

Summer 1999

## Nitrate Reductase Activity, Nitrate Uptake and Iodine Speciation in the Marine Environment

Chin-Chang Hung  
*Old Dominion University*

Follow this and additional works at: [https://digitalcommons.odu.edu/oeas\\_etds](https://digitalcommons.odu.edu/oeas_etds)



Part of the [Biochemistry Commons](#), and the [Oceanography Commons](#)

---

### Recommended Citation

Hung, Chin-Chang. "Nitrate Reductase Activity, Nitrate Uptake and Iodine Speciation in the Marine Environment" (1999). Doctor of Philosophy (PhD), Dissertation, Ocean & Earth Sciences, Old Dominion University, DOI: 10.25777/c73v-fh64  
[https://digitalcommons.odu.edu/oeas\\_etds/38](https://digitalcommons.odu.edu/oeas_etds/38)

This Dissertation is brought to you for free and open access by the Ocean & Earth Sciences at ODU Digital Commons. It has been accepted for inclusion in OES Theses and Dissertations by an authorized administrator of ODU Digital Commons. For more information, please contact [digitalcommons@odu.edu](mailto:digitalcommons@odu.edu).

NITRATE REDUCTASE ACTIVITY, NITRATE UPTAKE AND IODINE  
SPECIATION IN THE MARINE ENVIRONMENT

by

Chin-Chang Hung

M.S. June 1993, National Taiwan University, R.O.C. Taiwan

A Dissertation Submitted to the Faculty of  
Old Dominion University in Partial Fulfillment of the  
Requirement for the Degree of


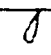
DOCTOR OF PHILOSOPHY

OCEANOGRAPHY

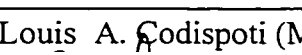
OLD DOMINION UNIVERSITY

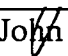
August 1999

Approved by:

 George T. F. Wong (Director) 

 William M. Dunstan (Member)

 Louis A. Codispoti (Member)

 John R. Donat (Member)

## ABSTRACT

### NITRATE REDUCTASE ACTIVITY, NITRATE UPTAKE AND IODINE SPECIATION IN THE MARINE ENVIRONMENT

Chin-Chang Hung  
Old Dominion University, 1999  
Director: Dr. George T. F. Wong

The present method for the determination of new production (NP) by measuring the uptake of added  $^{15}\text{NO}_3^-$  suffers from a number of limitations. In an attempt to improve this situation, this research examined the possibility of estimating  $^{15}\text{NO}_3^-$  uptake by measuring the activity of nitrate reductase (NRA). In addition, because it has long been suspected that the biological reduction of  $\text{IO}_3^-$  to  $\text{I}^-$  may be mediated by nitrate reductase (NR), this research investigated the ability of NR to catalyze the reduction of iodate to iodide.

An improved method for the determination of NRA was developed. The sensitivity of this method is about five times higher than methods used in previous studies. NRA and  $^{15}\text{NO}_3^-$  uptake (NU) were determined over a wide range of nitrate concentrations in the East China Sea and in the adjoining Kuroshio Current in May, 1996. In light- and nitrate-replete waters ( $[\text{NO}_3^-] > 1 \mu\text{M}$ , %PAR > 10%, PAR: photosynthetically active radiance), NRA was linearly related to NP so that NRA may be used for estimating NP. A high ratio of NU/NRA was found in nitrate-depleted ( $[\text{NO}_3^-] < 1 \mu\text{M}$ ) and light-replete (%PAR > 10%) conditions. The high ratio of NU/NRA data might have been caused by an overestimation of NU due to the stimulation of the addition of  $^{15}\text{NO}_3^-$  to nitrate-deficient water. This result revealed that NRA may be a reliable index for estimating new production in oligotrophic waters. In comparing NU in the literature with our NU values in different hydrographic realms, the NU values estimated from NRA fall well with recently reported values in similar types of waters.

NRA and iodine speciation were measured in the East China Sea in May, 1996. The results suggest that the reduction of iodate to iodide in the upwelling areas is caused by the enzyme NR. In the process of iodate reduction, the depletion of iodate and the enrichment of iodide relative to the composition of the source water of a surface water mass represent an integration of NRA through the residence time of the water mass.

A method for estimating the reduction of iodate to iodide by NR by using  $^{125}\text{IO}_3^-$  was developed. The reduction of  $\text{IO}_3^-$  to  $\text{I}^-$  by NR was observed in the cultures of *S. costatum* and in natural phytoplankton assemblages. The rates were 0.008 to 0.019 n mol  $\text{I}^- \mu\text{g chl } a^{-1} \text{ h}^{-1}$  in natural samples. The iodate reduction rate was linearly related to NRA, suggesting that iodate reduction may be coupled to nitrate reduction.

## ACKNOWLEDGMENTS

I would like to give my sincere thanks to Dr. George Wong who gave me much help and encouragement since I came to Old Dominion University. During the period of writing my dissertation, Dr. Wong spent much time in reading and correcting my dissertation. Also, I want to greatly express my thanks to my committee members-Drs. William Dunstan, Louis Codispoti and John Donat-who spent much time reading and correcting my dissertation and they assisted me greatly in my dissertation work.

I am deeply grateful to other professors, K. -K. Liu, James Yuan, G.-C. Gong , F. -K. Shiah, Y.-L.L. Chen, Gregory Cutter, and David Burdige who gave me much assistance in my field experiments and provided many significant discussions and comments on my dissertation. Additionally, I also want to give thanks to my friends and classmates: Vincent Kelly, Lisa Drake, Xianhao Cheng, Keun-Hyung Choi, Claudette Lajoi, Christina Dryden, Shi-Jun Fan, Rusty Hall, Carley Moritz, Paul Richardson, Li Zhang, Steve Kibler, and Rob Wardwell. They gave me help, comments, and encouragements about my experiments. Moreover, I greatly appreciate the help given to me by R.C. Kidd, Dana Oblak, Holly Park and Nikki Moore since I came to ODU. Furthermore, I want to thank the captains and the crew of R/V Ocean Researcher I and II for their assistance in taking sample collections.

Finally, I would like to dedicate this dissertation to my parents whose love and support fill my heart . My wife, Hsiao-Feng, has given me infinite support, sacrifice, and love so that I can finish my degree. I am constantly aware of how much I appreciate them.

## TABLE OF CONTENTS

	Page
LIST OF TABLES .....	viii
LIST OF FIGURES .....	ix
Chapter	
I. INTRODUCTION .....	1
Introduction .....	1
Hypothesis .....	3
Objective .....	3
Literature review .....	4
New production in the ocean .....	4
Measurement of new production .....	9
Nitrate assimilation and nitrate reductase .....	10
Iodine speciation in the ocean .....	14
Biological control of iodine speciation .....	16
II. AN IMPROVED METHOD FOR THE DETERMINATION OF NITRATE REDUCTASE ACTIVITY IN THE MARINE ENVIRONMENT.....	18
Introduction .....	18
Materials and methods .....	22
Reagents .....	22
Procedures .....	23
Calculation of nitrate reductase activity .....	26
Results and discussions .....	26
The effect of pH on nitrate reductase activity .....	26
The effect of the mode of mixing on nitrate reduction by NR .....	29
Effect of incubation time on enzyme activity.....	32
Nitrite quantification by using the method proposed here and a dipping probe colorimeter spectrophotometer .....	35
Precision and detection limit .....	38
Conclusions .....	40
III. NITRATE REDUCTASE ACTIVITY IN THE EAST CHINA SEA .....	41
Introduction .....	41
Review of the East China Sea .....	42
Materials and methods .....	45

(Continued)

Chapter	Page
Results and discussions .....	47
Distributions of water masses in the East China Sea .....	47
Depth distributions of NRA in the East China Sea .....	49
Distribution of NRA in the transect .....	60
Turnover time of nitrate in the transect .....	65
The relationship between specific NRA and PAR .....	69
The relationship between nitrate concentration and specific NRA .....	72
The relationship between NRA and chlorophyll <i>a</i> .....	75
Conclusions .....	77
 IV. THE EFFECTS OF LIGHT AND NITRATE LEVELS ON THE RELATIONSHIP BETWEEN NRA AND <sup>15</sup> NO <sub>3</sub> <sup>-</sup> UPTAKE: FIELD OBSERVATIONS IN THE EAST CHINA SEA .....	78
Introduction .....	78
Materials and methods .....	79
Sampling .....	79
Hydrographic and nutrient measurements .....	81
Chlorophyll <i>a</i> , primary production, <sup>15</sup> NO <sub>3</sub> <sup>-</sup> uptake and NRA assay .....	81
Results and discussions .....	84
Hydrography, light, nutrient and chlorophyll <i>a</i> .....	84
NRA and <sup>15</sup> NO <sub>3</sub> <sup>-</sup> uptake (NU) .....	97
Temporal variations .....	97
The influence of environmental conditions on NU/NRA .....	100
Relationship between NRA and NU .....	105
Relationship between NRA and chlorophyll <i>a</i> .....	109
Depth-integrated NRA and NU .....	114
Comparison of NU estimated from NRA and previous NU data .....	116
Conclusions .....	119
 V. THE RELATIONSHIP BETWEEN NRA AND IODINE SPECIATION IN THE SOUTHERN EAST CHINA SEA .....	120
Introduction .....	120
Materials and methods .....	122
Results and discussions .....	125
Hydrography .....	125
Depth profiles of hydrography, NRA, N-IO <sub>3</sub> <sup>-</sup> , and N-I <sup>-</sup> .....	128
Reduction of iodate to iodide .....	134
A conceptual model for the cycling of dissolved inorganic iodine .....	136

(Continued)

Chapter	Page
The estimation of new production using the production rate of iodate to iodide .....	138
Estimating global new production from global iodate depletion in the surface oceans .....	145
Conclusions .....	147
VI. THE REDUCTION OF IODATE TO IODIDE BY NITRATE REDUCTASE IN MARINE PHYTOPLANKTON .....	148
Introduction .....	148
Materials and methods .....	149
Reagents .....	149
Procedures .....	152
Results and discussions .....	156
Experimental blank .....	156
Comparison of commercial NR and marine NR .....	157
Effect of reaction time .....	160
Effect of the concentration of $\text{IO}_3^-$ .....	162
Iodate reduction by NR extracted from euxenic cultures of <i>S. costatum</i> and from natural phytoplankton assemblages .....	164
The relationship between IRA and NRA .....	166
Conclusions .....	168
VII. SUMMARY AND DIRECTIONS FOR FUTURE RESEARCH.....	169
Summary .....	169
Directions for future research .....	170
REFERENCES .....	172
APPENDICES .....	187
A. RECIPE OF F/2 SOLUTION .....	187
B. CALCULATION OF NRA .....	188
C. NRA, HYDROGRAPHY AND RELEVANT DATA IN THE EAST CHINA SEA .....	189
D. NRA, NU AND HYDROGRAPHIC DATA IN THE EAST CHINA SEA .....	194
E. IODATE, IODIDE, AND RELEVANT DATA IN THE SOUTHERN EAST CHINA SEA .....	197
VITA .....	200



## LIST OF TABLES

Table	Page
1-1	Estimates of global new production in the recent literature .....8
2-1	The nitrate reductase assay list from 1969 to 1995 .....21
2-2	The comparison of sensitivity in three different NRA assays (Eppley et al., 1969; Hochman et al., 1986; and this study) .....37
2-3	The precision of NRA in <i>S. costatum</i> and natural phytoplankton assemblages (from Chesapeake Bay) .....39
3-1	Properties of the waters in the mixed layer of the different hydrographic regimes of the East China Sea .....57
3-2	The turnover time of nitrate in the upwelling water of southern East China Sea .....68
4-1	Properties of the waters in the mixed layer of the different hydrographic regimes of the East China Sea .....90
4-2	Relationship between NU and NRA under different combinations of light- and nitrate- conditions .....108
4-3	Characteristics of the photic zone to PZD <sub>10</sub> in different hydrographic regimes of the East China Sea .....110
4-4	Properties of the photic zone to PZD <sub>01</sub> in different hydrographic regimes of the East China Sea .....112
4-5	Review of previous comparison of <sup>15</sup> NO <sub>3</sub> <sup>-</sup> new production vs new production via nitrate reductase activity from different hydrographic realms .....117
5-1	NU and turnover time of upwelled water in the southern East China Sea .....143
6-1	The reduction rate of iodate to iodide by nitrate reductase from natural phytoplankton that were collected in Chesapeake Bay, VA and from one phytoplankton culture ( <i>S. costatum</i> ) .....165

## LIST OF FIGURES

Figure	Page
1-1 A diagram of dissolved inorganic nitrogen species in the surface ocean .....	7
1-2 A general scheme of inorganic nitrogen uptake for phytoplankton .....	11
1-3 A possible role of nitrate reductase in iodate reduction .....	17
2-1 The analytical procedure for NRA measurement .....	25
2-2 The effect of pH on nitrate reductase activity in <i>S. costatum</i> .....	28
2-3 Comparison of continuous incubation (open) and one minute agitation incubation (solid) for nitrite formed in marine phytoplankton .....	31
2-4 Comparison of continuous agitation (open) and one minute agitation incubations (solid) for NRA in marine phytoplankton .....	34
2-5 Ratio of NRA at incubation time $t$ to time of $< 5$ min (open) .....	34
3-1 Sampling locations for NRA stations .....	44
3-2 The relationship between temperature and salinity at all stations .....	48
3-3 The depth profiles of hydrographic data and NRA at Sta. 30 (upper panel) and Sta. 15 (lower panel). Horizontal dotted line represents the MLD. Horizontal broken line represents the PZD .....	50
3-4 The depth profiles of hydrographic data and NRA at Sta. 51 (upper panel) and Sta. 53 (lower panel). Horizontal dotted line represents the MLD. Horizontal broken line represents the PZD .....	51
3-5 The depth profiles of hydrographic data and NRA at Sta. 52-1 (upper panel) and Sta. 52-3 (lower panel). Horizontal dotted line represents the MLD. Horizontal broken line represents the PZD .....	52
3-6 The depth profiles of hydrographic data and NRA at Sta. 49 (upper panel) and Sta. 50 (lower panel). Horizontal dotted line represents the MLD. Horizontal broken line represents the PZD .....	53
3-7 The depth profiles of hydrographic data and NRA at Sta. 11 (upper panel) and Sta. 45 (lower panel). Horizontal dotted line represents the MLD.	

## LIST OF FIGURES (Continued)

Figure	Page
Horizontal broken line represents the PZD .....	54
3-8 The depth profiles of hydrographic data and NRA at Sta. 26. Horizontal dotted line represents the MLD. Horizontal broken line represents the PZD .....	55
3-9 The depth profiles of hydrographic data and NRA at Sta. 55-3 (upper panel) and Sta. 55-5 (lower panel). Horizontal dotted line represents the MLD. Horizontal broken line represents the PZD .....	56
3-10 (a) The distribution of NRA in the Station 48-55 transect (upper panel) .....	62
(b) The distribution of S-NRA in the Station 48-55 transect (lower panel) .....	62
3-11 The distribution of nitrate in the Station 48-55 transect .....	63
3-12 The distribution of chlorophyll <i>a</i> in the Station 48-55 transect .....	64
3-13 The distribution of turnover time (day) of nitrate in the transect .....	67
3-14 The relationship between S-NRA and PAR at different stations .....	70
3-15 The relationship between S-NRA and PAR at different stations .....	71
3-16 The relationship between S-NRA and concentration of nitrate in upwelling areas (Stations 51, 52 and 53) .....	73
3-17 The relationship between S-NRA and concentration of nitrate at different stations .....	74
3-18 The relationship between I-NRA and I-chl <i>a</i> at all stations .....	76
4-1 The study area .....	80
4-2a The surface distribution of temperature (°C) in the East China Sea .....	85
4-2b The surface distribution of salinity in the East China Sea .....	86
4-2c The surface distribution of nitrate ( $\mu\text{M}$ ) in the East China Sea .....	87
4-2d The surface distribution of chlorophyll <i>a</i> ( $\text{mg m}^{-3}$ ) in the East China Sea .....	88

## LIST OF FIGURES (Continued)

Figure	Page
4-3 The vertical distribution of (a) temperature, salinity and $\sigma_\theta$ (b) nitrate, chlorophyll <i>a</i> and %PAR, (c) NRA and NU at Sta. 11 .....	91
4-4 The vertical distribution of (a) temperature, salinity and $\sigma_\theta$ (b) nitrate, chlorophyll <i>a</i> and %PAR, (c) NRA and NU at Sta. 15 .....	92
4-5 The vertical distribution of (a) temperature, salinity and $\sigma_\theta$ (b) nitrate, chlorophyll <i>a</i> and %PAR, (c) NRA and NU at Sta. 26 .....	93
4-6 The vertical distribution of (a) temperature, salinity and $\sigma_\theta$ (b) nitrate, chlorophyll <i>a</i> and %PAR, (c) NRA and NU at Sta. 30 .....	94
4-7 The vertical distribution of (a) temperature, salinity and $\sigma_\theta$ (b) nitrate, chlorophyll <i>a</i> and %PAR, (c) NRA and NU at Sta. 52-3 .....	95
4-8 The vertical distribution of (a) temperature, salinity and $\sigma_\theta$ (b) nitrate, chlorophyll <i>a</i> and %PAR, (c) NRA and NU at Sta. 55-3 .....	96
4-9 The vertical distribution of temperature and NRA from two casts at Sta.52 (a and b) and Sta. 55 (c and d) .....	99
4-10 The relationship between NU/NRA and nitrate at depth where %PAR > 10% ...	101
4-11 The relationship between NU/NRA and %PAR at locations where $\text{NO}_3^- > 1 \mu\text{M}$ and %PAR > 10% .....	104
4-12 The relationship between NU and NRA in waters with (a) nitrate > $1 \mu\text{M}$ and %PAR > 10%, (b) nitrate < $1 \mu\text{M}$ and %PAR > 10% and (c) nitrate > $1 \mu\text{M}$ and 1% < %PAR < 10%. The Model II regression line is shown as the solid line in (a) and as the dashed line in (b) and (c). The 1:1 line is shown as a dotted line in (a). The solid lines in (b) and (c) denote the regression relationship in (a) .....	107
4-13 The relationship between average NRA/chl <i>a</i> and the <i>f</i> ratio within $\text{PZD}_{10}$ .....	113
5-1 The study area of iodine species in the southern East China Sea .....	124
5-2 Contours of temperature in the transect along the southern East China Sea .....	126

## LIST OF FIGURES (Continued)

Figure	Page
5-3	Contours of salinity in the transect along the southern East China Sea .....127
5-4	The vertical distribution of $\text{N-IO}_3^-$ , $\text{N-I}^-$ , $\text{NO}_3^-$ , $\sigma\text{-}\theta$ , NRA at Sta. 49 .....129
5-5	The vertical distribution of $\text{N-IO}_3^-$ , $\text{N-I}^-$ , $\text{NO}_3^-$ , $\sigma\text{-}\theta$ , NRA at Sta. 53 .....131
5-6	The vertical distribution of $\text{N-IO}_3^-$ , $\text{N-I}^-$ , $\text{NO}_3^-$ , $\sigma\text{-}\theta$ , NRA at Sta. 55 .....133
5-7	The relationship between $\text{N-IO}_3^-$ and $\text{N-I}^-$ at all stations .....135
5-8	A conceptual model for the cycling of dissolved inorganic iodine species in the surface oceans .....137
5-9	The relationships between NRA and $\text{N-IO}_3^-$ (upper panel), and NRA and $\text{N-I}^-$ (lower panel) in the upwelling areas (Stations 51 to 53) .....139
5-10	The relationships between NRA and $\text{N-IO}_3^-$ (upper panel), and NRA and $\text{N-I}^-$ (lower panel) at Stations 49, 50 and 55. Dotted line is the relationship in the upwelling areas .....144
6-1	The analytical scheme of reduction of iodate to iodide mediated by nitrate reductase. AC: activated charcoal .....155
6-2	The concentration of iodide and iodate in iodate reduction experiment (NR from Sigma Co.) .....158
6-3	The concentration of iodide and iodate in iodate reduction experiment (NR from <i>S. costatum</i> ) .....159
6-4	The reduction of iodate to iodide by <i>S. costatum</i> NR at different reaction times .....161
6-5	The production of iodate and iodide catalyzed by NR at different iodate concentrations .....163
6-6	The relationship between iodide production activity (IRA) and nitrate reductase activity (NRA) in four field samples .....167

## CHAPTER I

### INTRODUCTION

#### **Introduction**

New production (NP) is the fraction of primary production that is supported by allochthonous nutrients (primarily nitrate) (Dugdale and Goering, 1967), and it should be equal to the export of particulate organic matter out of the euphotic zone under steady state conditions (Eppley and Peterson, 1979). This sinking flux of organic particles into the deep ocean is an important component in the global carbon cycle. Knowing the governing processes of new production and having an accurate estimation of new production is essential for a more accurate evaluation of the fate of anthropogenic CO<sub>2</sub> and its impact on global climatic changes (Platt et al., 1992; Siegenthaler and Sarmiento, 1993; Sarmiento and Le Quere, 1996).

NP is frequently estimated by the <sup>15</sup>N-labelled nitrate incubation technique (Dugdale and Wilkerson, 1986). However, this method suffers from several limitations. First, this method is inappropriate in oligotrophic waters where the nitrate concentration is too low to be accurately measured by conventional nitrate measurement (Eppley and Koeve, 1990). If the ambient concentration of nitrate is not known accurately, the added amount of <sup>15</sup>N-labelled nitrate may be excessive and stimulate nitrate uptake. As a result, high and variable uptake rates may be observed (Dugdale and Wilkerson, 1986; McCarthy et al., 1992, 1996; Allen et al., 1996). Second, the rate of nitrate uptake can be underestimated if nitrate is formed by nitrification during the incubation period (Ward et al. 1989; Eppley and Koeve,

---

The journal model for this dissertation was *Deep-Sea Research*.

1990). Third, the determination of  $^{15}\text{NO}_3^-$  uptake requires extensive sample manipulation and the use of a mass spectrometer. The cost and time for the analysis limit the number of samples that can be handled readily.

The uptake of nitrate involves three steps: nitrate reduction, nitrite reduction, and ammonia incorporation (Wada and Hattori, 1991). The first step is mediated by the enzyme nitrate reductase. If this is the rate determining step, then, nitrate reductase activity (NRA) will be proportional to the rate of nitrate uptake or NP. Thus, if a simple method can be developed for the determination of NRA, and a relationship between NRA and NP can be established. New production may be conveniently estimated from NRA. However, a consistent relationship between NRA and the rate of nitrate uptake has not been found in previous studies (Eppley et al., 1970; Collos and Slawyk, 1977; Dortch et al., 1979; Blasco et al., 1984). Possibly as a result of analytical difficulties (Berges and Harrison, 1995a) and a lack of appreciation of the effects of environmental factors such as light, nutrient conditions, and hydrographic conditions on NRA. By controlling the experimental conditions carefully, a strong correlation between the rate of nitrate incorporation and NRA was found in several more recent laboratory studies (Berges and Harrison, 1995a, 1995b; Berges et al., 1995). Thus, the first objective of this research is to evaluate the relationship between NRA and NP by using a modified NRA assay, and to try to apply the relationship between NP and NRA to estimate new production quantitatively.

Dissolved inorganic iodine in seawater exists primarily as iodate ( $\text{IO}_3^-$ ) and iodide ( $\text{I}^-$ ) (Tsunogai and Henmi, 1971; Trusdale, 1978; Wong, 1991), although the latter is thermodynamically unstable relative to the former in oxygenated seawater (Sillen, 1961;

Wong, 1980). Due to the chemical similarities between  $\text{IO}_3^-$  and  $\text{NO}_3^-$ , it has long been suspected that iodide is produced by the reduction of  $\text{IO}_3^-$  and the reaction is mediated by nitrate reduction. In this study, I have attempted to further investigate the relationship between NRA and NP as well as NRA and the speciation of iodine in the oceans.

### **Hypothesis**

The following two hypothesis are tested in this study:

1. Nitrate reductase activity is related to NP so that NRA may be used for estimating NP.
2. The reduction of iodate to iodide can be catalyzed by nitrate reductase in phytoplankton.

### **Objectives**

The specific objective in this study are:

1. To design an improved method for the determination of NRA.
2. To determine the relationship between NRA and NP in the field.
3. To measure the spatial variation of NRA in the field.
4. To determine the relationship between NRA and iodine speciation in the field.
5. To test whether nitrate reductase extracted from phytoplankton can catalyze the reduction of iodate to iodide.



## Literature review

### *New production in the ocean*

The basic definition of new production (NP) was initially given by Dugdale and Goering (1967) who defined NP as phytoplankton production that is supported by nutrients supplied from outside a system. On the other hand, regenerated production (RP) is based upon recycling nutrients in a system. The sources of new nitrogen include nitrogen transported into the euphotic zone from upwelling, input of different nitrogen compounds from river runoff, and combined nitrogen formed by nitrogen fixation (Fig. 1-1). In other words, the nutrient sources for new production include nitrate, ammonium, dissolved organic nitrogen (DON) as well as  $N_2$ , with nitrate generally considered to be the dominant source in ocean waters. The major forms of regenerated nitrogen are ammonium, urea and DON, although there is some debate on the possible significance of nitrate and nitrite as represented nutrients. Generally, a stable  $^{15}N$  is chosen as a tracer for estimating biological production because it can easily be used to distinguish new (nitrate,  $N_2$ ) and regenerated (ammonium, DON) forms of nitrogen (this is usually considered as operational definition). However, the operational definitions of new and regenerated production are sometimes confused with the basic definition. For example, when ammonium is transported to an estuary or a coastal area from an outside source, the rate of  $^{15}NH_4^+$  uptake should be regarded as new production rather than regenerated production since the ammonium is also a new source of nitrogen in this system. Thus, it should be noted that the “true” definition of new production is primarily based on a new source of nitrogen being transported to a system rather than based on nitrogen species.

The supply of new nitrogen (primary nitrate) for the surface ocean from upwelling was estimated to be about  $1.2 \times 10^{15}$  g-N  $y^{-1}$  by Codispoti (1983) according to total nitrogen assimilation rate of  $\sim 5 \times 10^{15}$  g-N  $y^{-1}$  (Liu, 1979) and an average  $f$  ratio  $\sim 0.25$  (Eppley and Peterson, 1979). More recently, Chavez and Toggweiler (1995) have summarized relevant new nitrogen source from wind-driven upwelling and vertical mixing, and they estimated the amount of nitrate transported to the surface ocean to be  $1.2 \times 10^{15}$  g-N  $y^{-1}$ . Thus, the magnitude of new nitrogen is roughly about  $1.2 \times 10^{15}$  g-N  $y^{-1}$ . Garside et al. (1976) reported that the input of different N compounds (ammonium, urea, DON, nitrate and nitrite) in sewage discharges to the ocean was about 10 g-N per person per day. If the world population is  $5.5 \times 10^9$  people, the input rate of total N will be about  $2 \times 10^{13}$  ( $10 \times 365 \times 5.5 \times 10^9$ ) g-N  $y^{-1}$ . Recently, the flux of DON from river has been estimated to be  $3.4 \times 10^{13}$  (Gruber and Sarmiento, 1997). The input of nitrogen fixation was estimated about  $2.8 \times 10^{13}$  g-N  $y^{-1}$  (Delwiche, 1981). The nitrogen fixation (fixed by *Trichodesmium*) was estimated about 5 to  $100 \times 10^{12}$  g-N  $y^{-1}$  (Carpenter, 1983; Gruber and Sarmiento, 1997). Thus, the magnitude of nitrogen fixation is roughly about  $1.0 \times 10^{14}$  g-N  $y^{-1}$ . Comparing the new nitrogen source from upwelling to human activity and nitrogen fixation, the nitrogen source of human activity and nitrogen fixation is one order magnitude lower than that of upwelling even though considering the analytical uncertainty of these estimations. Because new production in the surface ocean is primarily supported by input of nitrate from deep ocean, the concept of new production is usually referred as the rate of nitrate uptake. As a consequence, the rate of  $^{15}\text{NO}_3^-$  uptake is often regarded as a new production (NP).

The sum of NP and RP are referred to as primary production (PP). The ratio of NP

to PP is called the *f*-ratio and is an important index of trophic status (Eppley and Peterson, 1979). Eppley and Peterson (1979) further indicated that NP should be equal to the export production of particulate organic matter out of euphotic zone over a sufficient time scale. As a consequence, NP may play a crucial role in the transfer of anthropogenic CO<sub>2</sub> into the deep oceans. An accurate estimation of NP flux and an understanding of the regulating processes of NP are necessary for deciphering the imbalance of anthropogenic CO<sub>2</sub>. NP has been studied and computed in different marine environments for almost three decades, but the recent estimations of global NP still vary by up to a factor of four (5 to 22 Gt C y<sup>-1</sup>, Table 1-1) with an average of 9 Gt C y<sup>-1</sup>. The principal discrepancy among these independent approaches might result from complicated factors, such as different methods, temporal and spatial variations of NP. Strictly speaking, the study of global NP estimation to date suggests there is not get a consensus on the global NP value. Thus, it is necessary to put in more effort on the estimation of global NP.

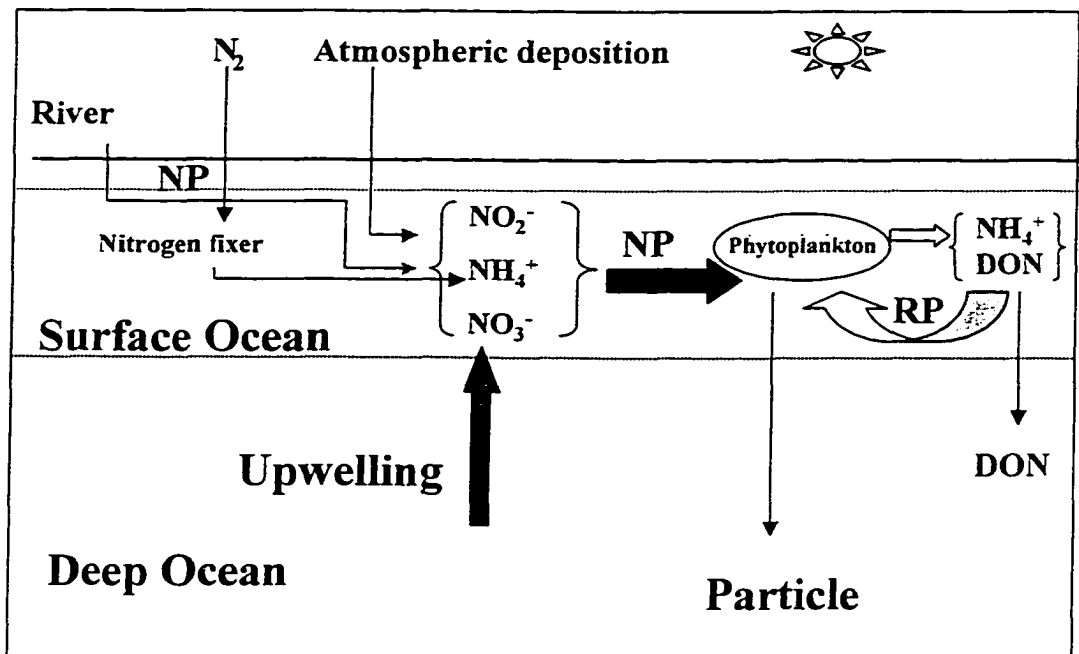


Fig. 1-1. A diagram of dissolved inorganic nitrogen species in the surface ocean. NP- new production. RP- regenerated production. RE - release of DON,  $NH_4^+$ .

*Table 1-1. Estimates of global new production in the recent literature*

Reference	Global new production (Gt C y <sup>-1</sup> )
Eppley & Peterson (1979)	3.4 ~ 4.7
Chavez and Barber (1987)	8.2
Martin et al. (1987)	7.4
Packard et al. (1988)	22
Berger (1989)	6.0
Bienfang & Zimann (1992)	7.7
Karl (1992)	5.5
Najjar et al. (1992)	12 ~ 15
Post et al. (1992)	15 ~ 22
Sarmiento et al. (1993)	8 ~ 12
Chavez & Toggweiler (1995)	7.2
Shaffer (1996)	5.0
Average (from 1979 to 1996)	9.0

*Measurement of new production*

A number of methods have been used for estimating new production: (a) the determination of the sinking particle flux from the euphotic zone by using sediment traps (b) the determination of the rate of nitrate uptake by using  $^{15}\text{N}$ -labelled tracer in bottle incubations, (c) the determination of sinking particle flux from the disequilibrium between Th and its parent nuclide U, (d) the estimation of nutrient or dissolved oxygen utilization and oxygen production (Eppley, 1989) and (e) the estimation of ocean color by using remote sensing (Sathyendranath et al., 1991). Of the above approaches, the uptake of stable  $^{15}\text{NO}_3^-$  is most widely used for estimating NP because its unique chemical nature can effectively distinguish between NP (based on nitrate and  $\text{N}_2$ ) and RP (based on ammonium and DON) (Dugdale and Goering, 1967, Dugdale and Wilkerson, 1986). Nevertheless, the  $^{15}\text{N}$  technique has some confounding problems such as (1) isotope dilution of the substrate due to recycling of substrate with the background isotope ratio (Glibert et al., 1982; Harrison, 1983); (2) difficulty in determining the extremely low concentration of nitrate in surface waters of oligotrophic oceans (Eppley et al., 1977); (3) bottle limitation including return of  $^{15}\text{N}$ -labelled back to the substrate pool (Laws et al., 1985) and depletion of substrate (nitrate or ammonium) under long-term incubations (Goldman et al., 1981); (4) stimulation from the addition of  $^{15}\text{N}$ -labelled substrate at low ambient nitrate concentrations (Glibert and Goldman, 1981; Eppley and Koeve, 1990); and (5)  $^{15}\text{N}$ -labelled disappearance during the incubation period (Laws, 1984; Ward et al., 1989). Among these problems, some have been overcome or at least circumvented with advanced instruments or improved techniques (Bronk et al., 1994; Ditullio and Laws, 1983; Fitzwater et al., 1982; Garside,

1982), but some problems still exist, particularly substrate stimulation in extremely low nitrate environments. In oligotrophic waters, the ambient nitrate concentration is too low to be accurately measured by the traditional nitrate analysis (Eppley and Koeve, 1990) so that the amount of added  $^{15}\text{N}$ -labelled nitrate in incubation experiments may result in a severe stimulation of nitrate uptake (Dugdale and Wilkerson, 1986; McCarthy et al., 1992, 1996; Allen et al., 1996). Although Garside (1982) proposed a chemiluminescence technique to measure extremely low nitrate concentrations, down to nanomolar concentration, the  $^{15}\text{N}$  method may still underestimate new production because the formation of nitrate via nitrification during the incubation periods (Ward et al., 1989; Eppley and Koeve, 1990). Furthermore, the upward flux of nitrate via upwelling is often regarded as a proxy for new production but this transported nitrate is not totally sequestered by phytoplankton since other factors such as iron deficiency (Martin, 1990), grazer regulation (Walsh, 1976), silicate limitation (Dugdale et al., 1995) and lack of seed of bloom-forming species (Chavez, 1989) may inhibit phytoplankton growth. Therefore, it is not surprising that estimates of the amount of global NP show large variations.

#### *Nitrate assimilation and nitrate reductase*

To assimilate nitrate, phytoplankton cells use an active transport system, ATP (adenosine triphosphate), to transport external nitrate through the cell membrane. Then the cells utilize a series of enzymes to reduce nitrate via nitrite to ammonium. The conversion process of nitrate to ammonium primarily includes three fundamental stages (Fig. 1-2) (Dortch et al. 1979; Solomonson and Barber, 1990; Wada and Hattori, 1991). The first step

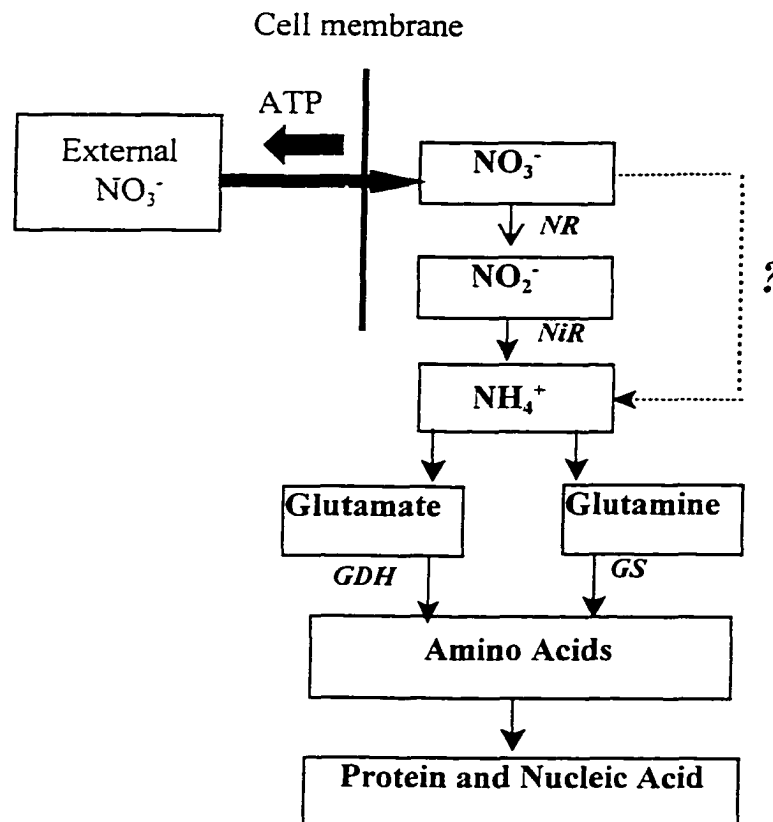
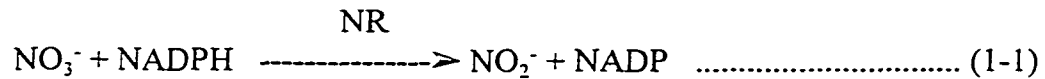


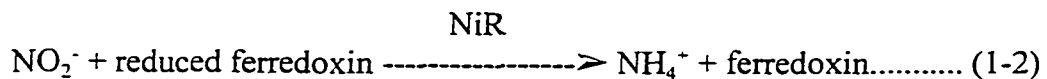
Fig. 1-2. A general scheme of inorganic nitrogen uptake for phytoplankton. Solid lines represent known reactions and dotted lines show possible reactions. NR: nitrate reductase; NiR: nitrite reductase; GDH: glutamate dehydrogenase; GS: glutamine synthase; ATP: adenosine triphosphate. (Referred from Dortch et al. 1979; Solomonson and Barber, 1990; Wada and Hattori, 1991)



is the reduction of nitrate to nitrite catalyzed by the enzyme nitrate reductase (EC 1.6.6.1, NADH nitrate oxidoreductase). NAD(P)H is used as the physiological electron donor for this reaction.



The second step is the reduction of nitrite to ammonia catalyzed by enzyme nitrite reductase (NiR, EC 1.7.7.1). This step is coupled to photosynthetic electron transport in algae via reduced ferredoxin which serves as the physiological electron donor for nitrite reductase.



The third step is the assimilation of ammonia by glutamate dehydrogenase (GDH) and glutamine synthetase (GS) to amino acids. NR is a complex enzyme containing several different redox-active prosthetic groups and encompasses flavin, heme (cytochrome  $b_{557}$ ) and Mo-pterin prosthetic groups in a 1:1:1 stoichiometry per subunit (Solomonson et al., 1975; Giri and Ramadoss, 1979). The molecular weights of the NR enzyme have a reported range 230,000 to 500,000 (Aparicio and Maldonado, 1978; Beavers and Hageman, 1980). Nitrate reduction is generally considered as the rate-limiting step in nitrate assimilation (Beavers and Hageman, 1969; Solomonson and Barber, 1990). Therefore, the characteristics of the activity of NR have been widely investigated in order to gain insights in nitrogen assimilation (references). About thirty years ago, NR enzyme was first used as an index of nitrogen source for the phytoplankton by Eppley and Coastworth (1968). Eppley et al. (1969) reported that NRA in the cells is significantly suppressed when phytoplankton are grown under nitrate-deplete and ammonium-replete conditions. Eppley et al. (1970), Packard et al. (1971) proposed that the activity of NR may be used to estimate the *in situ*

rate of nitrate uptake. Numerous investigations have been conducted in studying the relationship between nitrate reductase activity and the rate of nitrate uptake under different environmental conditions such as the concentration of nitrate, ammonium, and light irradiance (Eppley et al., 1970; Packard and Blasco, 1974; Collos and Slawyk, 1976; Dortch et al., 1979; Blasco et al. 1984). However, the relationship between NP and NRA is more perplexing than expected because many facets are still poorly understood. The discrepancies between NRA and NP may arise from several causes: (1) NRA is a property of phytoplankton at or before sampling time while new production is an integration of nitrate uptake after sampling time (Blasco et al., 1984); (2) NRA has a diel periodicity which may somewhat affect the comparison of the two parameters (Eppley et al., 1970; Blasco and Packard, 1974); (3) previous NRA assays were poorly optimized resulting in NRA that does not totally reflect the original enzyme activity (Berges and Harrison, 1995a; Berges, 1997); (4) the incubation time for  $^{15}\text{N}$ -label techniques in previous surveys was variable (4 ~ 24 hours) (Eppley et al., 1970; Blasco and Packard, 1974; Collos and Slawyk, 1976; Dortch et al., 1979; Blasco et al. 1984); and (5) the influence of light, nutrient concentration and hydrographic variability on NRA and NP measurements were not been taken into appropriate consideration. Recently, Hochman et al. (1986) developed an improved NRA assay and obtained higher NR signals for application in both phytoplankton cultures and field observations, compared to the methods of Eppley et al. (1969) and Packard et al. (1978). However, the NRA method of Hochman et al (1986) was not carried out in conjunction with  $^{15}\text{NO}_3^-$  uptake rate estimates in a field investigation. More recently, Berges and his co-workers (1995a,b,c) used a modified NR method to compare the

calculated rate of nitrate uptake with NRA in phytoplankton cultures and field samples under light and nutrient controlled conditions. They found a good relationship between the two variables. Thus, these promising results suggest that NRA is a potential candidate to estimate NP as long as an improved NRA assay can be developed and other interference factors can be appropriately eliminated.

### *Iodine speciation in the ocean*

Dissolved iodine is a biointermediate element and its total concentration in seawater is about 450-500 nM (Bruland, 1983; Wong, 1991; Truesdale, 1994). Dissolved iodine in the surface layer (0-200 m) primarily exists in two forms: iodate ( $\text{IO}_3^-$ ) and iodide ( $\text{I}^-$ ), whose depth distributions are more variable than the distribution of total dissolved iodine. (Tsunogai and Henmi, 1971; Truesdale, 1978; Luther and Cole, 1988). Low iodate concentrations (300 to 500 nM) are often observed in the surface oceans. The concentration gradually increases to a maximum level of 450 to 500 nM at depth. On the other hand, higher iodide concentrations (30 to 200 nM) are frequently found in the surface oceans. The concentration decreases with depth to an undetectable level ( $< 10$  nM) below the euphotic zone. Recently, dissolved organic iodine (DOI) may also be found in the estuaries, lagoon and high productive coastal waters (Wong and Cheng, 1997; Cheng, 1998).

According to thermodynamics, iodate should be the only detectable form of dissolved iodine in oxic seawater. At  $\text{pH} = 8.1$  and  $\text{pE} = 12.5$ ,  $\text{IO}_3^- / \text{I}^-$  should be equal to  $10^{13.5}$  (Sillen, 1961; Wong, 1980). In other words, iodate is a more stable form than iodide in oxic seawater. However, the prediction is inconsistent with field investigations

suggesting that chemical kinetics may significantly influence iodine speciation in surface ocean. Although the distributions of iodate and iodide in different marine environments have been relatively well known, the mechanism for the formation of iodine speciation is still unclear (Wong, 1991). According to the literature, some redox couples of bioactive elements, sulfide, nitrite, ammonia, methane, and methanol, may have potential to drive the oxidation state of iodate (Wong, 1991). Zhang and Whitfield (1986) reported that iodate can be reduced by bisulfide in seawater. Luther and Cole (1988) also indicated that bisulfide plays an important role regulating the iodine speciation in suboxic/anoxic waters in the Chesapeake Bay. In addition, a biochemical redox couple involving, NADPH (reduced nicotinamide-adenine-dinucleotide phosphate) and  $\text{NADP}^+$ , is considered as likely to promote the reduction of iodate to iodide. Thus, Tsunogai and Sase (1969) suggested that the reduction of iodate to iodide may also be catalyzed by NR. Besides chemical influences, photochemical reaction is also a possible factor to induce the reduction of iodate to iodide (Jickells et al., 1988). However, recent surveys suggest that iodide production arising from sunlight irradiance is supported by iodine speciation rather than from iodate (Brandão et al., 1994; Spokes and Liss, 1966; Cheng, 1998). These abiological sources explain certain circumstances of iodide formation, but it is difficult to expand these concepts to the global ocean scale because the above chemical redox-couples are deficient in oxic seawater. Thus, the question of dissolved iodine speciation conversion is still exiting "Where does the detectable iodide come from?"

*Biological control of iodine speciation*

Tsunogai and Sase (1969) first proposed that the formation of iodide is from the reduction of iodate mediated by bacterial nitrate reductase, but they did not quantitatively estimate the iodide production rate by bacterial NR and demonstrate NR produced by phytoplankton with the reducing ability for iodate reduction. Butler et al. (1981) indicated that *Skeletonema costatum* can incorporate iodate but other phytoplankton (*D. tertiolecta*, *A. japonica* etc.) can not. Wong and Zhang (1992) suggested that the reduction of iodate to iodide might be associated with nitrate reduction. Moisan et al. (1994) indicated that some marine phytoplankton can take up iodate and might release iodide during the process of iodate uptake. Udomkit (1994) also observed that the production of iodide in several species of phytoplankton in iodate batch phytoplankton cultures. Although Moisan et al. (1994) and Udomkit (1994) have determined the rate of  $\text{IO}_3^-$  uptake or production rate of  $\text{I}^-$  by phytoplankton, they did not determine that the reduction of iodate to iodide is caused by phytoplankton nitrate reductase. However, neither cultural experiment results nor field investigations were demonstrated that NRA is involved in the reduction of iodate to iodide. By consolidating previous studies: NR catalyzing the reduction of iodate to iodide is a possible avenue to interpret the detectable iodide in the surface oceans because of the formula of iodate similar to nitrate and nitrate uptake acting a predominate role within the microorganism food web (Fig. 1-3).

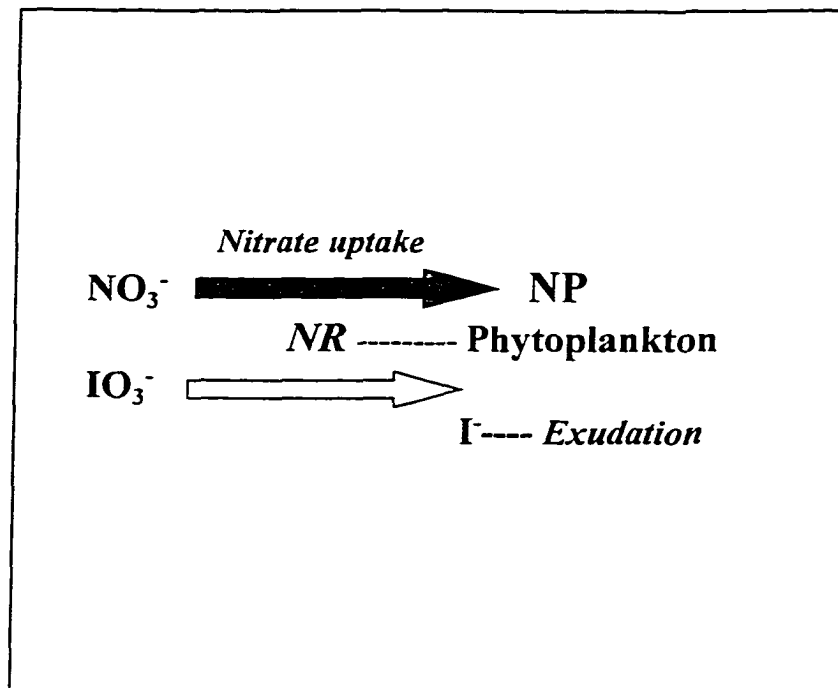


Fig. 1-3. A possible role of nitrate reductase in iodate reduction.  
NP: particulate nitrogen. NR: nitrate reductase.  
Solid arrow represent nitrate uptake.  
Blank arrow represents possible reaction.

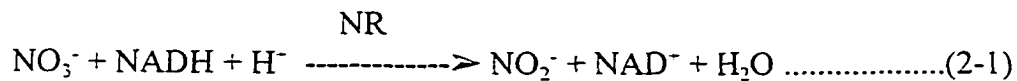
## CHAPTER II

### AN IMPROVED METHOD FOR THE DETERMINATION OF NITRATE REDUCTASE ACTIVITY IN THE MARINE ENVIRONMENT

#### Introduction

Attempts to utilize nitrate reductase activity (NRA) as an index of nitrate uptake in field observations in the marine environment have met with little success (Collos and Salwyk, 1977; Dortch et al., 1979; Blasco et al., 1984). Two possible reasons for these failures are: (1) the effects of variability of environmental factors, such as the concentration of nitrate, light conditions and hydrographic conditions have not been taken consideration adequately (Packard and Blasco, 1974; Collos, 1982; Blasco and Conway, 1982; Blasco et al., 1984) and (2) the method for the determination of NRA has not been optimized (Berges and Harrison, 1995a; Berges 1997). An improved method for the determination of NRA in marine samples is described in this chapter.

Nitrate reductase (NR) is the enzyme that mediates the reaction between  $\text{NO}_3^-$  and NADH so that



The activity of NR (nitrate reductase activity, NRA) is most commonly estimated by measuring the rate of production of  $\text{NO}_2^-$  in the presence of excess  $\text{NO}_3^-$  added and NADH in a NR extraction from a known biomass of phytoplankton cells. The analytical scheme includes three main components: (1) the extraction of the enzyme from phytoplankton cells; (2) the reduction of added nitrate to nitrite by NADH in the presence of nitrate reductase as well as other added reagents at a given pH in a given time interval; (3) the determination of

the nitrite formed. Since the observed NRA results from operatively defined experimental conditions, such as the pH, substrate concentration, incubation time and incubation temperature (Table 2-1), it represents a relative rather than an absolute nature rate. Thus, the primary objectives in an analytical scheme for the determination of NRA are to provide: (1) highly precise results and (2) the highest possible sensitivity in order to minimize the required sample volume. Eppley et al. (1969) first proposed a method for the determination of NRA in marine phytoplankton. Later, this method was widely used to study the relationship between NRA and new production (Collos and Salwyk, 1977; Packard et al., 1978; Dortch et al., 1979; Blasco et al., 1984). However, the precision in Eppley's method is about 20 % and the sensitivity is very low due to dilution (it required about 10  $\mu\text{g}$  chlorophyll *a* per sample) or the influence of other reagents. Berges and Harrison (1995a), and Berges (1997) pointed out that the Eppley et al. method (1969) is not optimized because the efficiency of extraction of NR was low and  $\text{MgSO}_4$  might affect the regulation of NR during incubation. Furthermore, Hochman et al. (1986) encountered great difficulty in measuring reasonable NRA in natural samples by using the Eppley et al. method (1969) even under nitrate-replete and ammonium-deplete conditions. Thus, they developed an improved method for measuring NRA. Hochman et al. (1986) reported that their method can obtain higher NRA and higher precision (8 -11 %) in both fresh and marine phytoplankton samples than other NR approaches (Eppley, 1978; Packard et al., 1978). However, this method has not yet been tested under field conditions in the marine environment. When considering the distinct analytical conditions of current NRA assays (Table 2-1), it becomes apparent that the enzyme incubation time, pH and nitrite detection



methods are quite inconsistent. Therefore, the tasks of this chapter are focused on developing improved reaction conditions for NRA in terms of pH value, incubation mode and/or time, and nitrite detection method with an axenic algal culture (*Skeletonema costatum*) and natural marine phytoplankton from the Chesapeake Bay.

Table 2-1. The nitrate reductase assay list from 1969 to 1995

Reference	Rupturing of cells	Grinding Temp. <sup>1</sup> , Time	Ext. <sup>2</sup>	pH	NO <sub>3</sub> <sup>-</sup> (mM)	NADH (mM)	Incubated Time (min) Temp.	Stop Reaction
Eppley et al. (1969 & 1978)	GT <sup>3</sup>	4 °C, 2 min	YES	7.9	10	0.089	30, RT	ZnOAC* ethanol
Harrison (1973)	GT	4 °C, 5 min	YES	8.1	11	0.047	45, 20 °C (in darkness)	ZnOAC ethanol
Packard et al. (1978)	GT	4 °C, 2 min	NO	7.9	3.5	0.106	20, 15 °C	ZnOAC ethanol
Hochman (1986)	Toluene	25 °C, 1 min	NO	7.6	10.5	0.68	20, at 25 °C	ZnSO <sub>4</sub> at 97 °C
Gao et al. (1992, 1993)	1-propanal	16 °C no mixing	NO	7.6	10	0.05	30, 15 °C (in darkness)	no reagent
Timmermans et al. (1994)	Toluene	RT no mixing	NO	7.8	100	6.5	10, 20 at RT	boiling distilled water
Berges and Harrison (1995)	GT	4 °C, 5 min	YES	7.9	10	0.2	10, 15 at RT	ZnOAC ethanol
This study	Toluene	RT continue mixing	NO	7.8	10.5	0.68	5, 10 at RT	ZnSO <sub>4</sub> at 97 °C

1-Ext.: extraction; 2-Temp.: temperature; GT<sup>3</sup>: Glass-Teflon; RT: room temperature (20 to 26 °C).

\* ZnOAC: zinc acetate.

## Materials and methods

### *Reagents*

Phosphate buffer solution (150 mM, pH 7.8): Dissolve 39.19 g of  $K_2HPO_4$  in a small volume of distilled deionized water (DDW) in a 1000-ml of volumetric flask. Dilute the solution to volume and adjust its pH to 7.8 with phosphoric acid and NaOH.

Potassium nitrate solution (0.1 M): Dissolve 8.088 g of  $KNO_3$  in a small volume of DDW and dilute to volume in a 1000-ml of DDW.

Sodium nitrite standard (10  $\mu$ M): Dissolve 0.1724 g of  $NaNO_2$  w in a small volume of DDW and dilute to volume in a 1000-ml of volumetric flask to form a 2.5 mM stock standard. Dilute this stock solution to 100  $\mu$ M of second standard by pipetting 4 ml of stock standard in a 100-ml of volumetric flask. Then dilute this second standard to 10  $\mu$ M by pipetting 10 ml of second standard in a 100-ml of volumetric flask.

NADH solution (6.5 mM): Dissolved 0.215 g Nicotinamide Adenine Dincieotide (NADH, reduced form, Sigma Co., N-6005) in a small volume of DDW in a 50-ml of flask and dilute the solution to volume. Keep this solution refrigerated ( 4 °C) and fresh.

Toluene: A. C. S. grade toluene (MCB) is used without further purification.

ZnSO<sub>4</sub> solution (0.11 M in 15% HCl): Dissolve 20.18 g of  $ZnSO_4$  in a small volume of DDW in a 1000-ml of flask and dilute the solution to volume.

NaOH solution (2 M): Dissolve 8 g of NaOH in a small volume of DDW in a 100-ml of flask and dilute the solution to volume.

Sulfanilamide solution (SUL, 2%): Dissolve 2 g of sulfanilamide in a small volume of 15%

(v/v) hydrochloric acid and dilute it to volume in a 100-ml of volumetric flask with 15% hydrochloric acid.

N-1-naphthylethylenediamine hydrochloride solution (NED, 0.3%): Dissolve 0.3 g of N-1-naphthylethylenediamine hydrochloride in a small volume of DDW in a 100-ml of flask and dilute it to volume.

### Apparatus

A Brinkmann Dipping Probe Colorimeter (Model PC-800) equipped with a probe tip of 2-cm light path (Pyrex-backed front surface mirrors) was used for all nitrite measurements without transfer of test solution to a cuvette. A narrow pass filter of 545 nm wavelength was the exact wavelength used for the detection of nitrite absorbance. The signal was then recorded by a digital readout. A Vortex mixer was used to agitate the phytoplankton cell solution.

### Phytoplankton culture

*Skeletonema costatum* (Greville) Cleve (SKEL) were obtained from the Provasoli-Guillard Center for the Culture of Marine Phytoplankton. *S. costatum* were cultured in 1000-ml borosilicate Erlenmeyer flasks in *f*/2 culture medium (Guillard and Ryther, 1962). Cultures were grown in the log phase at  $20 \pm 1$  °C on a 12:12 h light-dark cycle at an irradiance of  $65 \mu\text{mol photons m}^{-2} \text{s}^{-1}$ . The recipe for *f*/2 is shown in Appendix A.

### *Procedures*

#### Nitrate reductase activity assay

Sufficient phytoplankton cells are filtered through a Gelman Type A/E glass fiber filter which is first washed with 10 ml of deionized distilled water. (For oligotrophic waters, about 20 liters of the sample is filtered. In mesotrophic coastal water, use about 2-8 liters). Place the filter, with the cells facing upward, in a 50-ml beaker. Add 1 ml of the phosphate buffer and 50  $\mu$ L of toluene to the beaker. Agitate the mixture by placing into a slurry the beaker on a vortex mixer for 1 minute. Add 0.2 ml of the NADH solution and 0.2 ml of the potassium nitrate solution to the beaker. Agitate the mixture at room temperature ( $\sim$  20 to 25  $^{\circ}$ C) for 5 minutes by again placing the beaker on vortex mixer. Terminate the reaction by pipetting 1 ml of the mixture into a centrifuge tube containing 2 ml of  $\text{ZnSO}_4$ , which has been equilibrated in a water bath heated to 97  $^{\circ}$ C. Allow the centrifuge tube to stand in the water bath for 20 seconds. After the centrifuge tube has been removed from the water bath and cooled to room temperature, add 0.1 ml of NaOH to the centrifuge tube and centrifuge it for 20 minutes at 4000 rpm. Decant the clear supernatant liquid into a clean test tube. Add 0.1 ml of sulfanilamide solution, stir it for 10 seconds, and allow the solution to stand for 2 minutes. Then add 0.1 ml of NED solution and stir it for 10 seconds. The final volume of the solution in the test tube is about 2.2 ml. Allow the solution to stand for 10 minutes. Measure the absorbance of the pink azo dye formed by using a Brinkman Model PC-800 Probe colorimeter. As a blank, another subsample is processed in parallel identically without the addition NADH. Prepare a nitrite standard curve by substituting nitrite solution of known concentrations (0.1, 0.2, 0.3, 0.4, 0.5 and 0.6 ml of 10  $\mu$ M) in the place of the enzyme extract in the analytical scheme. A flow chart of the analytical scheme is shown in Figure 2-1.

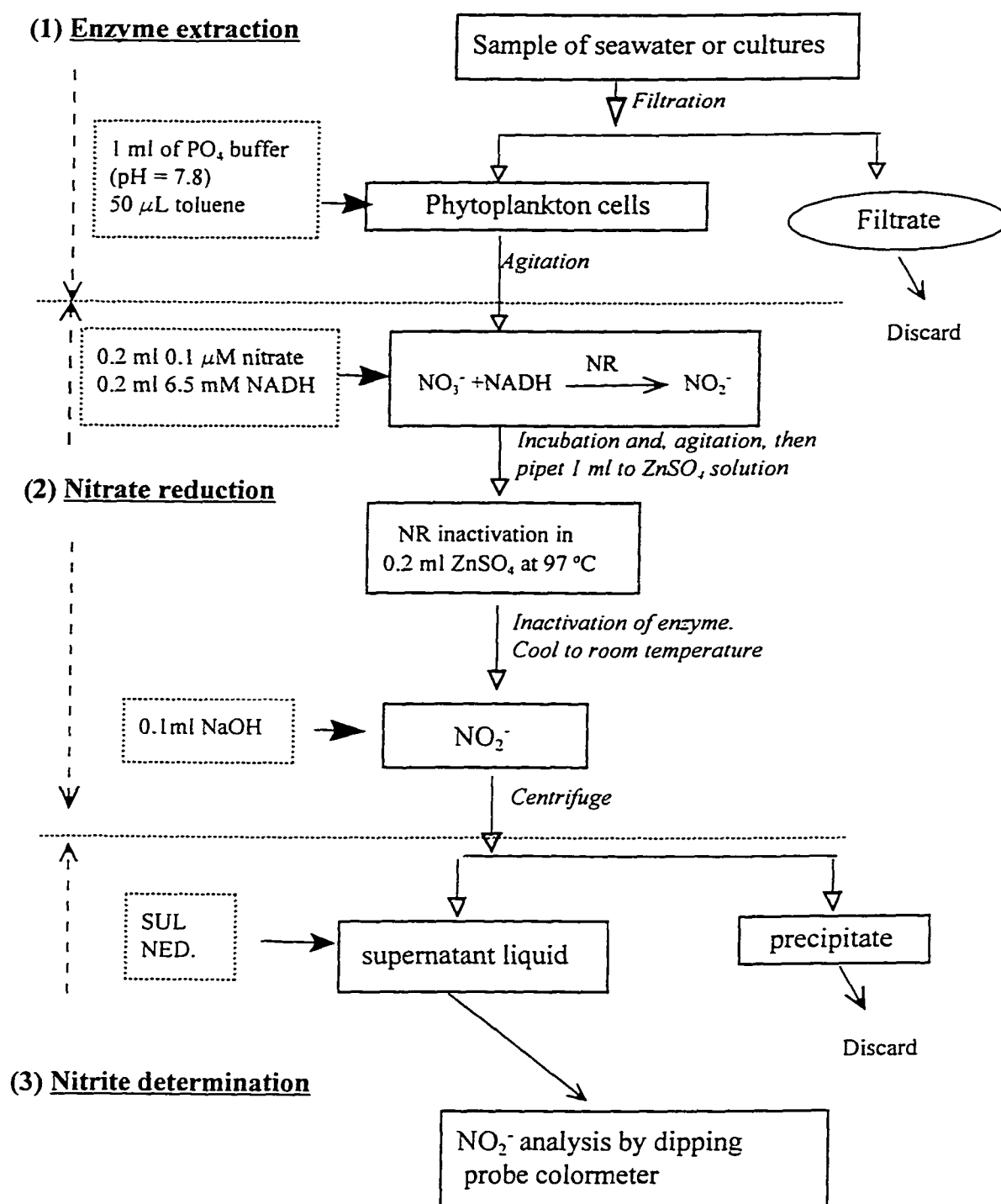


Fig. 2-1. The analytical procedure of NRA measurement.

### *Calculation of nitrate reductase activity*

The activity of NR is calculated as follows:

$$\text{NRA (nM-NO}_2^- \text{ h}^{-1}\text{)} = \frac{(A_{\text{sample}} - A_{\text{blank}})}{S_{\text{standard}} \times T} \times \frac{V_{\text{absorbance}} \times V_{\text{mixture}}}{V_{\text{nitrite}} \times V_{\text{sample}}}$$

$A_{\text{sample}}$  --- represents the absorbance of the sample

$A_{\text{blank}}$  --- represents the absorbance of the blank.

$S_{\text{standard}}$  --- is the slope of the calibration curve for nitrite standard.

$T$  --- is the incubation time.

$V_{\text{absorbance}}$  --- is the final volume for nitrite absorbance measurement.

$V_{\text{mixture}}$  --- is the volume of the phytoplankton extract.

$V_{\text{nitrite}}$  --- is the volume of extract analyzed for nitrite.

$V_{\text{sample}}$  --- is the volume of sample filtration. An example of the calculation procedure is given in Appendix B.

## **Results and discussions**

### *The effect of pH on nitrate reductase activity*

The pH used in the extraction of NR in the different NRA analytical scheme ranges from 7.6 to 8.1 (Table 2-1). Because of this, the optimal pH for this step was further evaluated. NR was extracted from a culture of *S. costatum* at pH of 7.6, 7.7, 7.8, 7.9, 8.0 and 8.1. The NRA in these sub-samples were then determined. Two series of experiments were conducted, one using 30 ml of the cultures (chlorophyll *a* > 70  $\mu\text{g/L}$ ) and the other using 20 ml of the culture in each sub-sample.

The effect of pH on the nitrate reductase activity is shown in Fig. 2-3. Curves A and B represent the results using 30-ml and 20-ml subsamples of the culture *S. costatum* respectively. In curve A, the concentration of nitrite stayed approximately the same between pH 7.6 and 7.9. At higher pH, the concentration of nitrite decreased steadily with increasing pH, reaching a minimum at the highest pH of 8.1. In curve B, the concentration of nitrite was stable at pH 7.6 and 7.7, and then increased steadily with pH, reaching a maximum between pH 7.8 and 7.9. The lowest concentration of nitrite was found at the higher pH of 8.1, similar to curve A. The results in curves A and B suggest that this optimal pH of NRA analysis ranges from 7.8 to 7.9 while NR does not function well at higher pH values (> pH 8). Comparing the results (7.8 to 7.9) to other reports (Table 2-1), it was found that the pH range is quite acceptable.



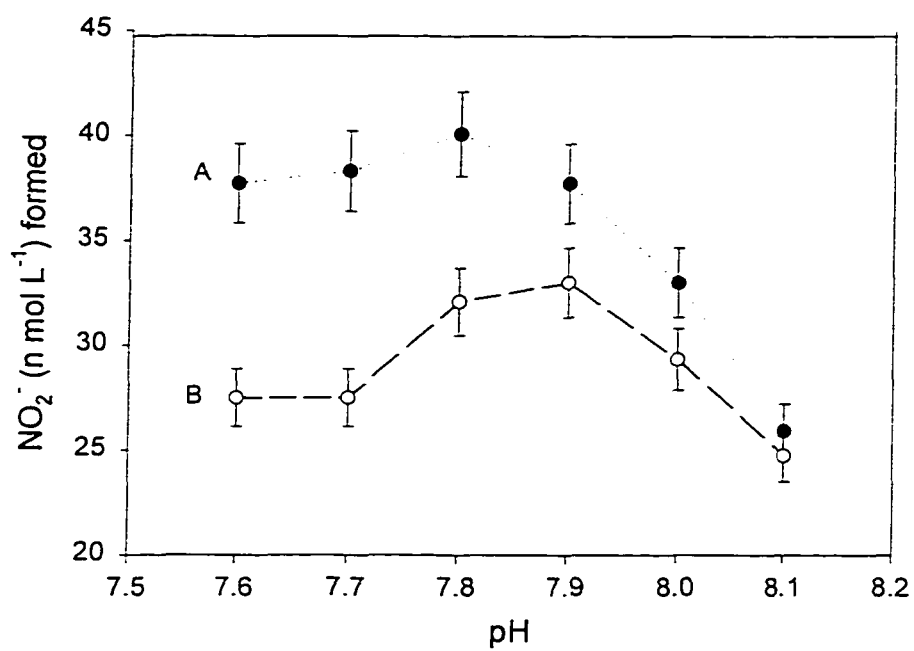


Fig. 2-2. The effect of pH on nitrate reductase activity in *S. costatum*. (A and B represent 30 and 20 ml of sample).

*The effect of the mode of mixing on nitrate reduction by NR*

NR was extracted from natural phytoplankton assemblages collected along the shore of Chesapeake Bay (36°58' N, 76°16' W). Water samples were first filtered through a 200  $\mu\text{m}$  mesh-size net to remove large particles. They were then separated into two 1600 ml subsamples for the NRA analysis. During the incubation step in the nitrate reduction step, one subsample was continuously agitated by using a vortex mixer. For the other subsample, the mixing scheme of Hochman (1986) was employed. It was agitated for 1 minute with a vortex mixer and then gently shaken on a shaker. Aliquots were then drawn from these subsamples for the determination of the nitrite formed at known time intervals.

The relationships between the concentration of nitrite formed and the time for agitation using these two modes of mixing are shown in Fig. 2-3. At a given incubation time, the concentration of nitrite formed was higher in all cases when continuous agitation of the sample with a vortex mixer was used. Thus, this mode of continuous mixing has been adopted in the proposed improved method. The linear relationship between the concentration of nitrite formed and reaction time in the first 10 minutes suggests that during this phase, the rate of this reaction might have been controlled by the availability of NR. Thus, it represents the real NRA. In the second phase, at a reaction time exceeding 15 minutes, the slower rate of formation of nitrite might have been caused by (1) an exhaustion of the added nitrate; (2) an exhaustion of the added NADH; (3) the deactivation of the added NADH; (4) deactivation of NR or a result of self-decomposition. The first and second explanations are unlikely since a large excess of nitrate and NADH have been added to the reaction mixture relative to enzyme activity. Both of the latter two explanations are

possible. NADH is an unstable compound which must be stored at low temperature (4°C). The self-decomposition rates of NADH and NR are not known exactly. Berges and Harrison (1995a) reported that NRA obtained from *Thalassiosira pseudonana* drops in activity by about 20 % after it is stored for 20 minutes, even at liquid nitrogen temperature (< -100 °C).

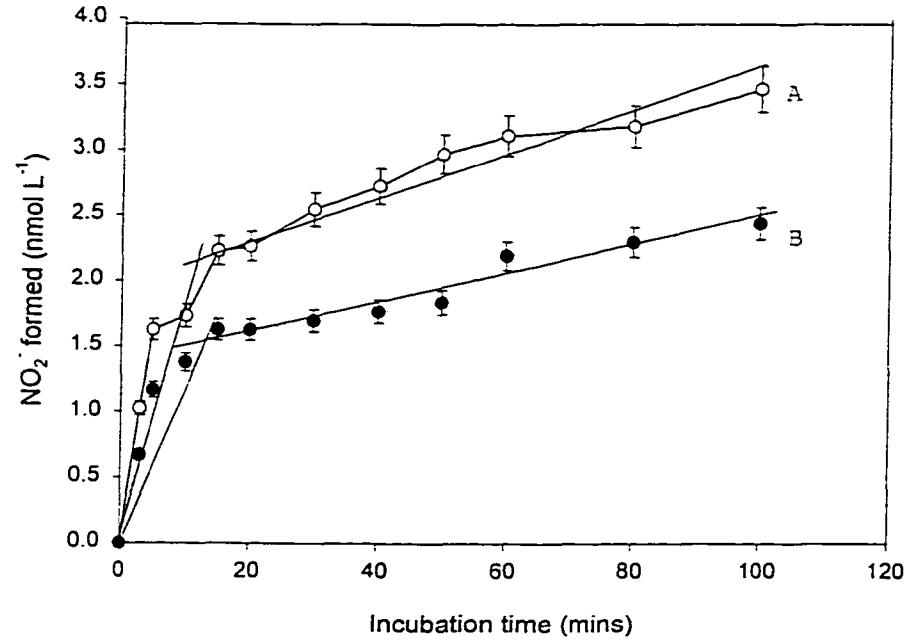


Fig. 2-3. Comparison of continuous incubation (open) and one minute agitation incubation (solid) for nitrite formed in marine phytoplankton.

*Effect of incubation time on enzyme activity*

In the continuous mixing mode, the concentration of nitrite formed was almost linear with time for the first 10 minutes at an average rate of 10 nM-N h<sup>-1</sup>. The concentration of nitrite formed increased approximately linear between 15 to 100 minutes at an average rate of 0.9 nM-N h<sup>-1</sup> (Fig. 2-3). In comparing the rate of nitrite production between the two different stages, the average rate of nitrite production in the former (10 nM h<sup>-1</sup>) is almost one order magnitude higher than in the latter (0.9 nM h<sup>-1</sup>). This suggests that NRA significantly mediated the reduction of nitrate to nitrite during the first 10 minutes after incubation, while NRA seemed to cease catalyzing the nitrate reduction from 15 to 100 minutes, due to deactivation of NR or self-decomposition. With the mixing scheme of Hochman (1986), the variation of concentration of nitrite formed with time was similar to that during continuous mixing with an average rate of 8.1 and 0.6 nM-N h<sup>-1</sup> for the first 10 minutes and from 15 to 100 minutes, respectively (Fig. 2-3). Although the mixing modes are different, the trends of the two cases are similar in that the highest rate of formation is during the first 10 minutes of incubation time with a subsequent lower rate during 15 to 100 minutes of incubation.

Fig. 2-4 shows the NRA calculated by using the data obtained at each incubation time. In the continuous mixing mode (curve A), NRA remained at a maximum rate (~20 nM h<sup>-1</sup>) when an incubation time of up to 5 minutes was used. At a longer incubation time, the rate decreased exponentially with time. The rate dropped to 10 nM h<sup>-1</sup> and 7 nM h<sup>-1</sup> at incubation times of 10 and 20 minutes respectively. With the mixing scheme (curve B) of Hochman et al. (1986), NRA shows an analogous distribution. The maximum rate

(13.5 nM h<sup>-1</sup>) also occurred at 3 - 5 minutes and the rate decreased exponentially with time. The rate dropped to 8 nM h<sup>-1</sup> and 5 nM h<sup>-1</sup> at incubation times of 10 and 20 minutes respectively. These results reveal that NRA is time independent at incubation times of 3 to 5 minutes, while NRA is strongly dependent on incubation time at 5 to 30 minutes. In other words, any inexact control of the incubation time will result in large error. In the proposed analytical scheme of NRA assay, an incubation time of 5 minutes has been adopted.

The ratio of NRA at each incubation time to NRA at incubation time of < 5 minutes in the mode of continue mixing is shown in Fig. 2-5 (open symbol). The percentages of NRA at incubation time of 10 and 20 minutes were 50 % and 34 % relative to initial rate, respectively. In comparison, the previous investigations frequently used longer incubation time (> 20 minutes) than this study (5 minutes). The results suggest the sensitivity of the previous NRA assays was low. In addition, the previous NRA assays also showed large variability because of the strong dependence on exact incubation time. Although there was no direct evidence in past reports to quantify the life time of NR after it was extracted from cells, the incubation time of the method developed in this study seems to be shorter than in previous methods (Table 2-1). Incubation time in previous methods varied from 30 minutes (Eppley et al., 1969; Gao et al., 1992) to 20 minutes (Packard et al., 1978; Hochman et al., 1986) to 10 minutes (Timmermans et al., 1994; Berges and Harrison, 1995).

The ratio of NRA at various incubation times using the mixing scheme of Hochman to incubation times of < 5 minutes in the mode of continue mixing is also presented in Fig. 2-5. NRA using the mixing scheme of Hochman was lower than in this study (60 % of NRA

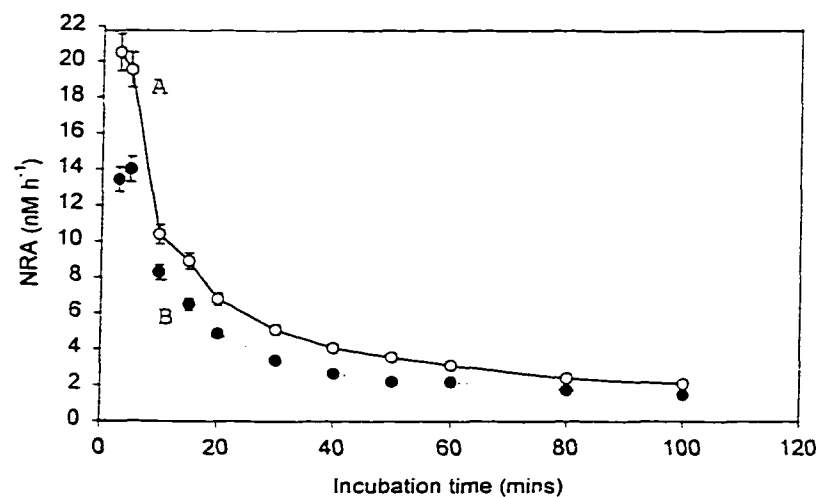


Fig. 2-4. Comparison of continuous incubation (open) and one minute agitation incubation (solid) for NRA in marine phytoplankton.

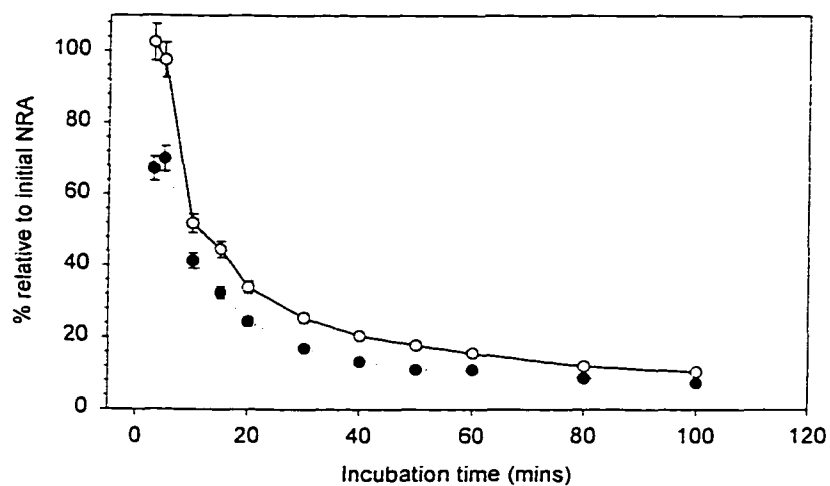


Fig. 2-5. Ratio of NRA at incubation time  $t$  to time of  $< 5$  min (open). Ratio of NRA at incubation time  $t$  in curve B to NRA at incubation time  $< 5$  min in curve A (solid).

from the new method) at times < 5 minutes. If the incubation time of 20 minutes in the Hochman assay is adopted, the ratio of NRA in the proposed assay to the Hochman assay is a ratio of 5. In other words, the sensitivity of the proposed assay is much higher than the scheme of Hochman et al. (1986).

*Nitrite quantification by using the method proposed here and a dipping probe colorimeter spectrophotometer*

The general scheme of the NRA assay includes three stages: (1) filtering and enzyme extraction; (2) nitrate reduction; and (3) nitrite detection. NRA is concentrated from filtration and dilution by reagent additions. For example, under the practical proposal here, the volume of phytoplankton extract is 1.5 ml and the volume of extract analyzed for nitrite is 1.0 ml. The final volume for absorbance measurement is 2.2 ml. If the size of the sample that is filtered is 1000 ml, then the concentration factor would be 303.

$$\text{Concentration factor} = \frac{1000ml}{1.5ml} \times \frac{1.0ml}{2.2ml} = 303$$

In Eppley's et al. (1969) method, the volume of phytoplankton extract, the volume of extract analyzed for nitrite and the final volume for absorbance measurement are 4.4, 1.5 and 3.0 ml, respectively. For the method of Hochman et al. (1986), the volumes are 1.9, 1.0 and 2.8 ml, respectively if all the volumes are 1000 ml. The concentration factors for Eppley's et al. (1969) and in Hochman's et al. method (1986) are 114 and 188 (Table 2-2). The final volume absorbance measurement in the methods of Eppley and Hochman are 3



ml and 2.8 ml because of the need to fill a 1-cm path length cuvette cell. In this study, using a dipping probe colorimeter provides a 2-cm path length with a smaller final volume. Therefore, the final ratio of absorbance in the Eppley et al and Hochman et al. method to the absorbance in the study is 0.2:1 and 0.3:1.(114x1: 188x1: 303x2). In other words, the sensitivity of the improved method is about five times higher than that in Eppley's method. Eppley et al. (1969) suggested that a successful measurement of NRA needs about 10  $\mu\text{g}$  of chlorophyll *a*. Assuming the chlorophyll *a* concentration in coastal area is 2  $\mu\text{g/L}$ , one needs five liters of seawater to satisfy the NRA analysis using Eppley's et al. method while one just needs 1 liter of seawater using the improved NRA assay. Similarly, if the chlorophyll *a* in oligotrophic ocean is 0.1  $\mu\text{g/L}$ , one must collect 100 liter of seawater using the Eppley's et al. method, while one only needs 20 liters of seawater using the improved NRA assay.

Table 2-2. The comparison of sensitivity in three different NRA assays  
(Eppley et al., 1969 ; Hochman et al., 1986; and this study)

	Eppley et al. (1969)	Hochman et al. (1986)	This study
Sample Volume (ml) : V1	1000	1000	1000
Volume of phytoplankton extract (ml): V2	4.4	1.9	1.5
Volume of extract analyzed for nitrite (ml): V3	1.5	1.0	1.0
Final volume for absorbance measurement (ml): V4	3.0	2.8	2.2
Concentration factor	114	188	303
Path length (cm)	1	1	2
Ratio of absorbance	0.2	0.3	1

V1 = the volume of filtration

V2 = the volume of phosphate buffer + NADH + Nitrate

V3 = volume used from V2

V4 = the volume of supernatant liquid (V3 + ZnSO<sub>4</sub> + NaOH) after centrifuge  
+ NED + SUL

### **Precision and detection limit**

The NRA in a culture of *S. costatum* and a sample of surface seawater collected from Chesapeake Bay were determined repeatedly in order to establish the precision of the proposed method. In each case, the sample was analyzed four times. The NRA formed were  $555 \pm 28$  (or  $\pm 5\%$ ,  $1\sigma$ ) and  $7.2 \pm 0.3$  (or  $\pm 5\%$ ,  $1\sigma$ ) respectively (Table 2-3). In comparison, Eppley et al. (1969) and Hochman et al. (1986) reported NRA uncertainties of  $\pm 20\%$  and  $\pm 8\%$  respectively. Thus, the precision of the proposed method is much better than that of Eppley et al. (1969) and is comparable to that of Hochman et al. (1986). The detection limits for NRA can be estimated from the detection limit for the determination of nitrite, about  $0.1 \mu\text{M}$ . If 5 liters of a sample is processed, the detection limit is about  $0.4 \text{ nM h}^{-1}$  (equation 2-1). If 20 liters of a sample is processed, it can be decreased to  $0.1 \text{ nM h}^{-1}$  (e.g. oligotrophic ocean).

Table 2-3. The precision of NRA in *S. costatum* and natural phytoplankton assemblages (from Chesapeake Bay)

	<i>S. costatum</i>	Natural phytoplankton
Volume of subsample	20 ml	2000 ml
chlorophyll <i>a</i>	> 70 mg m <sup>-3</sup>	4.2 mg m <sup>-3</sup>
Subsample 1	561	7.6
Subsample 2	583	7.4
Subsample 3	561	7.0
Subsample 4	516	7.0
Average	555	7.23
Std.	28	0.34
RSD	5	5

The unit of NRA is nM hr<sup>-1</sup>.

## **Conclusions**

An improved method for the determination of NRA was developed in this research. The sensitivity of this NRA assay is about three and five times higher than that used in Hochman et al. (1986) and in Eppley et al. (1969), respectively. In other words, the volume of sample can be largely reduced by using the modified NRA assay. Furthermore, the improved NRA assay in this study showed a superior reproducibility (RSD = 5 %) than did previous research (RSD = 20 % and 8 % for Eppley et al. (1969) and Hochman et al. (1986)). In addition, this improved NRA assay is less time consuming than that of Eppley et al. (1969) and Hochman et al. (1986), and it can be finished within 1 hour after sampling.

## CHAPTER III

### NITRATE REDUCTASE ACTIVITY IN THE EAST CHINA SEA

#### Introduction

Nitrate reductase activity (NRA) has been widely used for investigating the physiological mechanisms of nitrate uptake and determining the status of eutrophic conditions since Eppley and Coatsworth (1968) first proposed to utilize NRA to study phytoplankton ecology. NRA was suggested to study the rate of nitrate assimilation by Eppley et al. (1969) and Packard et al. (1971), but the successful cases to date are few because the physiological characteristics of NRA are still unclear (Blasco et al., 1984; Berges and Harrison, 1995a). Although it has been suggested that NRA can be used to estimate nitrate uptake under light- and nitrate-replete conditions (Berges and Harrison, 1995; Chapter IV), knowledge about NRA is still poorly understood, particularly the effects of NRA from ambient nutrient concentrations, hydrographic characteristics and changes of light intensity. In order to sufficiently utilize NRA to study nitrate uptake and estimate new production, it is first necessary to understand the influence of environmental factors on NRA.

The East China Sea is a suitable place where the nutrient supply is plentiful (one upwelling system) and variable (from oligotrophic to eutrophic). Thus, the purpose of this chapter is to study how NRA is affected by environmental factors such as light, nutrient concentrations and hydrographic conditions. In addition, the turnover time of nitrate in the upwelling water is also estimated in this region.

## Review of the East China Sea

The East China Sea (ECS) is one of the larger and more productive marginal seas of the world (Fig. 3-1). It is located to the north of Taiwan and bounded on the west by continental China and bounded on the east by the Kuroshio Current. When the Kuroshio Current passes the ECS along the northeast coast of Taiwan, the warm, saline, nutrient-impoverished Kuroshio Surface Water sometimes intrudes onto the shelf due to the topographical effect. The abrupt topographical variations also induce the cold and nutrient-rich Kuroshio Subsurface Water to upwell onto the shelf edge (Chern and Wang, 1990; Chern et al., 1990; Su et al., 1990; Wong et al., 1991; Hsueh et al., 1992; Liu et al., 1992a,b; Chen et al., 1995; Gong and Liu, 1995; Chen, 1996). As a result, a dome-shaped plume of upwelled Kuroshio Subsurface Water has been found at the shelf break northeast of Taiwan (Gong, 1992; Liu et al., 1992a; Gong et al., 1995). However, the phenomenon of upwelling is sometimes suppressed by either shelf water outflow under the southwest monsoon (Gong, 1992) or intrusion of Kuroshio Surface Water (Sun, 1987; Lin et al., 1992; Tang and Yang, 1993; Chuang and Liang, 1994). The East China Sea also receives outflow water from the Changjiang, one of the larger rivers of the world, with a flow rate of  $979 \text{ km}^3 \text{ yr}^{-1}$  (Milliman and Jin, 1985; Zhang, 1996), and Minjiang (Zhang, 1996; Chen, 1997). The outflow of river waters results in the presence of the fresh, cold and nutrient-rich Changjiang Diluted Water along the Chinese coast (Wong et al., 1998). Another source of surface water to the Sea is the Taiwan Current Warm Water which enters the East China Sea through the Taiwan Strait from the south. This water is nutrient poor while its temperature and salinity are slightly lower than those of the Kuroshio Surface Water. Thus, the major

surface water masses in the East China Sea are the Changjiang Diluted Water (CDW), the Taiwan Current Warm Water (TCWW), the Kuroshio Surface Water and the upwelled Kuroshio Subsurface Water (Liu et al., 1992a; Chen et al., 1995).



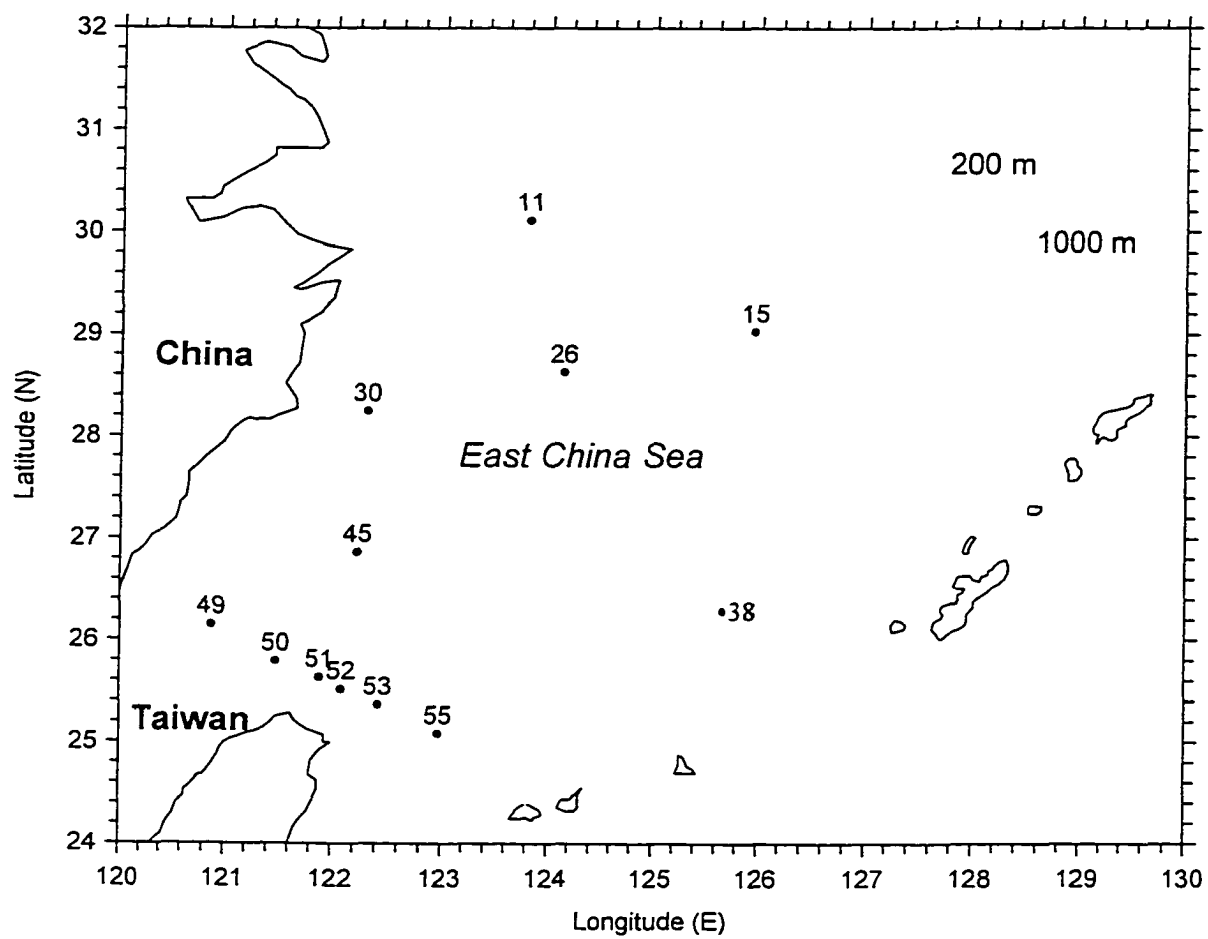


Fig. 3-1. Sampling locations for NRA stations. Sta. 38 is a hydrographic station.

## Materials and methods

Eleven stations were occupied in a transect across the southern East China Sea between May 2 and 15, 1996 aboard the R/V Ocean Research I during Cruise ORI-449 of the Kuroshio Edge Exchange Processes (KEEP) Study. The cruise track and the locations of the stations are shown in Figure 3-1. At each station, the profiles of temperature, salinity and fluorescence were recorded with a SeaBird model SBE9/11 conductivity-temperature-depth (CTD) recorder. Photosynthetically active radiance (PAR) was recorded with a PAR sensor (QSP200L; Biospherical). Discrete water samples were collected with GO-FLO bottles mounted onto a Rosette sampling assembly (General Oceanic). Sub-samples were then obtained for the determination of salinity, nitrite and (nitrate plus nitrite).

Sub-samples were transported to the shore based laboratory for the determination of salinity with an Autosal salinometer with a precision of  $\pm 0.003$ . Nitrite and (nitrate plus nitrite) were determined on board a ship by the standard pink azo dye method which has been adapted for use with a flow injection analyzer (Morris and Riley, 1963; Strickland and Parsons, 1972; Gardner et al., 1976; Pai et al., 1990; Gong, 1992; Liu et al., 1992a,b). The precision for the determination of nitrate and nitrite was 1% at 10 to 20  $\mu\text{M}$  levels. The detection limits for nitrite and nitrate were 0.05 and 0.1  $\mu\text{M}$ , respectively.

Sub-samples were obtained at 11 stations for the determination of chlorophyll *a* (chl *a*) and NRA. Chl *a* was determined by the method of Strickland and Parsons (1972) and Gong et al. (1993). The detailed procedures were similar to the previous analysis of chl *a* in Chapter VI.

Nitrate reductase activity was determined on board a ship by a slight modification of the method of Hochman et al. (1986). Seawater (20 liters at Sta. 55 and 4 to 8 liters at the other stations) was collected at Stations 11, 15, 26, 30, 45, 49, 52, 53 and 55 during the day, and at Sta. 50 and 51 after sunset. The samples collected during the day were immediately filtered through 47 mm Gelman Type A/E glass fiber filters. The samples collected after sunset were stored in a polyethylene bottle on the deck and then determined the next morning. The filter was transferred to a beaker together with 1 ml of a phosphate buffer (150 mM of  $K_2HPO_4$ , adjusted to a pH of 7.6), 50  $\mu$ M of toluene, 0.2 ml of 6.5 mM NADH (Sigma Chemical Co.) and 0.2 ml of 0.1 M potassium nitrate. The beaker was placed on a vortex mixer and mixed for 5 min at room temperature ( $\sim 20^\circ C$ ). Then, the reaction was terminated by pipetting 1 ml of the slurry from the beaker into a centrifuge tube containing 1.7 ml of 0.13 M  $ZnSO_4$  at  $97^\circ C$ . After the solution was allowed to cool, 0.2 ml of 1 N NaOH was added and the mixture was centrifuged for 20 min at 4000 rpm. Two ml of the supernatant liquid was removed for the determination of nitrite by adding 0.1 ml of a 2 % (w/v) N-1-naphthylethylenediamine hydrochloride solution to the supernatant liquid and measuring the absorbance of the azo dye formed at 545 nm (Strickland and Parsons, 1972) with a Brinkman PC-800 Probe Colorimeter equipped with a probe tip with a 2-cm light path. The precision in repeated determination of NRA in a sample was  $\pm 5\%$ . Since nitrite could be detected down to about 0.1  $\mu$ M, the corresponding detection limits for the determination of NRA would be 0.4 and 0.1 nM-N  $hr^{-1}$  when 5 and 20 liters of sample were processed respectively. The procedural blank of the method included the reagent blank and the blank due to the presence of intra-cellular nitrite. The reagent blank

corresponded to 0.03 and  $<0.01$  nM-N hr<sup>-1</sup> when sample volumes of 5 and 20 liters were used. The presence of intra-cellular nitrite gave rise to a blank that corresponded to NRA of 0.2 nM-N mg chl-a<sup>-1</sup> m<sup>3</sup>. The results reported here have been corrected for these blanks.

## **Results and discussions**

### *Distributions of water masses in the East China Sea*

The properties of temperature and salinity at all study stations are shown in Fig. 3-2. Sta. 38 represents typical Kuroshio water with its highest temperature and highest-salinity. About five major surface water masses were clearly identified in this study area. The coldest, freshest and nutrient-rich Changjing Diluted Water (CDW; Gong, 1992; Liu et al., 1992b; Gong et al., 1995; Wong et al., 1998) was observed at Sta. 30. The cold, high salinity and nutrient rich upwelled Kuroshio Subsurface Water (UKSW) was found at the shelf edge near the northeastern tip of Taiwan (Stations 51, 52 and 53, Wong, et al., 1991; Liu et al., 1992a, 1992b); the warm and nutrient-poor Kuroshio Surface Water (KSW) with highest salinity was observed at Sta. 55. A cold Coastal water (CW) with intermediate salinity was found at Sta. 49. Warm nutrient deplete Taiwan Current Warm Water (TCWW) with high salinity might be presented at Sta. 50. The characteristics of Stations 11, 15, 26 and 45 were different from the above water masses. Stations 11, 26 and 45 were located at the seaward frontal region between the CDW and Kuroshio water, while Sta. 15 was located at the shelf-ward frontal zone of the Kuroshio.

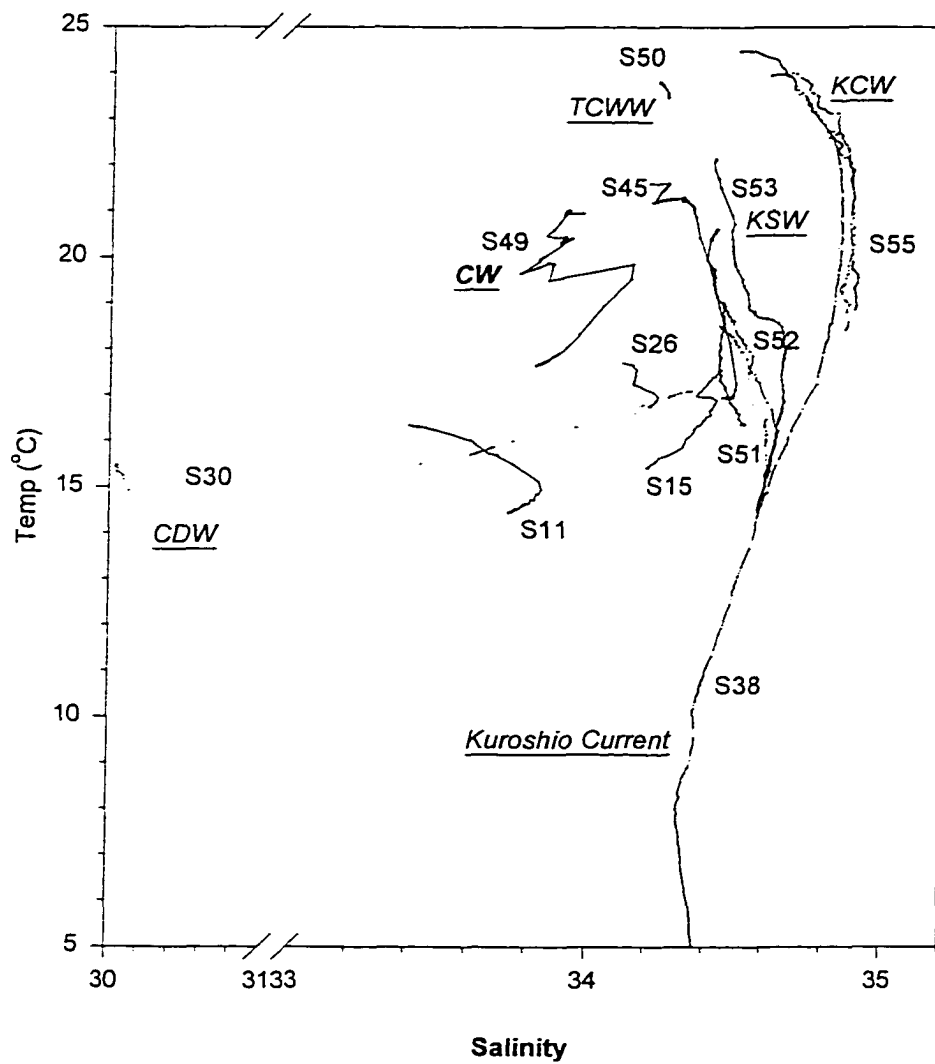


Fig. 3-2. The relationship between temperature and salinity at all stations.

*Depth distributions of NRA in the East China Sea*

The depth distributions of NRA and relevant hydrographic data in the study area are shown in Figures 3-2 to 3-7. The detailed data of NRA and relevant hydrographic data are shown in Appendix C. The mixed layer depth (MLD) is the depth at which the density gradient increased by a factor of 2 or higher. The photic zone depth (PZD) represents the depth of %PAR (photosynthetically active radiance) from surface layer to 1% of PAR%. Both MLD and PZD are indicated in the figures. The hydrographic properties and NRA in the mixed layer at different water masses are summarized in Table 3-1. The detailed data are shown in Appendix C. NRA in the coastal area (Stations 15 and 30) showed the shallow subsurface maximum, and their activities decreased with depth to background level below the PZD. NRA in the upwelling zone (Stations 51, 52 and 53), in coastal water (Sta. 49) and at Stations 11, 50 and 51 exhibited a surface maximum, and NRA gradually decreased to background level below the PZD excluding Sta. 49. NRA gradually decreased to a low level at a depth of 25 m above the PZD.

Low NRA was found in the surface layer in the oligotrophic ocean (Stations 55-3 and 55-5) and its activity increased with increasing depth to a subsurface maximum between 70 and 90 m. The distribution of NRA roughly parallels that of chl *a*. Similarly, observable NRA was found at a depth below the PZD mirroring the behavior of chl *a*.

The vertical distribution of NRA within the mixed layer was roughly uniform in the frontal area between the coastal plume and Kuroshio water (Sta. 26). The distribution of NRA above the PZD was similar to that of chl *a*. Although the observable NRA was still observed below the PZD, it quickly dropped to background levels at slightly greater depths.

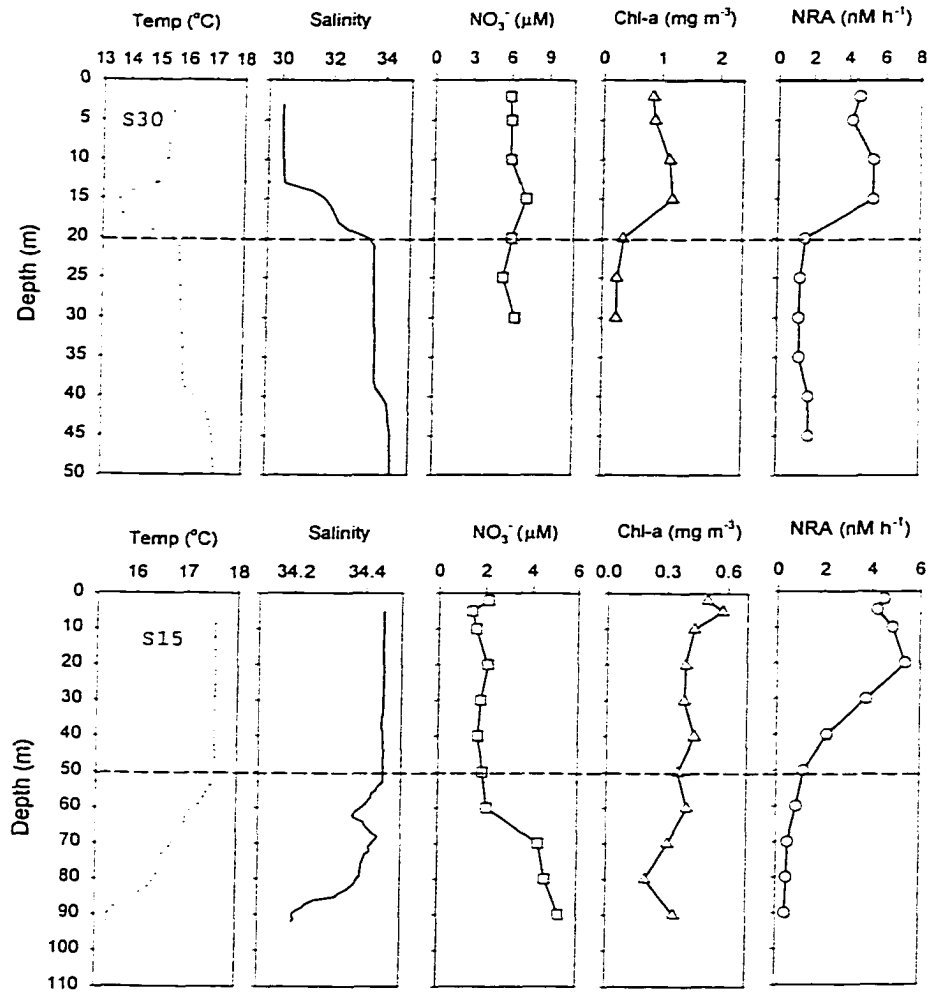


Fig. 3-3. The depth profiles of hydrographic data and NRA at Sta. 30 (upper panel) and Sta. 15 (lower panel). Horizontal dotted line represents the MLD. Horizontal broken line represents the PZD.

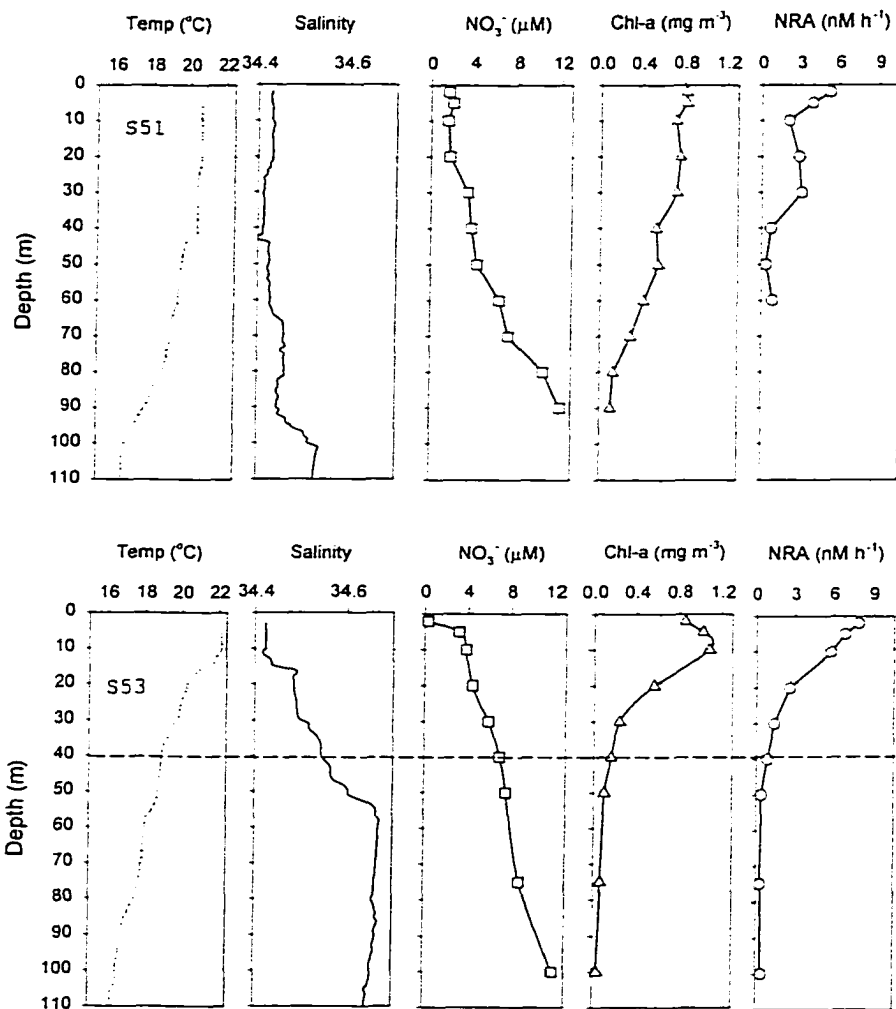


Fig. 3-4. The depth profiles of hydrographic data and NRA at Sta. 51 (upper panel) and Sta. 53 (lower panel). Horizontal dotted line represents the MLD. Horizontal broken line represents the PZD.



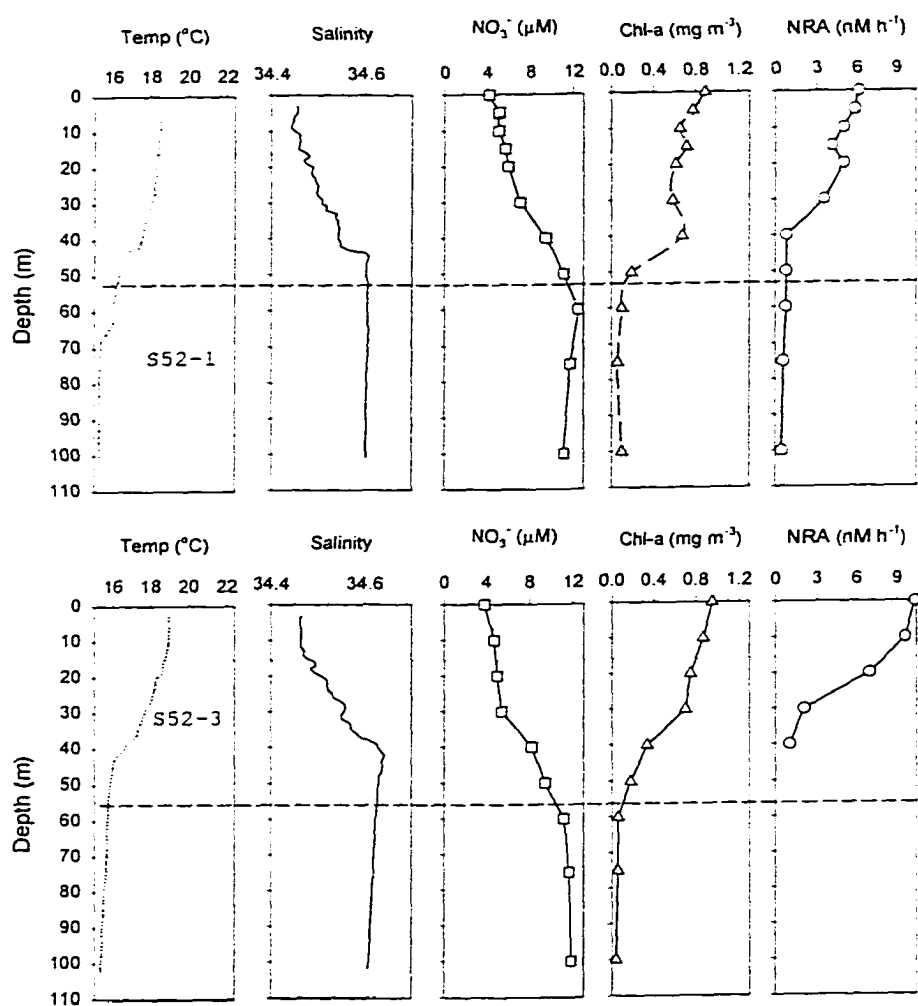


Fig. 3-5. The depth profiles of hydrographic data and NRA at Sta. 52-1 (upper panel) and Sta. 52-3 (lower panel). Horizontal dotted line represents the MLD. Horizontal broken line represents the PZD.

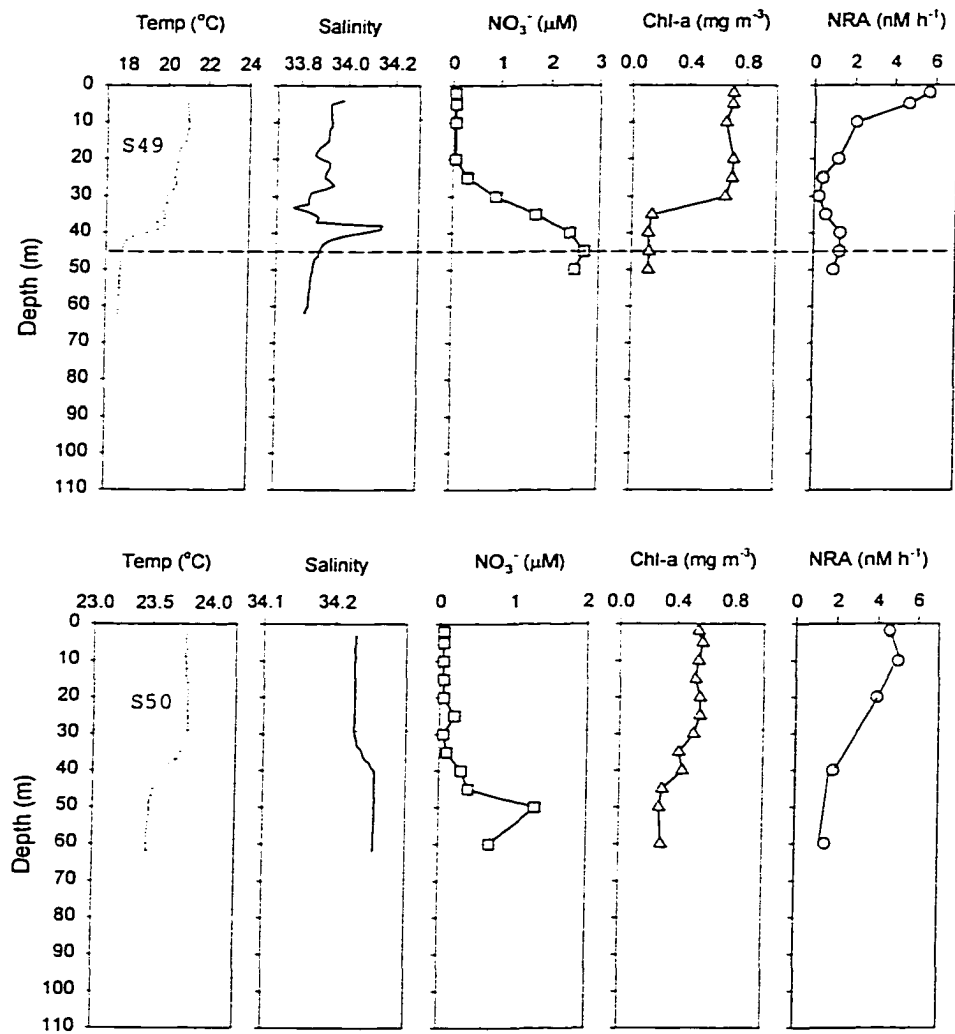


Fig. 3-6. The depth profiles of hydrographic data and NRA at Sta. 49 (upper panel) and Sta. 50 (lower panel). Horizontal dotted line represents the MLD. Horizontal broken line represents the PZD.

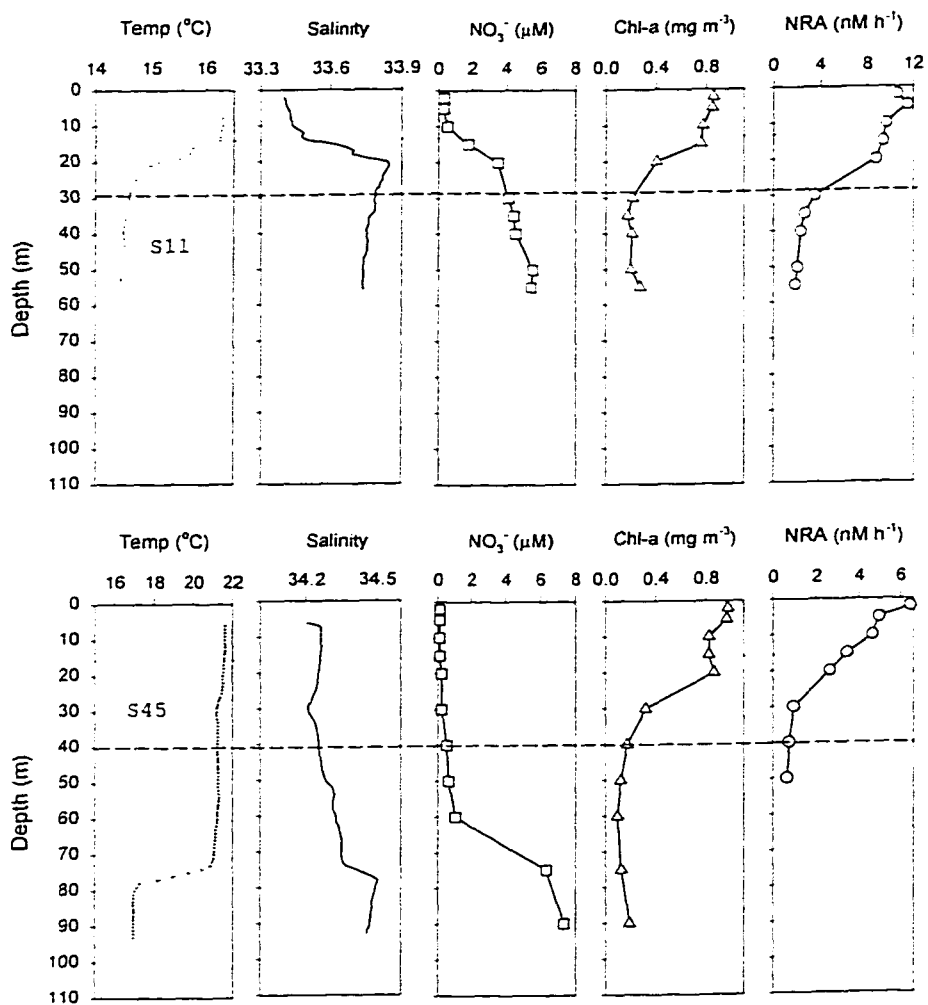


Fig. 3-7. The depth profiles of hydrographic data and NRA at Sta. 11 (upper panel) and Sta. 45 (lower panel). Horizontal dotted line represents the MLD. Horizontal broken line represents the PZD.

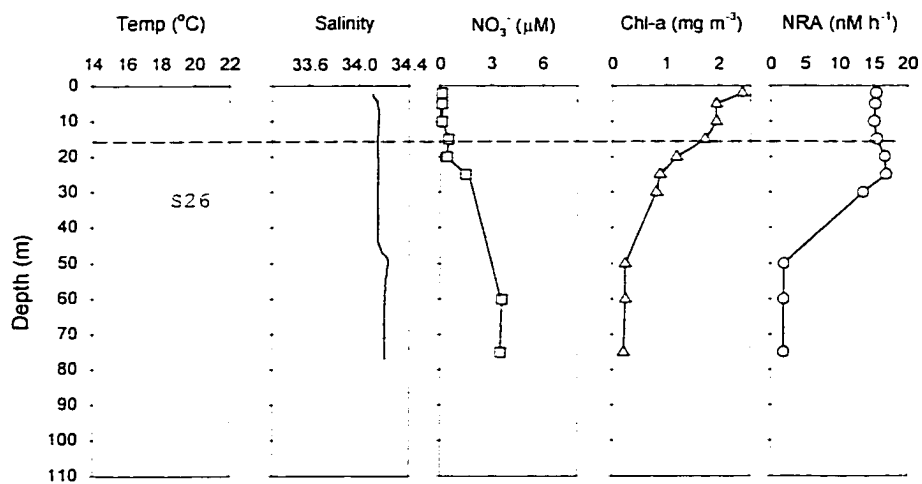


Fig. 3-8. The depth profiles of hydrographic data and NRA at Sta. 26. Horizontal dotted line represents the MLD. Horizontal broken line represents the PZD.

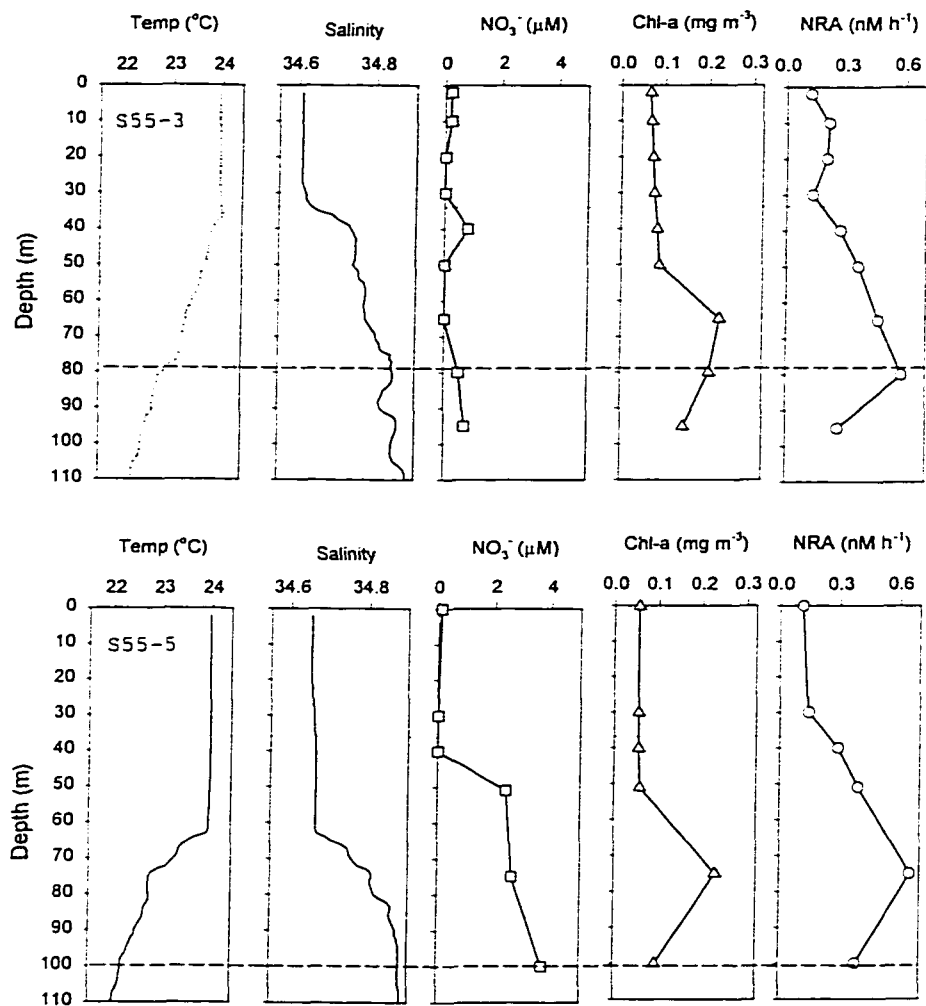


Fig. 3-9. The depth profiles of hydrographic data and NRA at Sta. 55-3 (upper panel) and Sta. 55-5 (lower panel). Horizontal dotted line represents the MLD. Horizontal broken line represents the PZD.

*Table 3-1. Properties of the waters in the mixed layer of the different hydrographic regimes of the East China Sea*

Hydrographic Regimes	Sta	MLD m	PZD 1%	S	T °C	NO <sub>3</sub> <sup>-</sup> μM	Chl-a mg m <sup>-3</sup>	NRA nM h <sup>-1</sup>	I-chl a 1%	I-NRA 1%
In coastal plume	30	13	20	30.1	15.4	6.0	0.96	4.7	21.9	103
Shelf/Kuroshio frontal region	15	52	50	34.4	17.5	1.8	0.43	3.7	21.3	196
Upwelling	51	5	nd	34.4	20.6	1.3	0.81	4.6	22.5	111
	53	10	40	34.5	22.1	2.4	0.98	6.8	22.2	141
	52-1	15	40	34.5	18.5	4.8	0.77	5.3	26.7	168
	52-3	15	55	34.5	18.7	4.3	0.90	10.0	29.6	243
Coastal plume/ shelf front region TCWW	11	12	29	33.4	16.3	0.4	0.83	10.6	18.1	261
	49	5	45	33.9	20.9	0.0	0.70	5.1	23.6	78
	50	30	nd	34.2	23.8	0.0	0.55	4.6	16.4	56
Shelf	26	3	19	34.1	17.7	0.1	2.44	15.4	37.3	308
	45	15	40	34.2	21.5	0.1	0.90	4.9	26.0	105
Kuroshio	55-3	33	78	34.6	23.9	0.0	0.07	0.17	9.2	25
	55-3	35	100	34.6	24.0	0.0	0.06	0.13	10.3	35

MLD - Mixed layer depth;

PZD 1%: photic zone depth to 1% of %PAR; I-NRA 1%: integrated NRA to 1% of PAR;

nd - no data; TCWW: Taiwan current warm water.

The NRA distributions in these different hydrographic regimes can be roughly divided into four types: (1) type A: NRA shows a shallow subsurface maximum (10 to 15 m) at Stations 15 and 30; (2) type B: NRA shows a surface maximum in the upwelling zone (Stations 11, 45, 49, 50, 51, 52-1, 52-3 and 53); (3) type C: NRA shows an almost uniform distribution within the mixed layer at the Station 26 while NRA was still detectable below the PZD (4) type D: NRA shows a deep subsurface maximum (60 to 90 m) in the oligotrophic ocean (Stations 55-3 and 55-5);

With respect to type A, it is difficult to explain the shallow subsurface maximum at Stations 15 and 30. Theoretically, maximum NRA should occur in the surface layer because light and nitrate ( $4-8 \mu\text{M}$ ) are not limiting while the maximum NRA was found at depths of 10 to 15 m rather than in the surface layer. Three possibilities may be used to explain this result: (1) high biomass in the shallow subsurface layer; (2) phytoplankton uptake of other nitrogen sources ( $\text{NH}_4^+$ ); and (3) deficiency of phosphoric acid in the surface layer. The appearance of  $\text{NH}_4^+$  will suppress the formation of NRA. Neither  $\text{NH}_4^+$  nor DON was measured in this study, but a plume of high  $\text{NH}_4^+$  is often observed in Changjiao Diluted water (Edmond, 1985). Consequently, higher  $\text{NH}_4^+$  in the surface layer higher than in the subsurface layer could help to explain the maximum NRA in the subsurface layer. Another possibility may be from phosphorous deficiency in the surface layer ( $\text{NO}_3^-/\text{PO}_4 = 120$  to 180) because phytoplankton need ATP to transport external  $\text{NO}_3^-$  to internal  $\text{NO}_3^-$  passing through cell membranes (Solomonson and Barber, 1990; Wada and Hattori, 1991). Once the phosphate becomes limiting, the transport of  $\text{NO}_3^-$  from outside to inside of cell will be reduced. As a consequence, NRA may be inhibited due to interior nitrate deficiency

in cells. Collos and Slawyk (1977) and Dortch et al. (1979) suggested that NR is induced by internal nitrate concentration rather than external concentrations. Thus, low NRA could be found in the surface layer under high-nitrate and low-phosphoric conditions. Conversely, the ratio of  $\text{NO}_3^-/\text{PO}_4$  decreased from 20 to 60 in shallow subsurface layer (10 to 15 m). This suggests that phosphoric acid is a significant factor affecting the production of NRA. Below the subsurface layer, the ratio of  $\text{NO}_3^-/\text{PO}_4$  decreased to 16, but the light became a limiting factor.

For type B, the surface maximum NRA in upwelling water and at Sta. 45 can be interpreted as follows: When a cold and nitrate rich water was introduced into the surface layer by an upwelling event, originally, the use of nitrate by phytoplankton is low due to the low autotrophic biomass and unstable conditions (cold and light-deplete). When the phytoplankton are kept transporting to the surface layer, the upwelled water is gradually stabilized under a well-lit environment which results in the nitrate being readily assimilated by phytoplankton. Thus, NRA is readily induced in the upper layer more than in the deep layer. However, the concentration of nitrate in the surface layer at Stations 11, 49 and 50 was almost exhausted, but the surface maximum NRA were found at these stations. One possibility which might explain this phenomenon is that NRA is induced by the internal nitrate from cells (Collos and Slawyk, 1977; Dortch et al., 1979). Thus, NRA still can be induced even though the concentration of ambient nitrate is low.

For type C, NRA showed an approximate uniform distribution within the mixed layer at Sta. 26. The uniform distribution of NRA in this frontal region could be explained by the vertical mixing of water masses or the vertical migration of phytoplankton. In



addition, the higher NRA around the PZD could be a memory of a previous sunny conditions. With respect to type D, it occurs where the PZD is deepest in the study area. In addition, nitrate in the surface layer at the oligotrophic site is almost exhausted and little nitrate diffuses to the subsurface layer from the deep ocean. NRA is low in surface layer due to nitrate limitation, and maximum NRA is found in the subsurface when appropriate light and nutrient support co-exist. In the upwelling system, the level of NRA in the oligotrophic area is one order of magnitude lower than that in the upwelling. With respect to the observable NRA below the PZD, the distribution of NRA is similar to that of chl *a* in the subsurface water (70 to 120 m) because the penetration depth of light is dependent on the intensity of surface light and the characteristics of water.

#### *Distribution of NRA in the transect*

The section of NRA in the transect is shown in Fig. 3-10a. The isolines of NRA rose steadily from the inner shelf to the upwelling region and then rose to the maximum level near the area between the upwelling region (Sta. 53) and the oligotrophic ocean (Sta. 54). For example, at inner shelf Sta. 50, the isoline of  $2 \text{ nM-N h}^{-1}$  was found at a depth of 40 m, while at upwelling Sta. 53 it was found at 25 m and at Sta. 54 at a depth of about 20 m. However, this upward trend of the NRA isolines was different from the isolines of nitrate (Fig. 3-11), but was similar to the trend of chl *a* isolines (Fig. 3-12). Furthermore, the isoline of highest NRA ( $> 6 \text{ nM-N h}^{-1}$ ) was found in the surface water of the upwelling region (Stations 51, 52 and 53), and the intermediate NRA ( $\sim 3 \text{ nM-N h}^{-1}$ ) was spread throughout the surface water in the shelf (Stations 49 and 50). The lowest NRA ( $< 0.3 \text{ nM-N h}^{-1}$ )

$\text{N h}^{-1}$ ) was found at the surface and the maximum NRA ( $0.5 \text{ nM-N hr}^{-1}$ ) appeared in the subsurface in the Kuroshio Current (Sta. 55). The spatial distribution of NRA seemed related to the trend of chl *a* suggesting that higher nitrate uptake occurred in adjacent waters of the upwelling center rather than in the upwelling center.

The section of S-NRA is shown in Fig. 3-10b. The high S-NRA clusters occurred in the surface layers of Stations 51 and 53, while the S-NRA in the surface layer at Sta. 52. was much lower than that at Stations 51 and 53. The discrepancy between these waters may reflect a "shift-up" hypothesis that the phytoplankton assemblage undergoes an acceleration from low specific rates of nitrate utilization up to higher rates (MacIsaac et al., 1985; Zimmerman et al., 1987; Garside, 1991). The results suggest that S-NRA may be a potential tool for studying the physiological mechanism of nitrate uptake (Blasco et al., 1984).

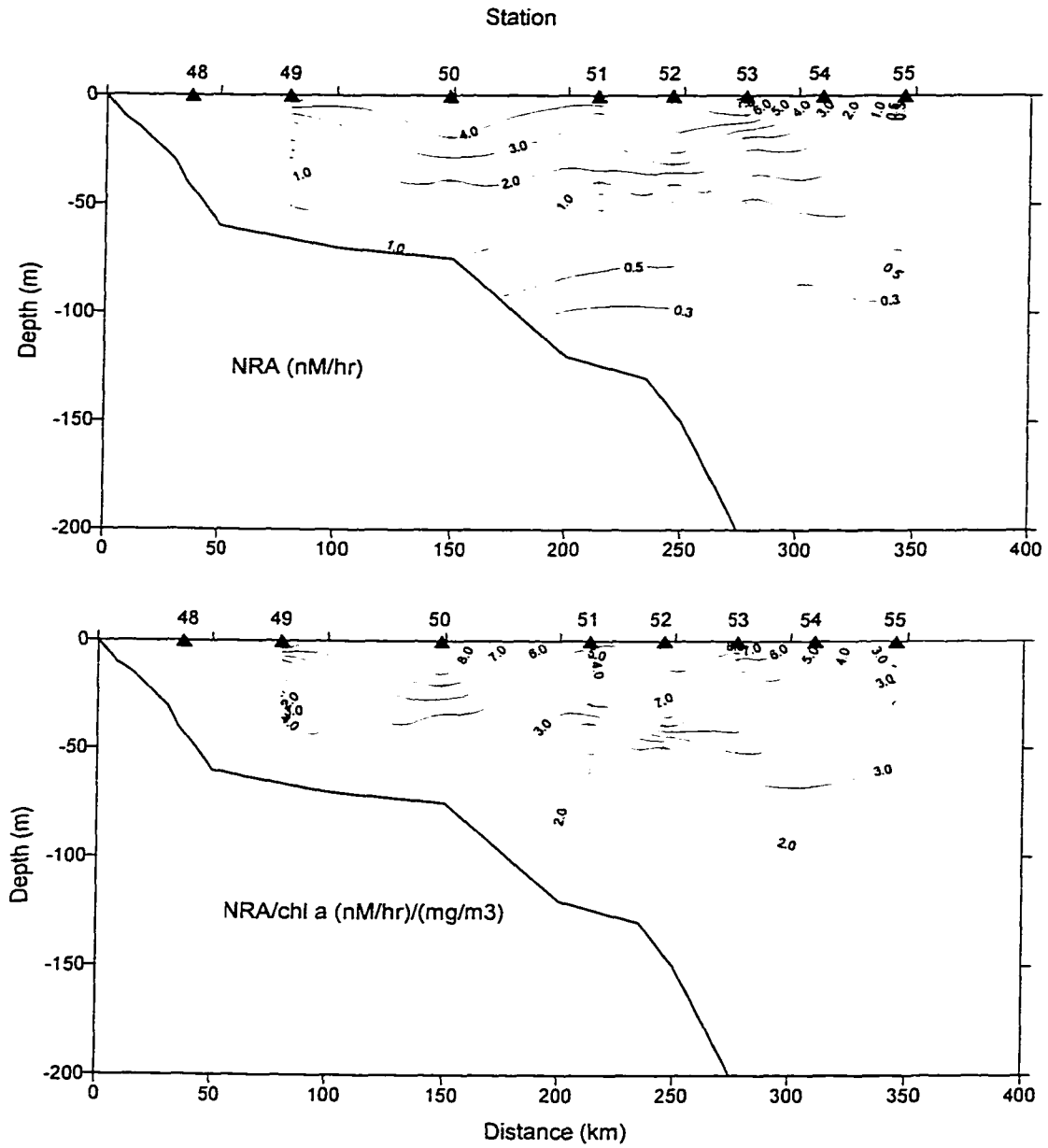


Fig. 3-10. (a) The distribution of NRA in the Stations 48-55 transect (upper panel).

(b) The distribution of S-NRA in the Stations 48-55 transect (lower panel).

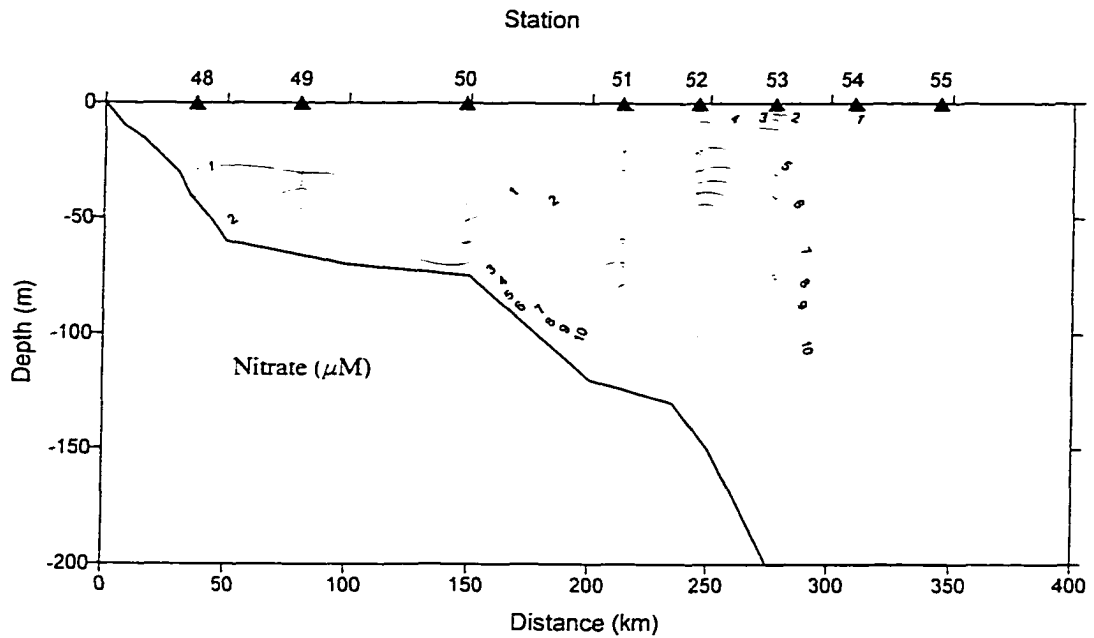


Fig. 3-11. The distribution of nitrate in the Station 48-55 transect.

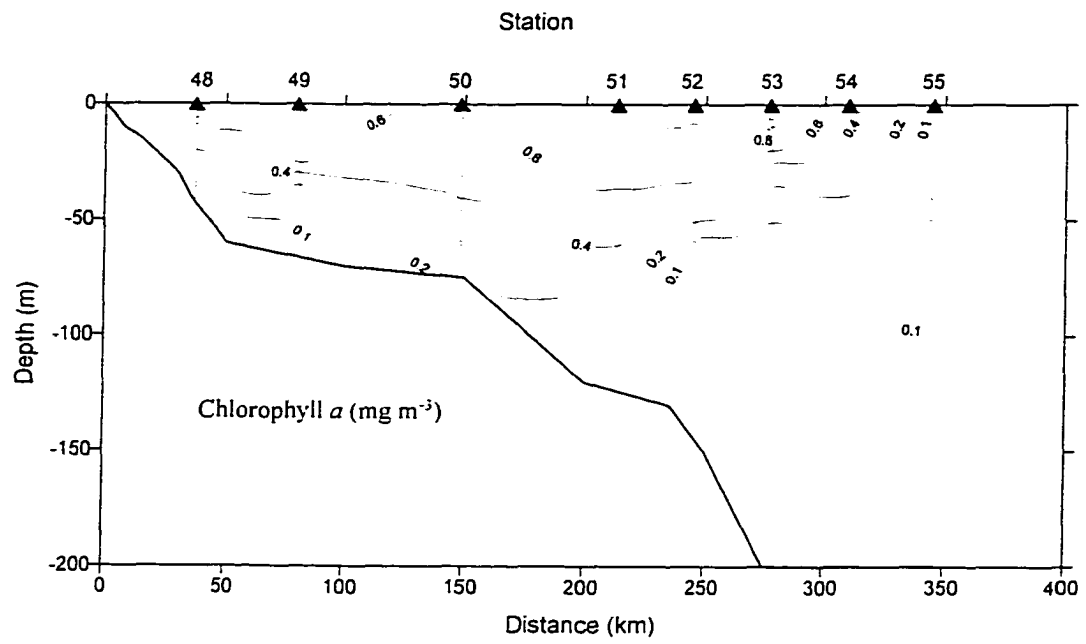


Fig. 3-12. The distribution of chlorophyll  $a$  in the Station 48-55 transect.

*Turnover time of nitrate in the transect*

In order to accurately estimate the nitrate transport into the East China Sea by the upwelling water of Kuroshio, the turnover time of the upwelling water must be determined. Assuming nitrate uptake (expressed as NRA) is the principle process controlling ambient nitrate concentration in the upwelling waters, at a steady state, the turnover time of nitrate ( $\tau\text{-NO}_3^-$ ) in the upwelling waters can be calculated by following equation:

$$\tau_{\text{NO}_3^-} = \frac{[\text{NO}_3^-]}{\frac{d\text{NO}_3^-}{dt}} = \frac{[\text{NO}_3^-]}{\text{NRA}}$$

where  $[\text{NO}_3^-]$  is the nitrate concentration and  $d\text{NO}_3^-/dt$  (or NRA) is the rate of nitrate uptake by phytoplankton within the  $\text{PZD}_{10}$ .  $\tau\text{NO}_3^-$  is the turnover time of nitrate which is controlled by nitrate input and nitrate consumption in the upwelling system. The contour of estimated  $\tau\text{NO}_3^-$  in the transect is shown in Fig. 3-13. In general, the turnover time increased with depth with 30 days in the surface layer and quickly increased to several hundred days in the subsurface. A short turnover time was found in the upwelling area of about 30 days and the shortest turnover time ( $< 10$  days) was found in the coastal region (Sta. 49 and 50). The short  $\tau\text{NO}_3^-$  in the former was caused by high productivity while the shortest  $\tau\text{NO}_3^-$  in the latter was caused by little supply of nitrate. The longer  $\tau\text{NO}_3^-$  was always found in the deepest depth suggesting that the consumption of nitrate is very little due to low phytoplankton biomass, low light and a high concentration of nitrate.

The estimates of  $\tau\text{NO}_3^-$  within  $\text{PZD}_{10}$  in the upwelling water are shown in Table 3-2. The shortest  $\tau\text{NO}_3^-$  (37 and 28 days) occurred at the edge of the upwelling water (Stations 51 and 53) while the longest  $\tau\text{NO}_3^-$  (83 and 43 days) were observed near the

center of upwelling waters (Stations 52-1 and 52-3). These results suggest that phytoplankton can take up nutrients more effectively in aged upwelled waters than in newly upwelled waters because aged upwelled waters contain more autotrophic biomass than newly upwelled waters. In addition, the water in aged upwelled waters was more stable than in newly upwelled waters. Analogous results have been described from numerous upwelling systems (MacIsaac et al., 1985; Dugdale and Wilkerson, 1989; Wilkerson and Dugdale, 1987; Dugdale et al., 1990).

The turnover time of upwelling water was estimated at  $20 \pm 10$  days using the dissolved oxygen mass balance approach (Liu et al., 1992b). In addition, the turnover time was also estimated to be one month from an examination of the dissolved inorganic iodine system (see Chapter V). Thus, the turnover time calculated in this work for the upwelling system compares well with previous estimates.

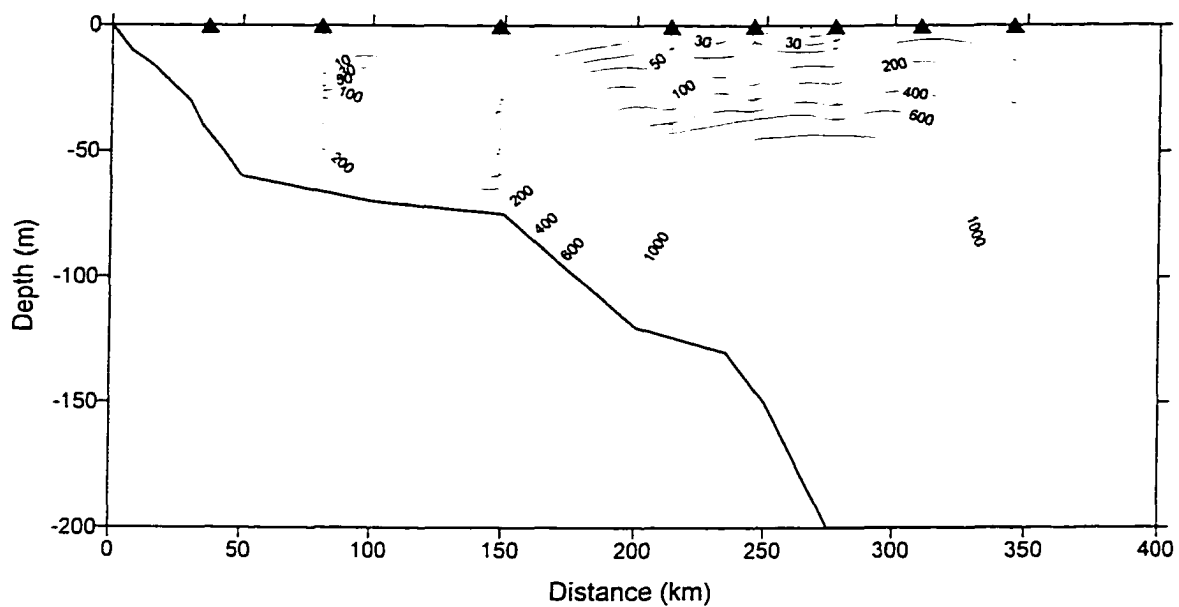


Fig. 3-13. The distribution of turnover time (day) of nitrate in the transect.



*Table 3-2. The turnover time of nitrate in the upwelling water of southern East China Sea*

Station	PZD <sub>10</sub> (m)	*NO <sub>3</sub> <sup>-</sup> (μM)	*NRA (nM-N h <sup>-1</sup> )	Turnover Time (day)
51	17	1.7	3.8	37
52-1	18	5.0	5.0	83
52-3	25	4.5	8.8	43
53	19	2.4	7.1	28

\*- average amount within PZD<sub>10</sub>.

*The relationship between specific NRA and PAR*

The relationship between PAR and chl *a* specific NRA (S-NRA) is shown in Fig. 3-14 where S-NRA was almost linear with PAR for weak light intensities, and S-NRA then increased to a maximum value when PAR was higher than  $80 \mu\text{E m}^{-2} \text{s}^{-1}$  at stations 11 and 45, excluding Sta. 52-3 in which the saturated PAR was about  $300 \mu\text{E m}^{-2} \text{s}^{-1}$ . The result demonstrates that light is a limiting factor for nitrate reduction under low light intensity. There was no photoinhibition in the relationship between S-NRA and PAR under high intensity of light. The maximum value of S-NRA ranged from 5.8 to 12.9 mmol-N mg chl  $\alpha^{-1} \text{h}^{-1}$ . However, in Fig. 3-15, S-NRA at low PAR conditions seemed to have higher value than high PAR conditions suggesting that nitrate is a limiting factor under high light intensity. The relationship between S-NRA and PAR at Fig. 3-14 was similar to a P-I curve (photosynthesis verse irradiance) so that it can be expressed as following equation:

$$S - NRA = NRA_{\max} \times (1 - e^{-S \times PAR / NRA_{\max}})$$

where  $NRA_{\max}$  represents the highest specific NRA when PAR is high; S is the initial slope of specific NRA and PAR; PAR is the intensity of light. The curve fitting was conducted using a non-linear regression program (Sigma Plot) to calculate the  $NRA_{\max}$  and S. The derived curves fitted with the observed data well suggesting that specific NRA can be a tool to estimate new production in the same way as a P-I curve was utilized to estimate primary production (Platt et al., 1980, 1988, 1992; Harrison et al., 1985; Sathyendranath et al., 1995). However, additional work is required to understand the relationship between specific NRA and PAR.

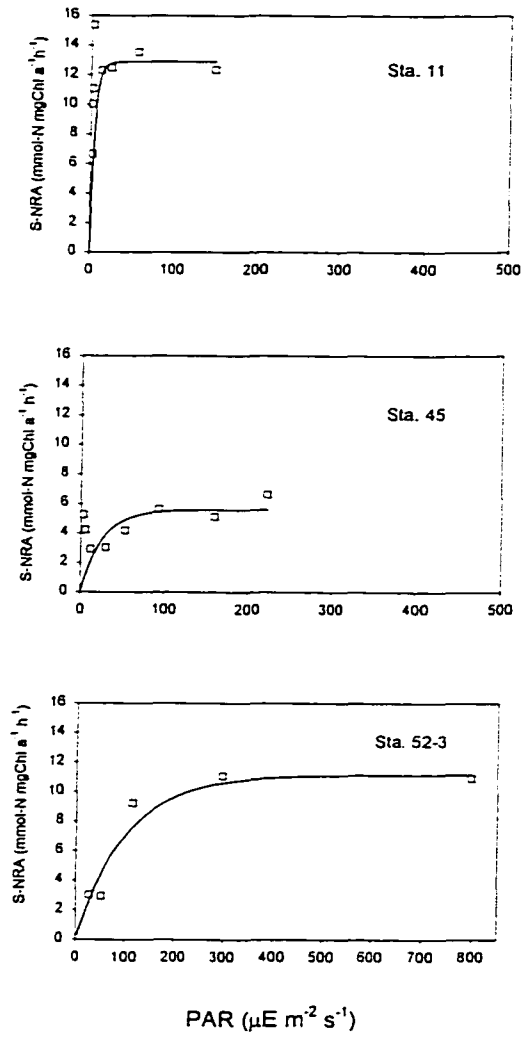


Fig. 3-14. The relationship between S-NRA and PAR at different stations.

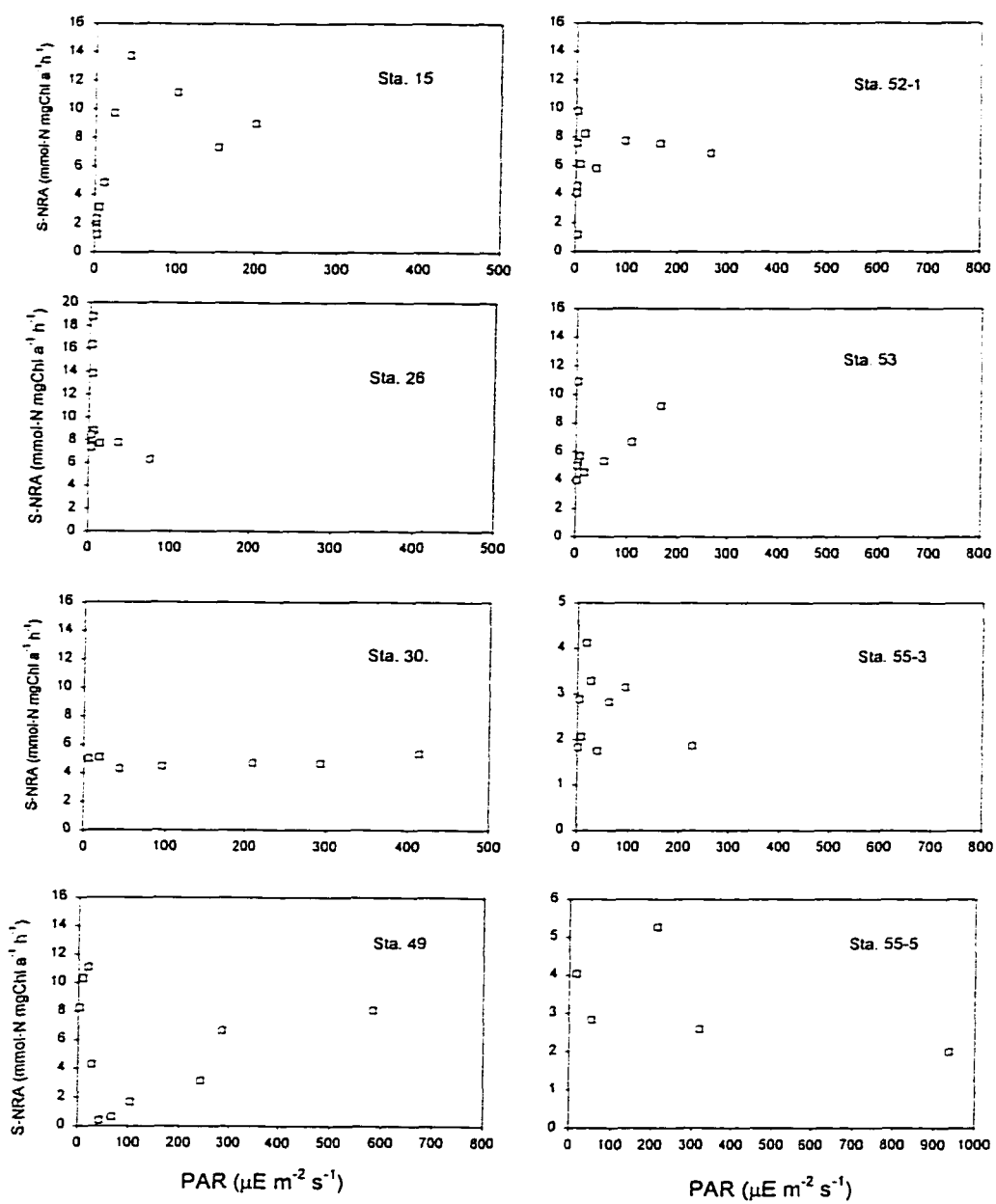


Fig. 3-15. The relationship between S-NRA and PAR at different stations.

*The relationship between nitrate concentration and specific NRA*

The relationships between the concentration of nitrate and chlorophyll specific NRA (S-NRA) in upwelling areas (Stations 51, 52 and 53) are shown in Fig. 3-16. In the Fig. 3-16, the S-NRA was almost reversely proportional to nitrate concentration in upwelling regions with high S-NRA at low nitrate concentration and low S-NRA at high nitrate concentrations. The result indicates that S-NRA was high under well-lit and nitrate-replete conditions while S-NRA was low even though the concentration of nitrate reached 8 to 12  $\mu\text{M}$  where phytoplankton was little due to the lack of light. The result also suggested that light is a limiting factor for NRA at deep depth where nitrate is replete. This coupling relationship between nitrate concentration and specific NRA can be used in estimating NRA by measuring chl *a* and nitrate in upwelling regions. However, as shown in Fig. 3-17, the relationship between the concentration of nitrate and S-NRA shows a random distribution, suggesting that phytoplankton utilize other nitrogen sources other than nitrate.

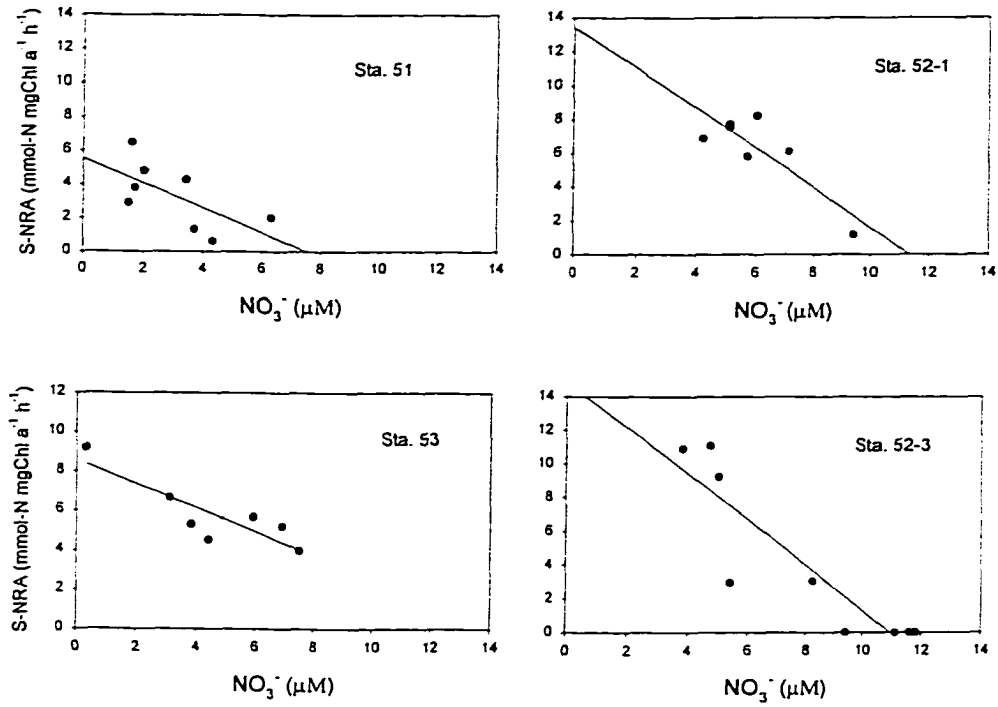


Fig. 3-16. The relationship between S-NRA and concentration of nitrate in upwelling areas (Stations 51, 52 and 53).

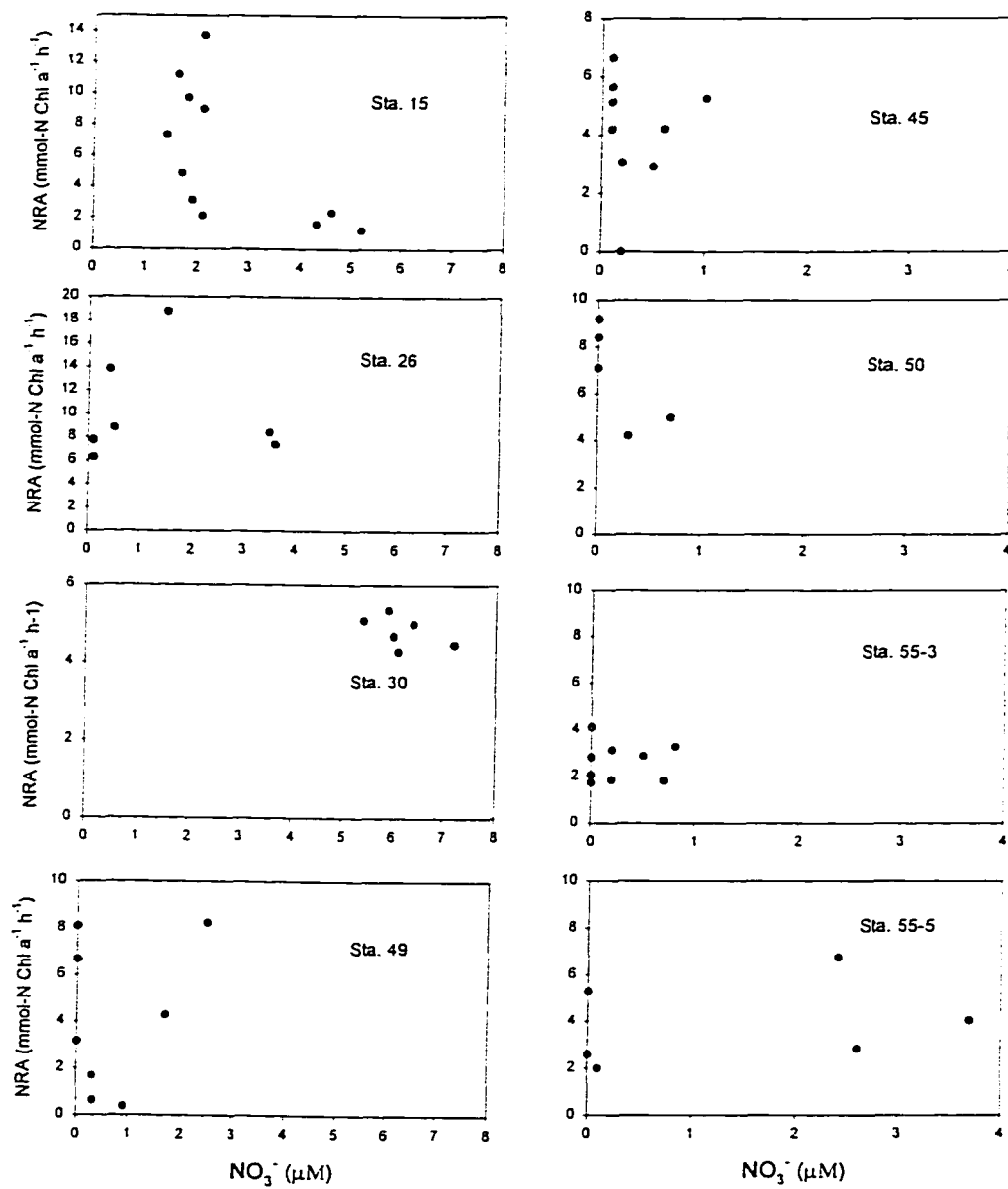


Fig. 3-17. The relationship between S-NRA and concentration of nitrate at different stations.

*The relationship between NRA and chlorophyll  $a$*

The relationship between integrated NRA (I-NRA) and integrated chlorophyll  $a$  (I-chl  $a$ ) within the photic zone where % PAR exceeded 1% at all the stations is shown in Fig. 3-18. In the Fig. 3-18, I-NRA is roughly proportional to the I-NRA so that

$$\text{NRA} = -49(\pm 56) + 8.7(\pm 2.4)\text{chl } a, r^2 = 0.53.$$

The intercept is close to zero according to statistical uncertainty, and the slope of the line is about 8.7. This result demonstrates that the production of NRA is totally from phytoplankton cells although some data points escaped from the best regression line. In other words, the higher the phytoplankton biomass, the higher the NRA. Once the relationship between NRA and chl  $a$  can be established, NRA can be readily estimated by measuring the chlorophyll  $a$ , multiplying the relationship between them. This approach is better used in dark conditions because NRA is difficult or impossible to measure at night. Thus, more research is required to understand the relationship between NRA and chlorophyll  $a$ .



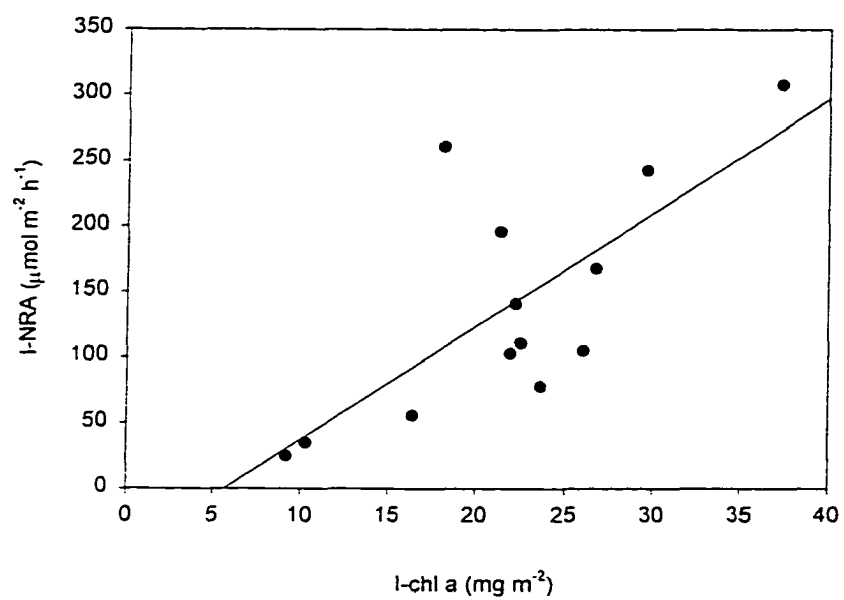


Fig. 3-18. The relationship between I-NRA and I-chl  $a$  at all stations.

## Conclusions

NRA showed a surface maximum in the upwelling area when the concentration of nitrate was high in the surface layer and light was abundant. NRA showed a sub-surface maximum level in coastal areas where NRA in the surface layer may be inhibited by other nitrogen sources (ammonium or DON). NRA in the strong vertical mixing area showed a uniform distribution above the mixed layer. NRA may be significantly underestimated or over estimated when water masses are well mixed and the intensity of light is weak during the sampling time. NRA in the oligotrophic oceans showed a deep sub-surface maximum suggesting that nutrient is a limiting factor at this depth.

NRA in the upwelling system can be used to study the physiology of phytoplankton for nitrate uptake because it can quickly reflect the rate of nitrate uptake. In addition, a good relationship between S-NRA and PAR was found in this study, suggesting that NRA can be estimated by chlorophyll *a* and light intensity. The turnover time (3 to 57 days, the average being 29 days) in the surface layer in upwelling regions estimated by the NRA system suggests that this estimation is similar to other approaches.

## CHAPTER IV

### THE EFFECTS OF LIGHT AND NITRATE LEVELS ON THE RELATIONSHIP BETWEEN NRA AND $^{15}\text{NO}_3^-$ UPTAKE: FIELD OBSERVATIONS IN THE EAST CHINA SEA

#### Introduction

The determination of new production using the  $^{15}\text{NO}_3^-$ -labeling technique suffers from a variety of limitations. Although nitrate reductase activity (NRA) has been suggested to be a promising tool for measuring new production, the successful cases are few. The reasons for failure are complicated, may arise from two major factors: (1) the previous NRA assays respond inadequately the real NRA; and (2) the effects of environmental variations in nutrients, light and hydrography on NRA and new production were not taken into appropriate consideration. However, it is very difficult to distinguish between these possibilities because they are intertwined with each other. In chapter two, an improved NRA assay has been developed for the determination of NRA. The goal of this chapter is to examine the possibility of estimating nitrate uptake by using an improved NRA approach.

Because major investigations concerning the relationship between NRA and  $^{15}\text{NO}_3^-$  uptake (NU) were conducted in upwelling areas (Eppley et al., 1970; Collos and Slawyk, 1977; Blasco et al., 1984; Slawyk et al., 1997), the relationship between NU and NRA in other oceanic sub-environments, such as coastal, shelf and oligotrophic waters, has not yet been fully examined. The East China Sea is a suitable site for this study due to waters with a wide range of nutrients, from oligotrophic ocean to upwelling water, to highly productive coastal water. Thus, the effects of light and nutrient (nitrate) concentration on the

relationship between nitrate reductase activity and  $^{15}\text{NO}_3^-$  uptake in the East China Sea were examined. In addition, primary production in the East China Sea was also measured to acquire more insight about the relationship between NRA and primary production.

## **Materials and methods**

### *Sampling*

40 stations were occupied in five transects across the East China Sea between May 2 and 15, 1996 aboard the R/V Ocean Research I during Cruise ORI-449 of the Kuroshio Edge Exchange Processes (KEEP) Study. The cruise track and the locations of the stations are shown in Figure 4-1. Small black circles represents the hydrographic stations and large black circles (Stations 11, 15, 26, 30, 52 and 55) represent the stations of nitrate reductase activity and  $^{15}\text{NO}_3^-$  uptake.

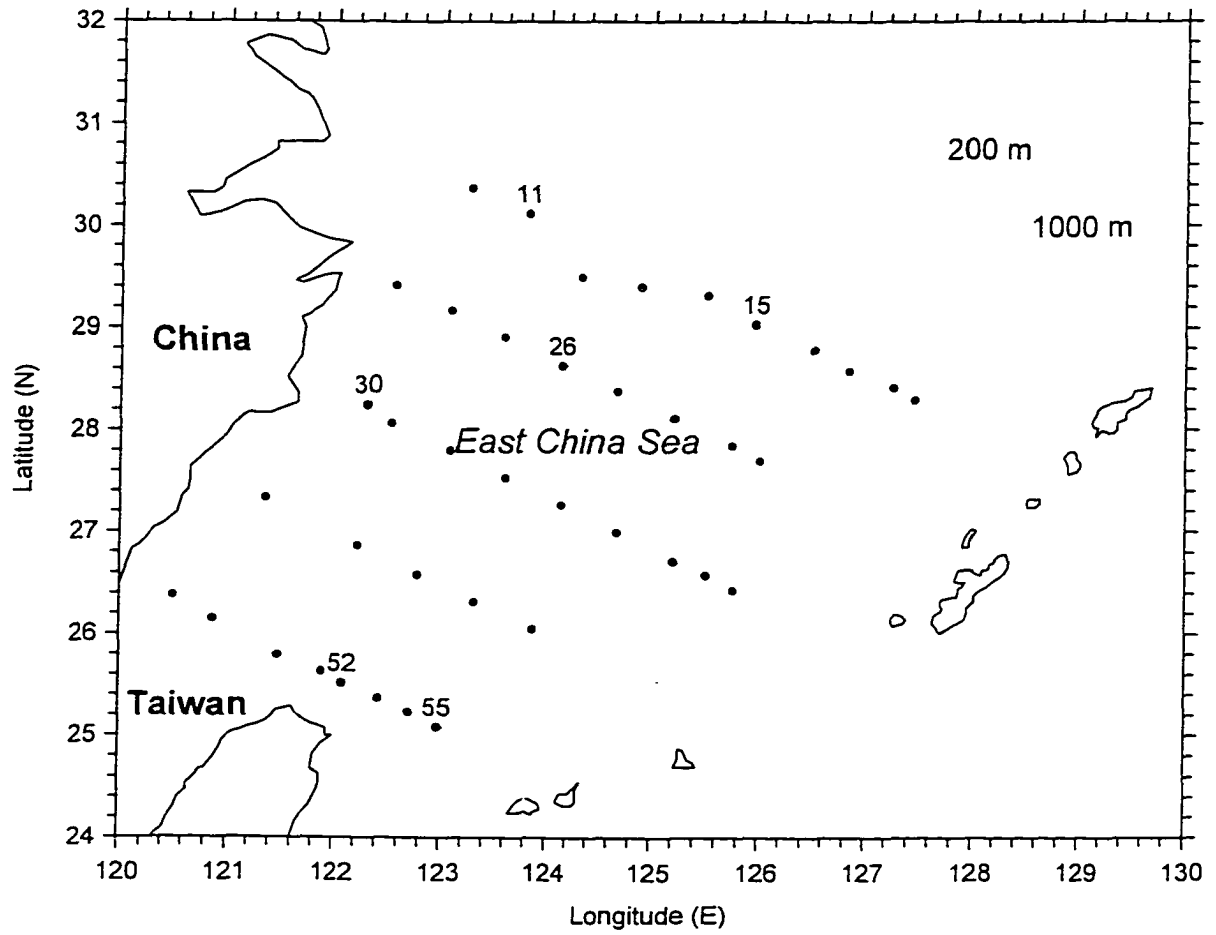


Fig. 4-1. The study area. Large circle –locations of stations where NRA and  $^{15}\text{NO}_3^-$  uptake (NP) were determined. Small circle: locations of hydrographic stations.

*Hydrographic and nutrient measurements*

At each station, the distributions of temperature, salinity and fluorescence were recorded with a SeaBird model SBE9/11 conductivity-temperature-depth (CTD) recorder. Photosynthetically active radiance (PAR) was recorded with a PAR sensor (QSP200L; Biospherical), while the depth of the euphotic zone was defined as 1% of the surface light level. Discrete water samples were collected with GO-FLO bottles mounted on a Rosette sampling assembly (General Oceanics). Sub-samples were then obtained for the determination of salinity, nitrite and (nitrate+nitrite).

Sub-samples were returned to the shore based laboratory for the determination of salinity with an Autosal salinometer. The precision for this measurement was  $\pm 0.003$ . Nitrite and (nitrate+nitrite) were determined on board ship by the standard pink azo dye method which has been adapted for use with a flow injection analyzer (Morris and Riley, 1963; Strickland and Parsons, 1972; Gardner et al., 1976; Pai et al., 1990; Gong, 1992; Liu et al., 1992a, b). The precision for the determination of nitrate and nitrite was 1% at 10 to 20  $\mu\text{M}$  levels. The detection limits for nitrite and nitrate were 0.1 and 0.05  $\mu\text{M}$ , respectively.

*Chlorophyll  $a$ , primary production,  $^{15}\text{NO}_3^-$  uptake and NRA assay*

Sub-samples were obtained at 6 stations: Stations 11, 15, 26, 30, 52 and 55 for the determination of chlorophyll  $a$  (chl  $a$ ),  $^{15}\text{NO}_3^-$  uptake and NRA. Stations 52 and 55 were occupied twice to study the temporal changes in these parameters. Chl  $a$ , was determined by the method of Strickland and Parsons (1972) and Gong et al. (1993). Seawater (100 ml)

was filtered through 47 mm Whatman GF/F glass fiber filters on board ship, then stored immediately at  $-20\text{ }^{\circ}\text{C}$  and returned to the laboratory for further processing. In the laboratory, the filters were ground in and extracted with 10 ml of 90% acetone at  $4\text{ }^{\circ}\text{C}$  for 2 hours. Then, the mixture was centrifuged for 10 min at 3000 rpm. The concentration of Chl- $a$  in the supernatant liquid was measured fluorimetrically with a Turner model 10-AU-005 fluorometer. The fluorometer was calibrated against a standard prepared from pure chl  $a$  (Sigma chemical Co.) The precision in the determination of chl  $a$  was about 1 % at  $200\text{ mg/m}^3$ .

Primary productivity (PP) was measured by the  $^{14}\text{C}$  assimilation method (Parsons et al., 1984; Shiah et al., 1995). Acid-cleaned polycarbonate bottles (250 mL, Nalgene) were filled with seawater pre-screened through  $200\text{ }\mu\text{m}$  mesh to remove large organisms and particles, and then inoculated with  $10\text{ }\mu\text{Ci NaH}^{14}\text{CO}_3$ . Samples were incubated in situ conditions for 6 hours. Following retrieval, the samples were filtered through 25 mm Whatman GF/F glass fiber filters under low vacuum ( $< 100\text{ mm Hg}$ ). The filters were placed in scintillation vials and stored in the dark. The filters were returned to the shore-based laboratory and analyzed for their  $^{14}\text{C}$  content by a liquid scintillation counter (Packard 2700TR). The precision in the counting statistics was approximate 1 %.

The uptake of nitrate was determined by the method of Dugdale and Wilkerson (1986) by measuring the uptake of added  $^{15}\text{NO}_3^-$ . On shipboard, seawater was filtered through a  $200\text{ }\mu\text{m}$  mesh-size net. The concentration of nitrate in the sample was determined on shipboard. An amount of  $^{15}\text{NO}_3^-$  equivalent to 10% of the nitrate present in the sample was added to the filtrate in a 1-liter polycarbonate bottle. (If the concentration of nitrate was

below detection limit, 100 nM of  $^{15}\text{NO}_3^-$  was added to the sample.) The mixture was incubated under *in situ* conditions for 6 hours. Upon the termination of the incubation, the samples were filtered through 25 mm Whatman GF/F glass fiber filters which were stored in a freezer at  $-20^\circ\text{C}$ . The filters were returned to the shore-based laboratory and analyzed for their  $^{15}\text{N}$  content by mass spectrometry with a Carlo-Erba NA1400 elemental analyzer which fed into a VG 622 Micromass mass spectrometer. The precision on the mass spectrometer for measuring N-15/N-14 atomic ratio was about 0.006 %.

Nitrate reductase activity was determined on board ship by the slightly modified version of the method of Hochman et al. (1986). The detailed procedure of NRA was the same as previous NRA assay in Chapter III. The use of Gelman A/E filters (nominal pore size  $1.0\ \mu\text{m}$ ) for the determination of NRA and Whatman GF/F filters (nominal pore size  $0.7\ \mu\text{m}$ ) for the determination of primary production,  $^{15}\text{NO}_3^-$  uptake and chl *a* may lead to an undersampling of the picoplankton. However, the difference in the retention efficiency between these two types of filters should be minimal since the difference in efficiency to retain total chlorophyll between filters with even larger difference in nominal pore size (between  $0.45\ \mu\text{m}$  and  $1.2\ \mu\text{m}$ ) has been reported to be  $< 9\%$  (Venrick et al., 1987). Furthermore, the dominant types of phytoplankton in the study area are the larger phytoplankton, such as *Skeletonema costatum*, *Thalassiosira* spp., *Thalassionema nitzschioides* and *Trichodesmium* spp. (Chen, 1995). They should be retained by both kinds of filters effectively.



## Results and discussions

### *Hydrography, light, nutrient and chlorophyll a*

The surface distributions of temperature, salinity, nitrate and chlorophyll *a* (chl *a*) are shown in Figures 4-2a, 4-2b, 4-2c and 4-2d. The four major surface water masses were distinctly identifiable. The Changjiang Diluted Water, salinity < 33, temperature < 17 °C, nitrate concentrations > 1 μM, and chl *a* > 0.75 mg m<sup>-3</sup>, was found along the Chinese coast. It spread seaward most extensively around the mouth of the Changjiang in the northwestern corner of the study area. Sta. 30 was located within this plume of fresher water while Stations 11 and 26 were located at the seaward frontal region of this plume. The highest concentration of chl *a* in the study area, 2.44 mg m<sup>-3</sup>, was found at Sta. 26. The Kuroshio Surface Water was found along the shelf edge, salinity > 34.5, temperature > 22 °C and chl *a* < 0.25 mg m<sup>-3</sup>. Sta. 55 was located in the Kuroshio while Sta. 15 was located at the shelf-ward frontal zone of the Kuroshio. The upwelling Kuroshio Subsurface Water manifested itself as a patch of cold, < 21 °C, nutrient-rich, nitrate concentration > 1 μM, water with intermediate chl *a* > 0.75 mg m<sup>-3</sup>. It was located northeast of Taiwan and Sta. 52 was located around the center of this upwelling dome. A small patch of warm (>22 °C) water was found northwest of Taiwan in the Taiwan Strait and it was probably the Taiwan Current Warm Water.

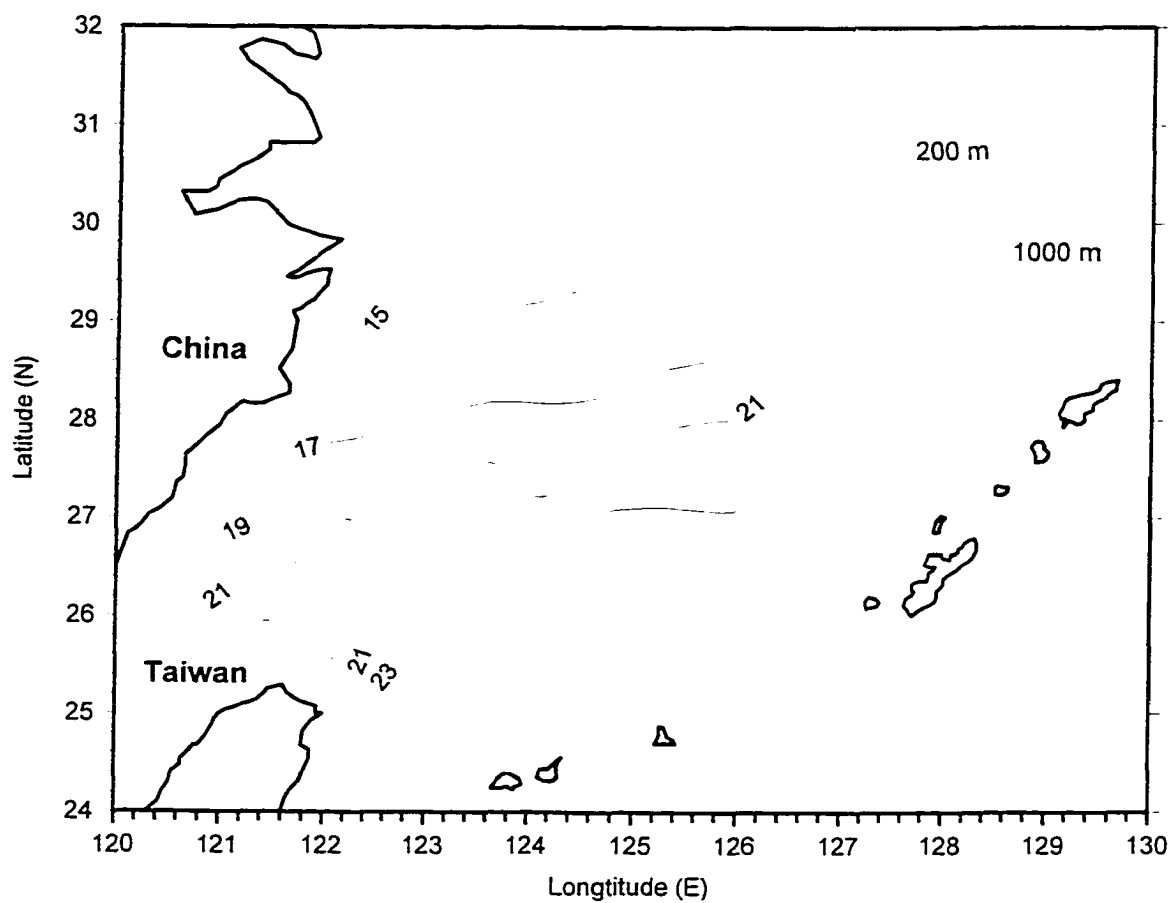


Fig. 4-2a. The surface distribution of temperature (°C) in the East China Sea.

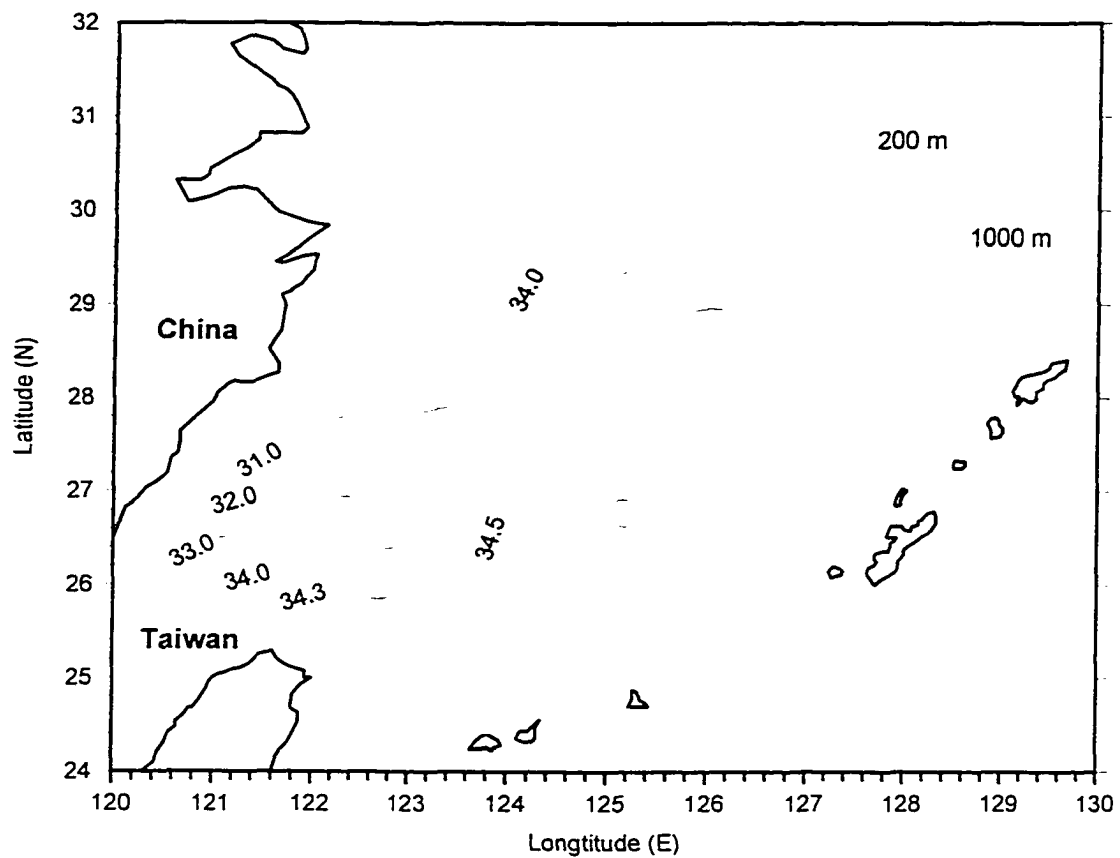


Fig. 4-2b. The surface distribution of salinity in the East China Sea.

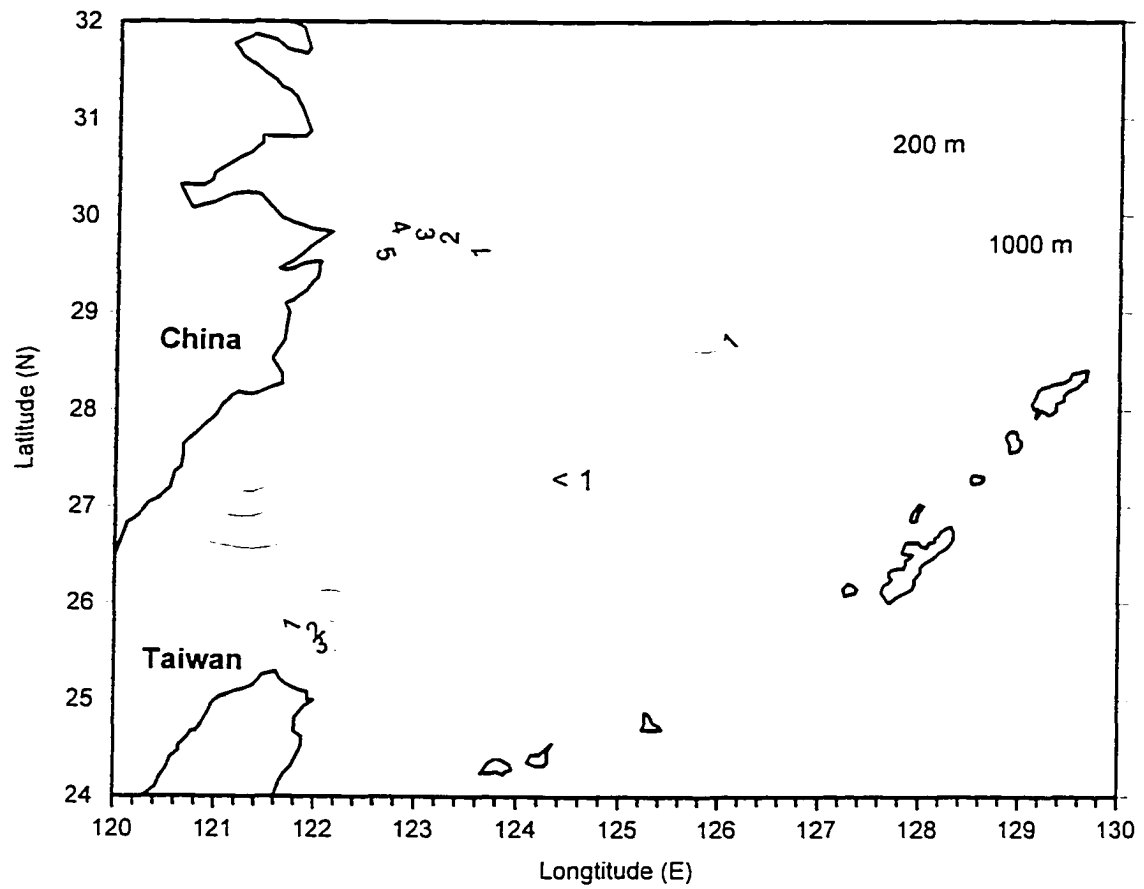


Fig. 4-2c. The surface distribution of nitrate ( $\mu\text{M}$ ) in the East China Sea.

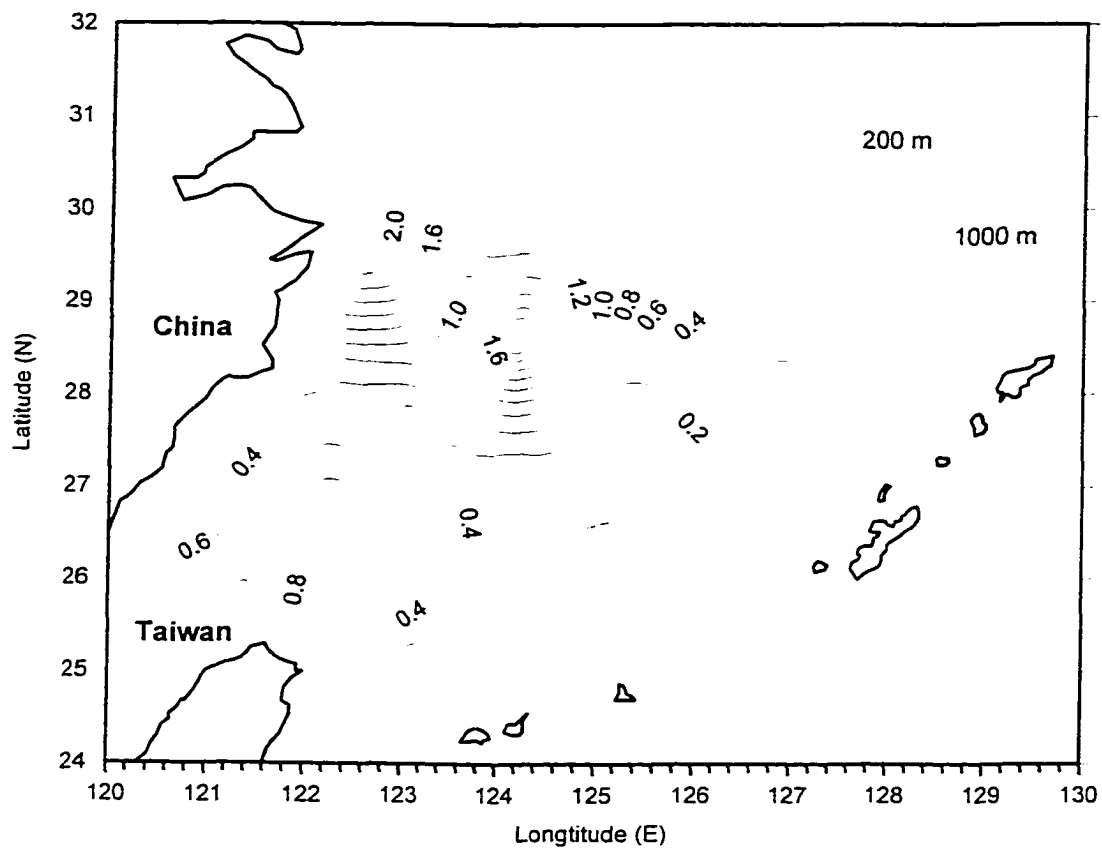


Fig. 4-2d. The surface distribution of chlorophyll *a* ( $\text{mg m}^{-3}$ ) in the East China Sea.

The vertical distributions of temperature, salinity, sigma- $\theta$ , nitrate, chl  $a$  and %PAR (% of the photosynthetically active radiance at the sea surface) at Stations 11, 15, 26, 30, 52 and 55 are shown in Figures 4-3 to 4-8. The detailed NRA and relevant data are shown in appendix D. The MLD (mixed layer depth) represents the depth at which in the density gradient increased by a factor of 2 or higher and PZD<sub>01</sub> represents the photic zone depth from surface to 1% PAR. MLD and PZD<sub>01</sub> are indicated in the Figures 4-3 to 4-8. The characteristics of the water within the MLD at these stations are summarized in Table 4-1. Shallow MLD (<15 m), PZD<sub>10</sub> ( $\leq$ 20 m), strong pycnoclines and high chl  $a$  (0.8 to 2.4 mg m<sup>-3</sup>) were found in the coastal fresh water plume (Sta. 30) and at the frontal region of the plume (Sta. 11 and 26). However, high concentrations of nitrate ( $\sim$  6  $\mu$ M) were found only at Sta. 30. The concentrations of nitrate at the other two stations were < 0.5  $\mu$ M. At Sta. 26, the MLD (3 m) was particularly shallow and the concentration of chl- $a$  was exceptionally high (2.4 mg m<sup>-3</sup>). A temperature inversion layer was found at Sta. 30 below 13 m, resulting from intrusion of more saline and warmer Taiwan Warm Current Water underneath the Changjiang Diluted Water (Beardsley et al., 1985). In the upwelling region at Sta. 52, as in the coastal plume, similarly shallow MLD (15 m) and PZD<sub>10</sub> (24 m), and high chl  $a$  (0.8 mg m<sup>-3</sup>) together with high nitrate (5  $\mu$ M) were found. In contrast, in the oligotrophic Kuroshio at Sta. 55, the MLD (33 m) and PZD<sub>10</sub> (41 m) were much deeper while the concentrations of nitrate (<0.5  $\mu$ M) and chl  $a$  (<0.1 mg m<sup>-3</sup>) were low. At the frontal region between the Kuroshio and the shelf water, at Sta. 15, the MLD (52 m) was the deepest among these six stations and it exceeded the PZD<sub>10</sub> (34 m). They were accompanied by intermediate levels of nitrate (2  $\mu$ M) and chl  $a$  (0.4 mg m<sup>-3</sup>).

*Table 4-1. Properties of the waters in the mixed layer of the different hydrographic regimes of the East China Sea*

Hydrographic Regimes	Sta	MLD m	S	T °C	NO <sub>3</sub> <sup>-</sup> μM	Chl <i>a</i> mg m <sup>-3</sup>	NU nM-N hr <sup>-1</sup>	NRA nM-N hr <sup>-1</sup>	NU/NRA
Coastal plume/ shelf front region	11	12	33.4	16.3	0.4	0.83	11.8	10.6	1.11
Shelf/Kuroshio frontal region	15	52	34.4	17.5	1.8	0.43	3.6	3.7	0.98
Coastal plume/ shelf frontal region	26	3	34.1	17.7	0.1	2.44	36.5	15.4	2.38
In coastal plume	30	13	30.1	15.4	6.0	0.96	3.3	4.7	0.71
Upwelling center	52-1	15	34.5	18.5	5.0	0.77	nd	5.3	nd
Upwelling center	52-3	15	34.5	18.9	4.3	0.90	13.5	10.0	1.35
Kuroshio	55-3	33	34.6	23.9	< 0.1	0.07	1.4	0.17	8.65
Kuroshio	55-5	35	34.6	24.0	< 0.1	0.06	nd	0.13	nd

nd - no data

MLD-Mixed layer depth

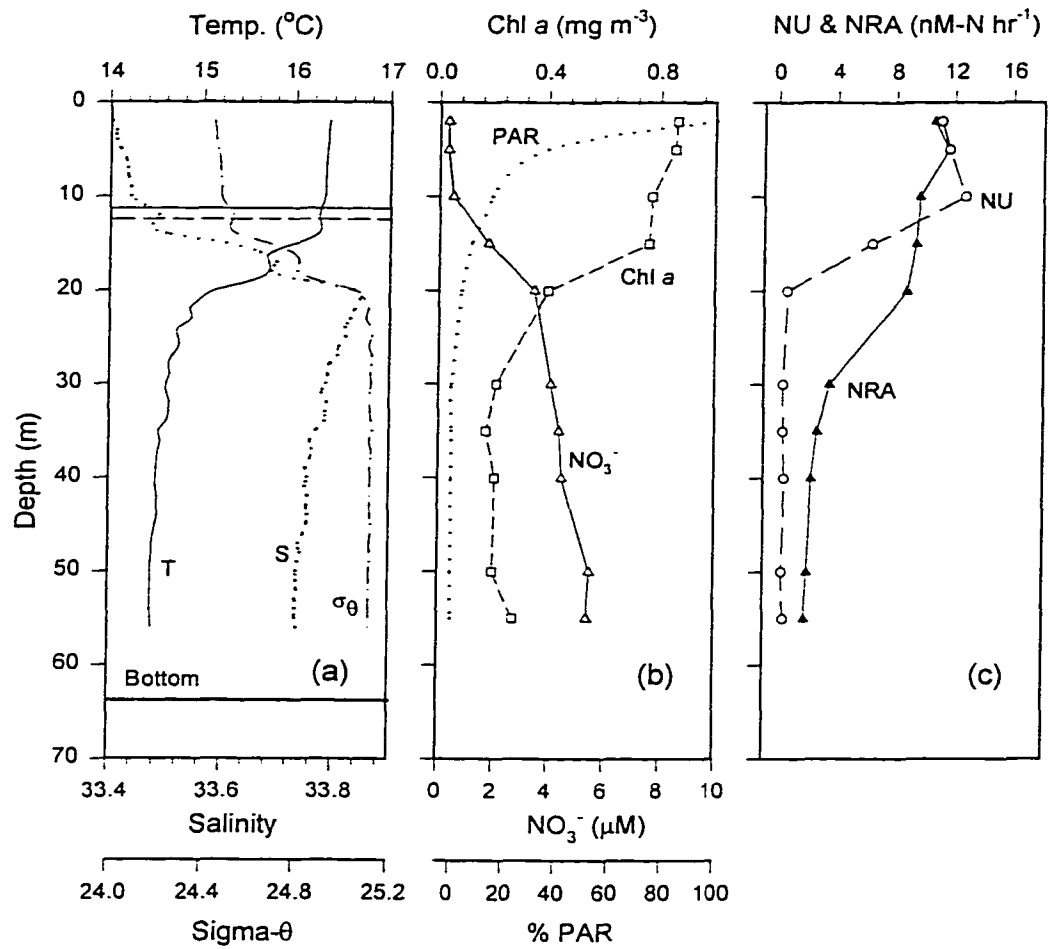


Fig. 4-3. The vertical distribution of (a) temperature, salinity and  $\sigma_\theta$ , (b) nitrate, chlorophyll *a* and %PAR, (c) NRA and NU at Sta. 11. Horizontal dashed line denotes PZD<sub>10</sub>. Horizontal thin solid line denotes MLD.



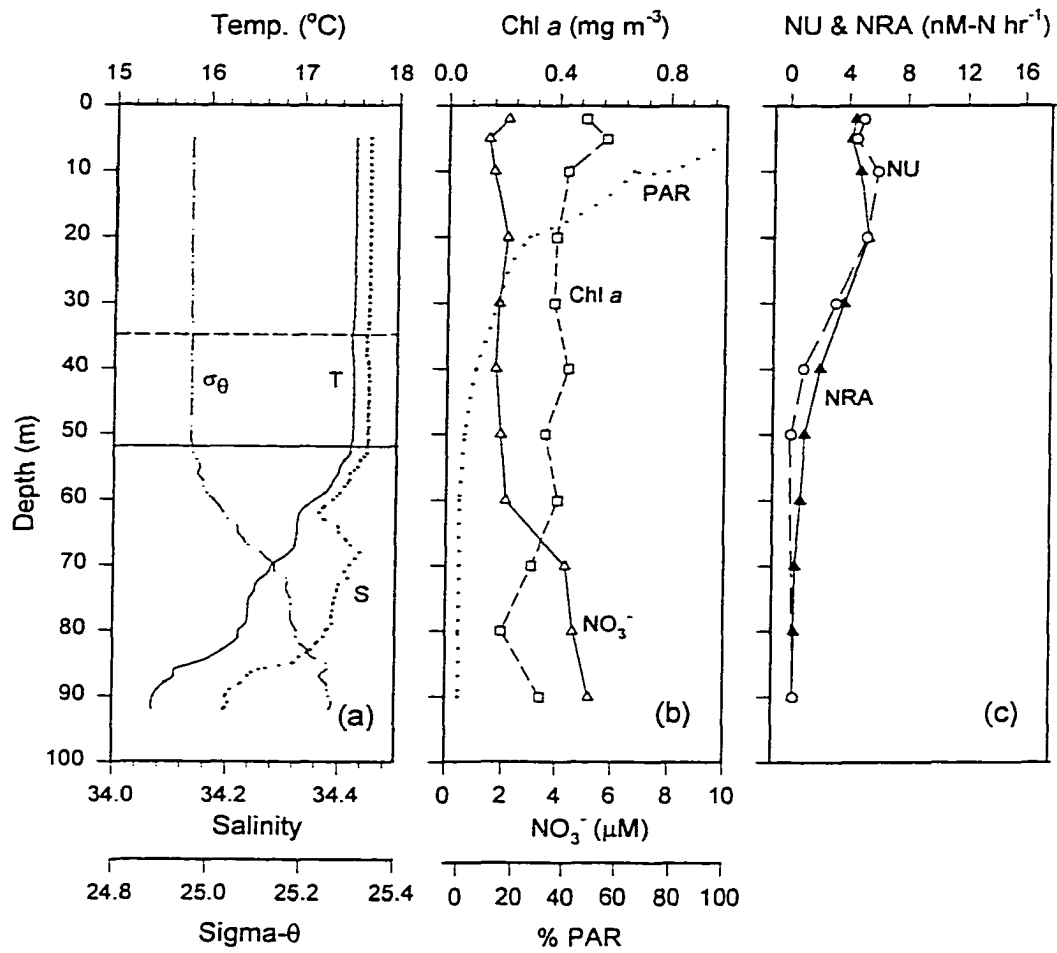


Fig. 4-4. The vertical distribution of (a) temperature, salinity and  $\sigma_\theta$ , (b) nitrate, chlorophyll *a* and %PAR, (c) NRA and NU at Sta. 15. Horizontal dashed line denotes PZD<sub>10</sub>. Horizontal thin solid line denotes MLD.

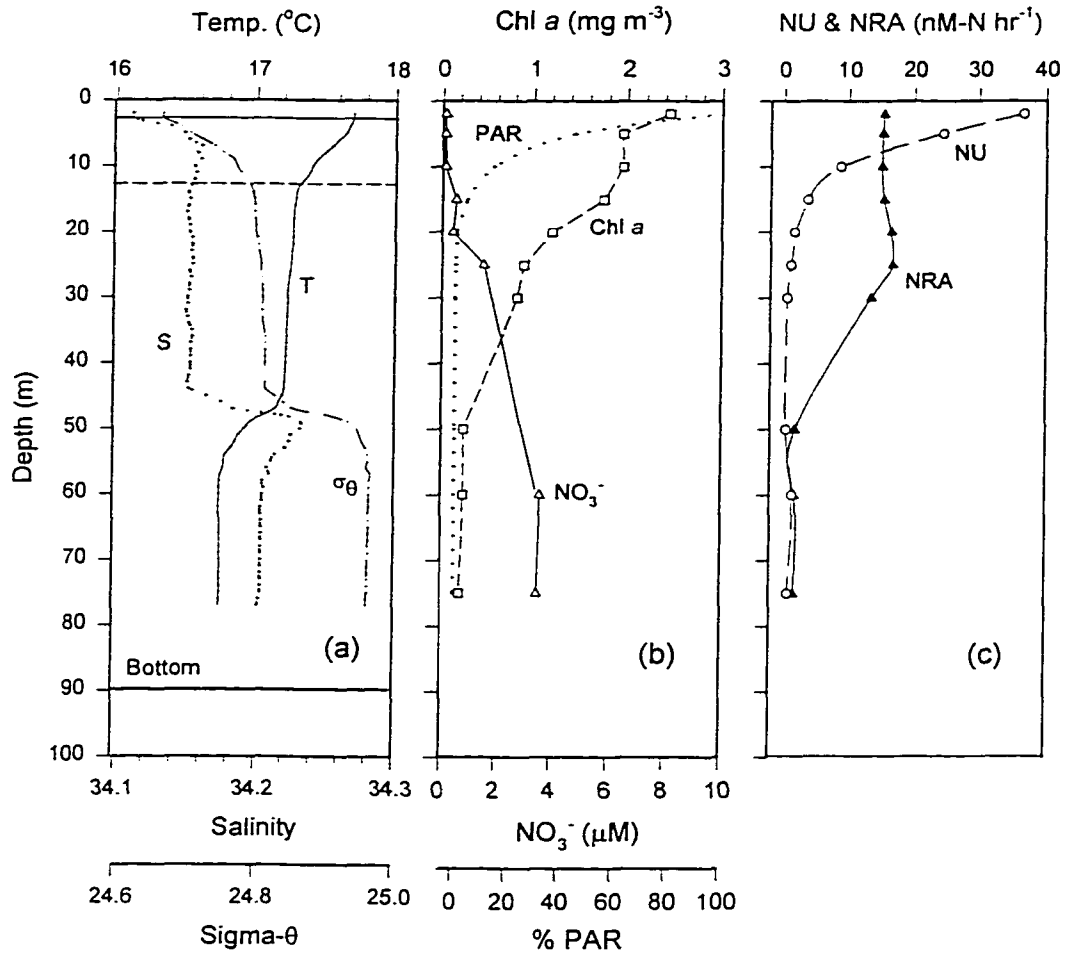


Fig. 4-5. The vertical distribution of (a) temperature, salinity and  $\sigma_\theta$ , (b) nitrate, chlorophyll *a* and %PAR, (c) NRA and NU at Sta. 26. Horizontal dashed line denotes PZD<sub>10</sub>. Horizontal thin solid line denotes MLD.

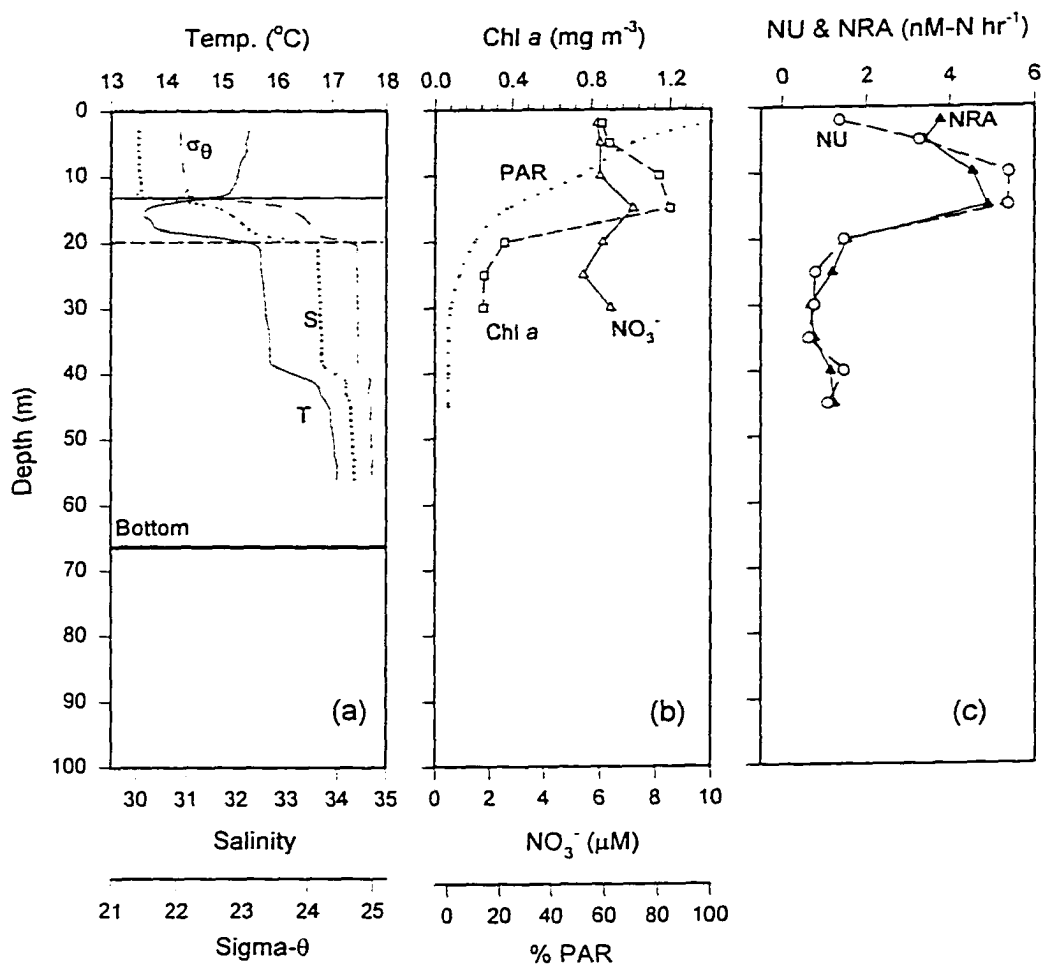


Fig. 4-6. The vertical distribution of (a) temperature, salinity and  $\sigma_{\theta}$ , (b) nitrate, chlorophyll  $a$  and %PAR, (c) NRA and NU at Sta. 30. Horizontal dashed line denotes PZD<sub>10</sub>. Horizontal thin solid line denotes MLD.

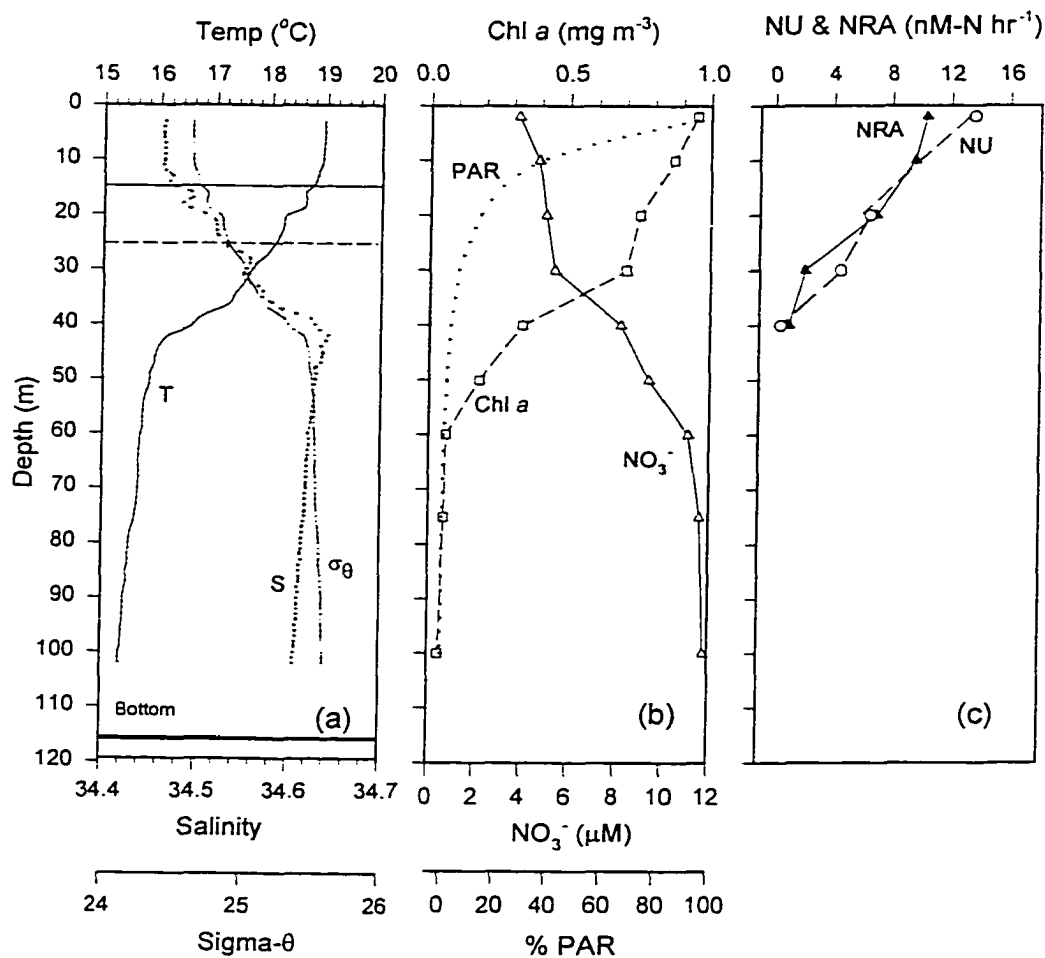


Fig. 4-7. The vertical distribution of (a) temperature, salinity and  $\sigma_\theta$ , (b) nitrate, chlorophyll *a* and %PAR, (c) NRA and NU at Sta. 52-3. Horizontal dashed line denotes PZD<sub>10</sub>. Horizontal thin solid line denotes MLD.

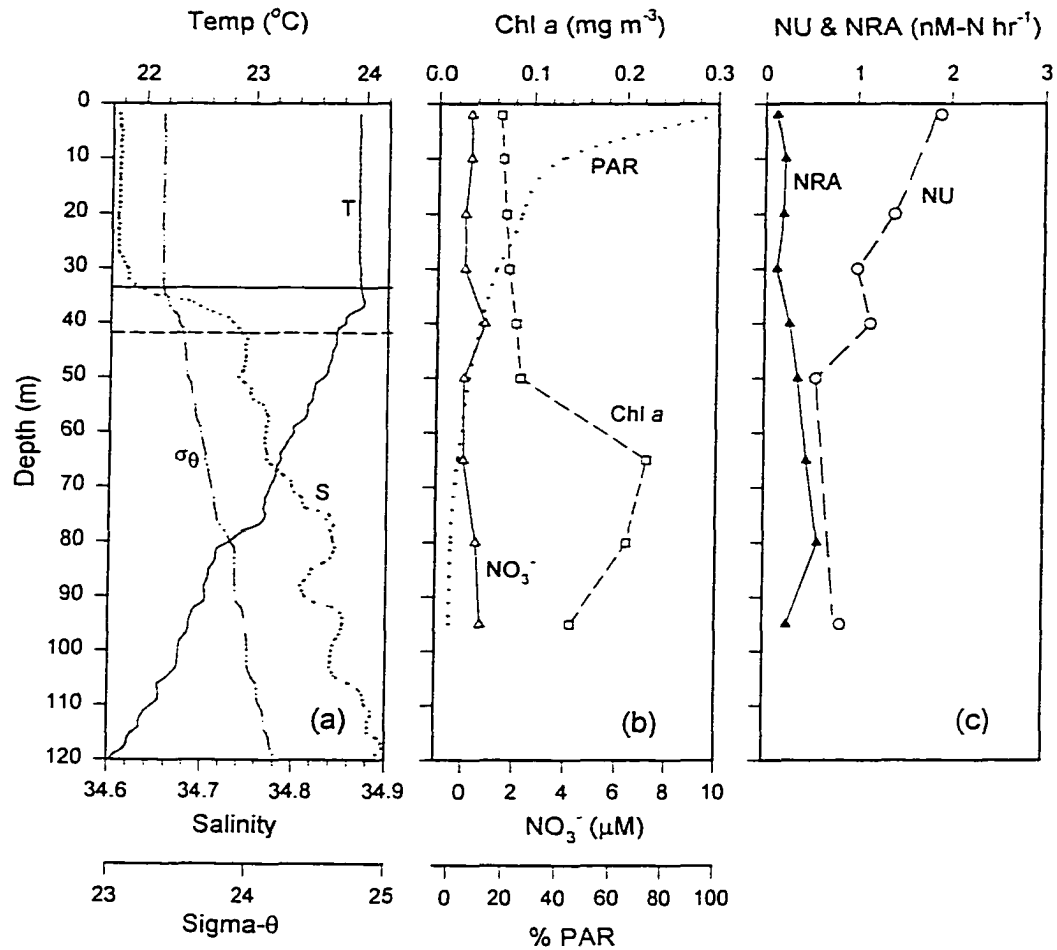


Fig. 4-8. The vertical distribution of (a) temperature, salinity and  $\sigma_{\theta}$ , (b) nitrate, chlorophyll *a* and %PAR, (c) NRA and NU at Sta. 55-3. Horizontal dashed line denotes PZD<sub>10</sub>. Horizontal thin solid line denotes MLD.

### *NRA and $^{15}\text{NO}_3^-$ uptake (NU)*

As a first approximation, the vertical distributions of NRA and  $^{15}\text{NO}_3^-$  uptake (NU), which is designated as new production or NU in this discussion, were usually similar to each other and to chl *a*. Significant levels of NRA and NU were confined primarily to within the MLD and/or the  $\text{PZD}_{10}$ . At greater depths, they dropped abruptly with depth to background levels. In the mixed layer, high NRA and NU were found at the frontal zone of the coastal plume at Sta. 11 (NRA = 11  $\text{nM h}^{-1}$ , NU = 12  $\text{nM h}^{-1}$ ) and at Sta. 26 (NRA = 15  $\text{nM h}^{-1}$ , NU = 30  $\text{nM h}^{-1}$ ) (Table 4-1). The values at Sta. 26 were exceptionally high. Within the plume, at Sta 30, NRA (4  $\text{nM h}^{-1}$ ) and NU (3  $\text{nM h}^{-1}$ ) were considerably lower. These values were similar to those observed at the frontal zone between the Kuroshio and the shelf water at Sta. 15 (NRA = 4  $\text{nM h}^{-1}$ , NU = 4  $\text{nM h}^{-1}$ ). High NRA (10  $\text{nM h}^{-1}$ ) and NU (14  $\text{nM h}^{-1}$ ) were also found in the upwelling zone at Sta. 52. The lowest NRA (0.2  $\text{nM h}^{-1}$ ) and NU (1.4  $\text{nM h}^{-1}$ ) were found in the oligotrophic Kuroshio at Sta. 55. Below the MLD, NRA sometimes did not decrease with depth in step with NU. NRA seemed to decrease less abruptly with depth. This phenomenon was clearly evident at Sta. 26 where high NRA persisted down to about 30 m while NU had decreased to residual level below 15 m.

### *Temporal variations*

Stations 52 and 55 were sampled twice over several hours at two different days and the results are shown in Fig. 4-9. At Sta. 55, the hydrography did not change significantly between the casts as indicated by their similar temperature profiles. The corresponding

distributions of NRA at Sta. 55 were also approximately the same. The high degree of reproducibility of these profiles gives credence to the reliability of our modified method of Hochman et al. (1986) for the determination of NRA. However, the two NRA profiles at Sta. 52 were inconsistent with each other. According to the temperature profiles, there was a water mass shift between the two casts at Sta. 52. Therefore, the discrepancy may result from the changes of water masses. It might also result from vertical migration and/or diel periodicity of NRA. It is difficult to distinguish between these possibilities with the available data.

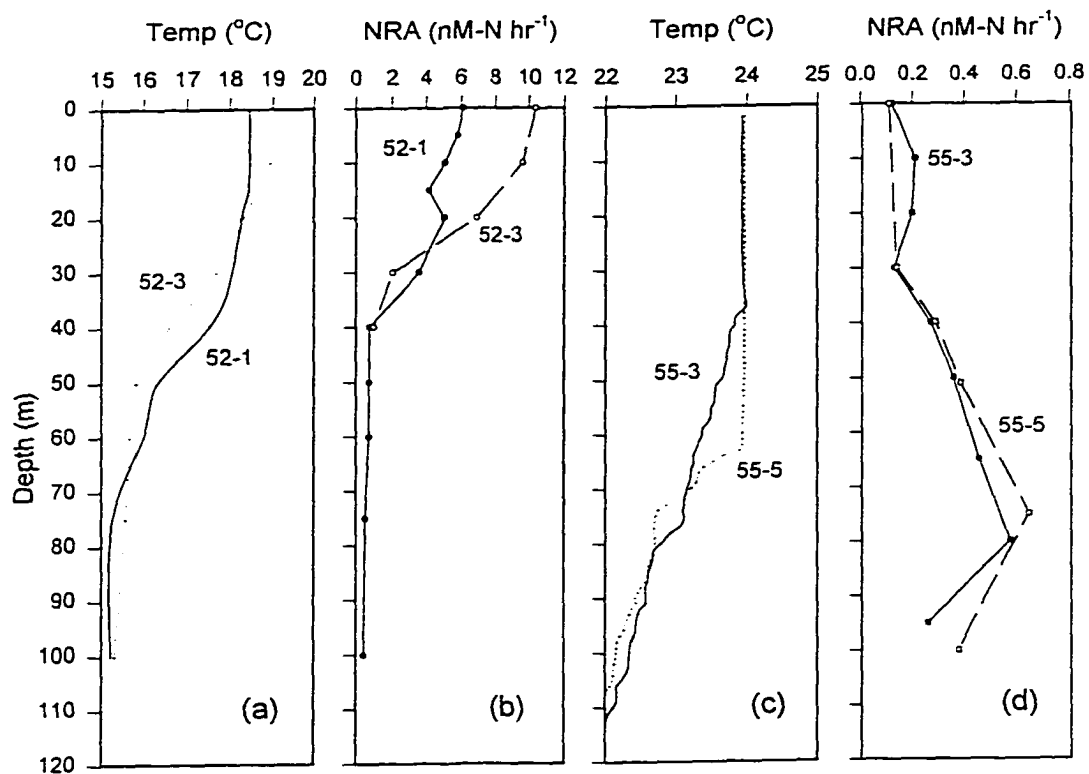


Fig. 4-9. The vertical distribution of temperature and NRA from two casts at Sta. 52 (a and b) and Sta. 55 (c and d).



*The influence of environmental conditions on NU/NRA*

Light is one of the primary environmental factors that can affect nitrate assimilation (Packard and Blasco, 1974; Gao et al., 1992; Smith et al., 1992; Berges et al., 1995). The depth at which PAR drops to 1% of the surface value (photic zone depth at 1% PAR or PZD<sub>01</sub>) is usually referred as the euphotic zone (Parsons and Takahashi, 1977). When the incident irradiance is below 1% PAR, light becomes a limiting factor for photosynthesis by phytoplankton. The relationship between NU/NRA and nutrient at depths where %PAR exceeded 10 % is shown in Fig. 4-10. At these depths, the availability of light should no longer be a limiting factor for nitrate assimilation. At nitrate concentrations above about 1  $\mu\text{M}$ , all the data points coalesced around a ratio of about 1. The average was  $1.0 \pm 0.3$ . Thus, there was an almost quantitative relationship between NRA and NU under light- and nutrient-replete conditions. Below a nitrate concentration of 1  $\mu\text{M}$ , there was much larger scatter. Some exceedingly high values of NU/NRA, up to 15.4, were found and the average was  $4 \pm 4$ . These excess NU values relative to NRA in light-replete but nutrient-deficient waters could have been an artifact which was caused by the  $^{15}\text{NO}_3^-$  added for the determination of NU (Eppley et al., 1977; Dugdale and Wilkerson, 1986; McCarthy et al., 1996). In nitrate-impoverishment waters, it is very difficult to measure very low nitrate concentrations ( $< 0.1 \mu\text{M}$ ) by the conventional nitrate method. Therefore, the amount of  $^{15}\text{NO}_3^-$  added (50 to 100 nM) for the measurement of  $^{15}\text{NO}_3^-$  uptake is often higher than 10% of the ambient concentration. As a consequence, the excess nitrate may easily induce nitrate uptake of phytoplankton. If there was a stimulative effect, NU would have been over-estimated by measuring  $^{15}\text{NO}_3^-$  uptake. NRA does not suffer from this source of error.

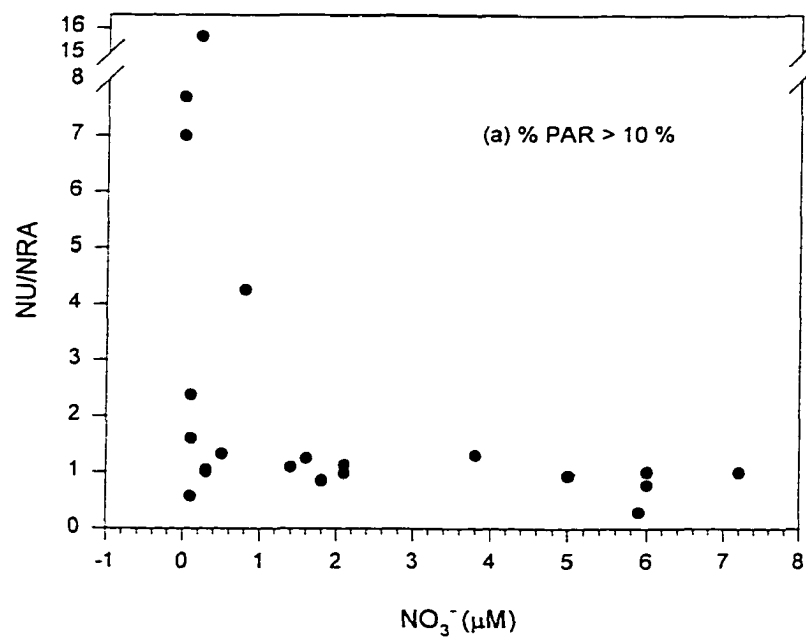


Fig. 4-10. The relationship between NU/NRA and nitrate at depth where %PAR > 10%.

Thus, in oligotrophic waters, NRA may be a more reliable indicator of NP.

The relationship between NU/NRA and %PAR at PAR >1% in waters with nitrate exceeding 1  $\mu\text{M}$  is shown in Fig. 4-11. In these waters, the availability of nitrate should no longer be a limiting factor for nitrate assimilation. At PARs above 10%, the ratio of NU/NRA is close to 1. Between PAR of 10% and 1%, there was much greater scatter. NU/NRA tended to be lower than those in the light-replete waters. The average NU/NRA was  $0.7 \pm 0.7$ . These low and highly variable NU/NRA may reflect the fact that NU and NRA measure slightly different facets of nitrate assimilation. NRA represents an instantaneous nitrate reducing potential at the sampling time, and it reflects the recent past nitrate uptake rate (Blasco et al., 1984) while NU represents a 6 hours  $^{15}\text{NO}_3^-$  uptake integration following sampling (Blasco et al., 1984; McCarthy et al., 1996; Slawyk et al., 1997). Under light-deficient and possibly light-limiting conditions, the history of the light conditions experienced by phytoplankton can be variable due to weather changes, vertical mixing of water masses and/or vertical migration of phytoplankton. Thus, it is not impossible that algal cells have experienced light-abundant conditions and contained higher enzyme activities at that light-deficient conditions just before sampling. Eppley et al. (1970), Goa et al. (1992) and Berges et al. (1995) reported that the cycling of phytoplankton cells between light and dark periods can affect the NRA of the cells. On the other hand, in the determination of NU, the light condition is fixed at the light-deficient condition during the incubation period. As a result, the nitrate reducing potential represented by NRA may be higher than the nitrate assimilation represented by  $^{15}\text{NO}_3^-$  uptake so that the latter may be a better indicator of new production under light-deficient condition. A number of the

samples that fell under this category ( $[\text{NO}_3^-] > 1 \mu\text{M}$ ;  $1\% < \% \text{PAR} < 10\%$ ) were found in or close to the nitraclines. Ward et al. (1989) and Eppley and Koeve (1990) suggested that nitrate may be formed in these waters by nitrification. The nitrate formed may dilute the  $^{15}\text{NO}_3^-$  added and cause an underestimation in nitrate uptake. If this were true, it would also contribute to the low values of NU/NRA in these waters.

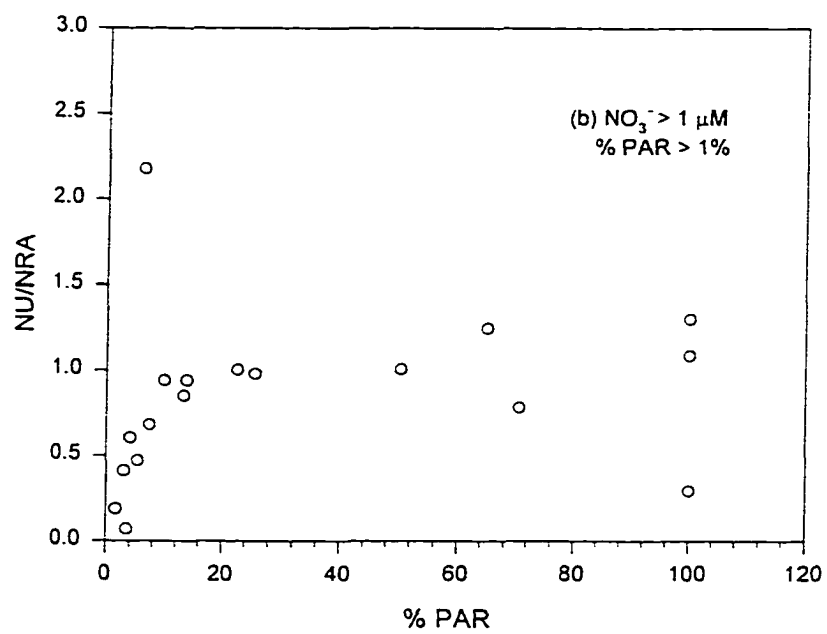


Fig. 4-11. The relationship between NU/NRA and %PAR at locations where  $\text{NO}_3^- > 1 \mu\text{M}$  and %PAR > 10%.

*Relationship between NRA and NU*

By considering the influences of low nitrate (NU may be overestimated) and of light-depletion (NRA may be overestimated), four types of water may be classified: (A) nitrate- and light-replete waters ( $[\text{NO}_3^-] > 1 \mu\text{M}$ ,  $\% \text{PAR} > 10\%$ ), (B) nitrate-deficient and light-replete water ( $[\text{NO}_3^-] < 1 \mu\text{M}$ ,  $\% \text{PAR} > 10\%$ ), (C) nitrate-replete and light-deficient water ( $[\text{NO}_3^-] > 1 \mu\text{M}$ ,  $\% \text{PAR} < 10\%$ ), and (D) nitrate- and light-deficient water ( $[\text{NO}_3^-] < 1 \mu\text{M}$ ,  $\% \text{PAR} < 10\%$ ). The linear regression relationships (Model II) with no intercept between NU and NRA in these four types of water are shown in Fig. 4-12a, b, and c, and they are summarized in Table 4-2. As expected from the previous discussion, NU was strongly correlated with NRA under nitrate- and light-replete conditions (Fig. 4-12a). The uncertainty of NU/NRA was about  $\pm 6\%$  according to the variation of coefficient. Thus, in this type of water, both NU and NRA may be used for estimating the rate of nitrate assimilation. This results demonstrated that NU may also be estimated from NRA once a relationship between the two rates can be established empirically by measuring both parameters simultaneously in a small number of samples. In type (B) water (Fig. 4-12b), although a slope similar to that in type (A) water was found, the correlation was significantly poorer. The uncertainty of the slope was  $\pm 13\%$ . If the poor correlation between NU and NRA in type (B) is indeed caused by the addition of  $^{15}\text{NO}_3^-$  during the determination of NU, NRA may be more reliable than NP for measuring nitrate assimilation. In type (C) water (Fig. 4-12c), the slope was about half of that in type (A) water while the correlation was even poorer than in type (B) water. The slope of the linear relationship had an uncertainty of  $\pm 33\%$ . Thus, NRA does not represent NU well and

cannot be used readily for estimating the rate of nitrate assimilation in this type of water. A relationship between NU and NRA cannot be estimated for type (D) water since there were only two data points from this type of water.

In previous field investigations, the relationships between NU and NRA were chaotic (Eppley et al., 1970; Collos and Slawyk, 1977; Blasco et al., 1984) and it is difficult to distinguish the failure possibilities which are from environment factors (variations of light, nutrients and hydrographic data) or the method of NRA. Similarly, it is not easy to demonstrate why the relationship between two variables in this study is better than before. The possible reasons may result from the different NRA assay used and appropriate eliminating the questionable data from hydrographic-based editing process.

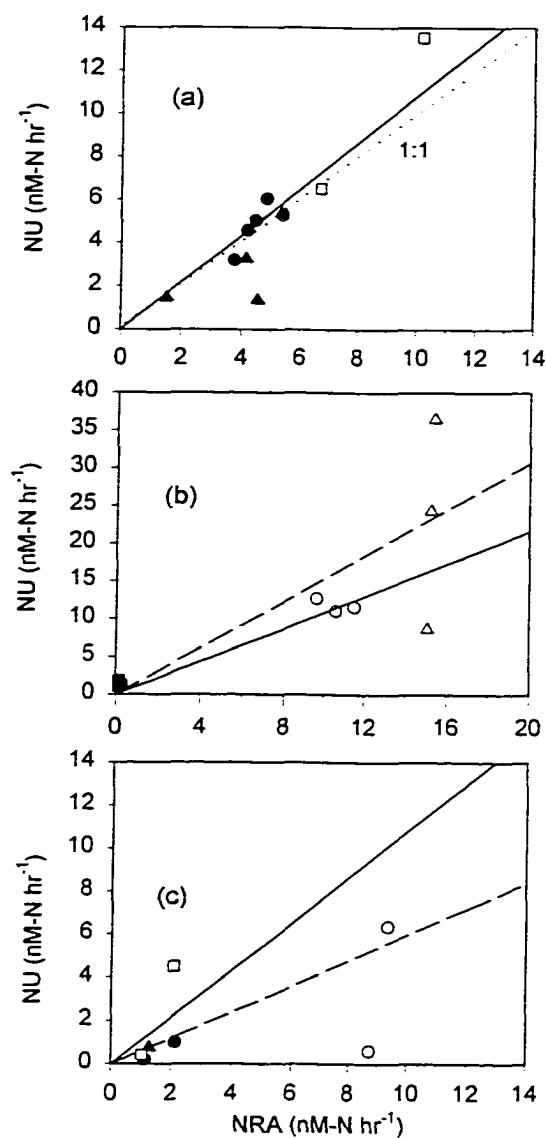


Fig. 4-12. The relationship between NU and NRA in waters with (a) nitrate  $> 1 \mu\text{M}$  and  $\% \text{PAR} > 10\%$ , (b) nitrate  $< 1 \mu\text{M}$  and  $\% \text{PAR} > 10\%$  and (c) nitrate  $> 1 \mu\text{M}$  and  $1\% < \% \text{PAR} < 10\%$ . The Model II regression line is shown as the solid line in (a) and as the dashed line in (b) and (c). The 1:1 line is shown as a dotted line in (a). The solid lines in (b) and (c) denote the regression relationship in (a).



*Table 4-2. Relationship between NU and NRA under different combinations of light- and nitrate- conditions*

Type	Light %PAR	NO <sub>3</sub> <sup>-</sup> (μM)	Average NU/NRA	Regression Analyses - NU vs NRA*			Characteristic of water type
				Slope	r <sup>2</sup>	n	
A	>10%	>1	1.0±0.3	1.08±0.07	0.79	12	NRA and NP are indicative of nitrate assimilation
B	>10%	<1	4 ± 4	1.5±0.2	0.65	10	NRA may be more indicative of nitrate assimilation
C	<10%	>1	0.7±0.7	0.6±0.2	0.19	7	NP may be more indicative of nitrate assimilation
D	<10%	<1	0.9±0.7	Insufficient data			2

\*- Model II linear regression through the origin. NU and NRA in nM-N hr<sup>-1</sup>.

n - Number of data points.

r - correlation coefficient.

*Relationship between NRA and chlorophyll *a**

The average ratios of NRA/chl *a* within the photic zone where %PAR exceeded 10% at all the stations are also listed in Table 4-3. Among the three major surface water masses: the oligotrophic Kuroshio Surface Water at Sta. 55, the upwelling Kuroshio Sub-surface Water at Sta. 52 and the Changjiang Diluted Water at Sta. 30, the highest NRA/chl *a*, 8.8 nM-N h<sup>-1</sup> mg<sup>-1</sup> m<sup>3</sup> (the average of Stations 52-1 and 52-3), was found in the upwelling water. In the other two water masses, NRA/chl *a* were less than half of this value. The average ratios of NRA/chl *a* at the other three stations (Stations 11, 15 and 26) were also similar or higher than that in the upwelling zone. One possible explanation may be linked to the potentially different nutrient conditions in the different zones (Rhees, 1979). In a natural marine environment, a variety of combined nitrogen, nitrate, nitrite, ammonia and dissolved organic nitrogen (DON), may be taken up by phytoplankton simultaneously, while NRA only reflects nitrate utilization. Thus, in an area where new production relative to primary production (*f* ratio) is high, the NRA/chl *a* will be high. On the other hand, when other forms of combined nitrogen are used to maintain the algal biomass, the NRA/chl *a* and *f* ratio will be low (Harrison et al., 1987). The *f* ratios in upwelling waters are expected to be higher than in the oligotrophic ocean where new production is limited by the availability of nitrate (Eppley, 1989). In the coastal waters, the presence of ammonia and DON may restrict the assimilation of nitrate and result in lower NRA/chl *a* (Eppley et al., 1969; Parkard and Blasco, 1974; Dortch et al., 1979; Eppley, 1989; Berges et al., 1995).

Table 4-3. Characteristics of the photic zone to  $PZD_{10}$  in different hydrographic regimes of the East China Sea

Sta.	$PZD_{10}$ Depth(m)	NRA/chl $a$	$NU_{10}$ (mg-N m <sup>-2</sup> hr <sup>-1</sup> )	$NU'_{10}$ (mg-N m <sup>-2</sup> hr <sup>-1</sup> )	$NU'_{10}/NU_{10}$
11	13	12.8	2.09	2.06	0.99
15	34	10.2	2.25	2.35	1.04
26	12	7.3	3.67	2.77	0.75
30	20	4.1	1.05	1.36	1.30
52-1	24	7.2	nd	1.85	nd
52-3	25	10.4	3.32	3.21	0.97
55-3	41	2.6	0.80	0.11	0.14
55-5	63	4.1	nd	0.23	nd

nd- No data

$PZD_{10}$  - Photic zone depth to 10% of surface photosynthetically active radiance (PAR).

$NU_{10}$ ,  $NU'_{10}$  - Depth integrated NU and NU estimated from NRA to  $PZD_{10}$ .

NRA/chl  $a$  in nM-N hr<sup>-1</sup> mg<sup>-1</sup> m<sup>3</sup>;  $NU_{10}$  and  $NU'_{10}$  in mg-N m<sup>-2</sup> hr<sup>-1</sup>.

A similar tendency of  $f$  ratio was found in this study (Table 4-4) and its value was low (0.08) in the oligotrophic water and increased to intermediate level (0.16 to 0.24) in the coastal Changjiang Diluted Water and upwelling water, and to highest level (0.46) in the frontal zones in the shelf. (Due to the stimulation problem of  $^{15}\text{NO}_3^-$  uptake in oligotrophic ocean, the estimation of NP is derived from the equation of  $\text{NU} = 1.08 \text{ NRA}$  rather than using the rate of  $^{15}\text{NO}_3^-$  uptake). These values agree well with those reported in similar types of marine sub-environments (Eppley, 1989). The suppression of nitrate uptake in the coastal Changjiang Diluted Water is a distinct possibility. Neither was DON nor ammonia measured in this study, but the eminent ammonium concentration, up to  $14.6 \mu\text{M}$ , has usually been found in the Changjiang estuary (Edmond et al., 1985; Zhang, 1996). This may explain the lower  $\text{NRA}/\text{chl } a$  at Sta. 30 relative to Sta. 52. The relationship between the  $f$  ratio and the averages of  $\text{NRA}/\text{chl } a$  within  $\text{PZD}_{10}$  is shown in Fig. 4-13. The  $\text{NRA}/\text{chl } a$  seems to be proportional to  $f$  ratio if the Sta. 26 (a peculiar hydrographic properties) is excluded. The best linear correlation between two variables are shown as below:

$$\text{NRA}/\text{chl } a \text{ (nM-N hr}^{-1} \text{ mg}^{-1} \text{ m}^3) = 36(\pm 4) f; r^2 = 0.83$$

The result suggests that  $\text{NRA}/\text{chl } a$  may potentially be used as supplement for measuring the  $f$  ratio because the measurements of  $\text{NRA}$  and  $\text{chl } a$  are much easier than those of new production and primary production. Furthermore,  $\text{chl } a$  can be estimated by an empirical equation of  $\text{chl } a$  and fluorescence obtained from fluorescence sensor (Gong et al., 1993).

Table 4-4. Properties of the photic zone to  $PZD_{01}$  in different hydrographic regimes of the East China Sea

Sta.	Depth (m)	$NU_{01}$	$NRA_{01}$ (mg-N m <sup>-2</sup> h <sup>-1</sup> )	$NU_{01}'$	$NU_{01}'/NU_{01}$	$NU_{01}$ (mg-C m <sup>-2</sup> d <sup>-1</sup> )	$PP_{01}$	$f$ ratio
11	29	2.61	3.59	3.90	1.50	178	556	0.32
15	36	2.31	2.25	2.44	1.06	157	645	0.24
26	19	4.06	4.09	4.43	1.09	276	604	0.46
30	29	1.17	1.43	1.55	1.32	80	489	0.16
52-1	40	nd	2.35	2.55	nd	nd	nd	nd
52-3	45	4.02	3.41	3.70	0.92	274	1155	0.24
55-3	78	1.16	0.34	0.36	0.32	25 <sup>#</sup>	294	0.08
55-5	100	nd	0.49	0.55	nd	nd	nd	nd

nd - no data

$PZD_{01}$  - Photic zone depth to 1 % of surface photosynthetically active radiance (PAR).

$NU_{01}$ ,  $NU_{01}'$ ,  $NRA_{01}$ ,  $PP_{01}'$  - Depth integrated NU, NU estimated from NRA,

NRA and primary production to  $PZD_{01}$ .

$f$  ratio -  $NU_{01}/PP_{01}$ , both in mg-C m<sup>-2</sup> d<sup>-1</sup>.

# - estimated from  $NRA_{01}$ .

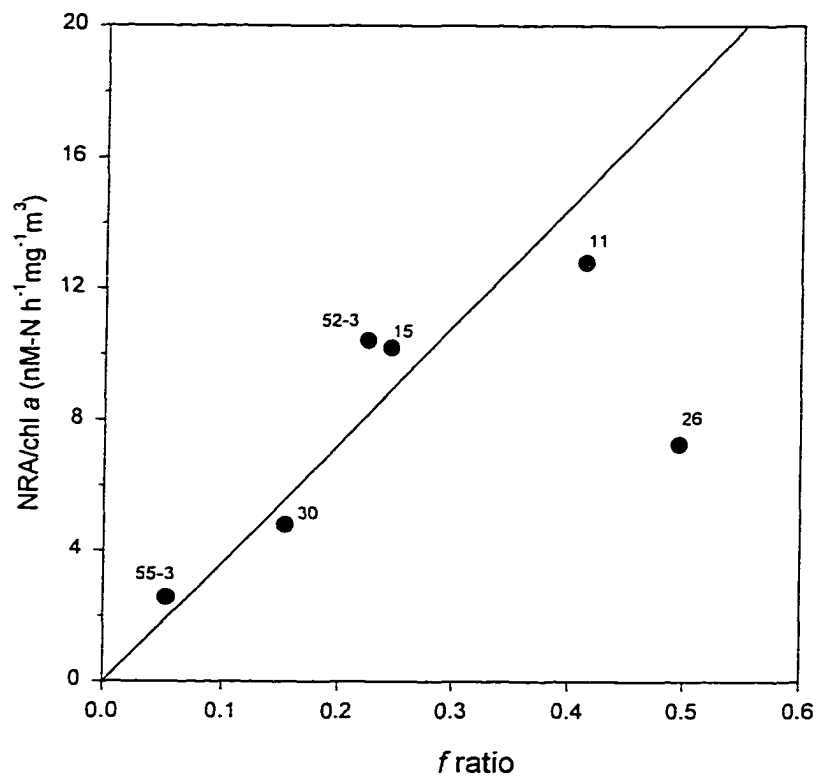


Fig. 4-13. The relationship between NRA/chl a and the f ratio within PZD<sub>10</sub>. The station number is indicated next to each data point. Solid line represents the Model II regression line when the data point from Sta. 26 is excluded.

### *Depth-integrated NRA and NU*

The depth-integrated NRA and NU down to PZD<sub>01</sub> at each station are also listed in Table 4-4. Higher values were found in the frontal zones at Stations 26, 11 and 15 (NRA<sub>01</sub> = 2.25 to 4.09 mg N m<sup>-2</sup> h<sup>-1</sup>, NU<sub>01</sub> = 2.31 to 4.06 mg N m<sup>-2</sup> h<sup>-1</sup>) and in the upwelling Kuroshio Subsurface Water at Stations 52-1 and 52-3 (NRA<sub>01</sub> = 2.35 to 3.41 mg N m<sup>-2</sup> h<sup>-1</sup>, NU<sub>01</sub> = 4.02 mg N m<sup>-2</sup> h<sup>-1</sup>). In contrast, even though the Changjiang Diluted Water is nitrate-rich, the depth-integrated NRA and NU in these waters at Station 30 (NRA<sub>01</sub> = 1.43 mg N m<sup>-2</sup> h<sup>-1</sup>, NU<sub>01</sub> = 1.17 mg N m<sup>-2</sup> h<sup>-1</sup>) were significantly lower. These suppressed levels of NRA and NU are consistent with the possibility that nitrate assimilation in coastal waters may be suppressed by the presence of other nitrogen forms (ammonia and/or DON) (Harrison et al., 1987). The lowest depth-integrated NRA and NU were found in the oligotrophic Kuroshio at Station 55-3 and 55-5 (NRA = 0.34 - 0.49 mg N m<sup>-2</sup> h<sup>-1</sup>, NU = 1.16 mg N m<sup>-2</sup> h<sup>-1</sup>). The lower NU and NRA in the Kuroshio relative to those in the upwelling region are consistent with the expected decrease in the *f* ratio from the upwelling region to open ocean waters (Eppley, 1989).

The depth-integrated of NU<sub>01</sub> can be estimated from NRA<sub>01</sub> by using the relationship between NU and NRA (NU = 1.08 NRA) in Table 4-4, and these estimated values, NU<sub>01</sub>', are summarized in Table 4-4. The estimated NU<sub>01</sub>' in the oligotrophic water (Sta. 55), the coastal plume (Sta. 30), the upwelling water (Sta. 52) and the shelf waters (the average of Stations 11, 15 and 26) were 0.4, 1.5, 3.3 and 3.6 mg-N m<sup>-2</sup> h<sup>-1</sup>, respectively. In comparing with <sup>15</sup>NO<sub>3</sub><sup>-</sup> uptake (NU<sub>01</sub>), the NU<sub>01</sub>' is slightly higher than NU<sub>01</sub> (except Sta. 55) while they are analogous to each other. The ratio of NU<sub>01</sub>' to NU<sub>01</sub> at these five stations

ranged from 0.92 to 1.5. The little high values ( $NU_{01}$ ) were probably caused by the decoupling between NRA and NP in waters with %PAR between 1% and 10%. When the estimated NU ( $NU_{10}$ ) and the measured NU ( $NU_{10}$ ) were integrated only down to  $PZD_{10}$ , the average ratio of the two rates dropped to  $1.01 \pm 0.17$  (Table 4-3). However, the contribution of this type of water (1 %PAR to 10%PAR) relative to the total  $NU_{01}$  was usually small, the effect was minimal in terms of other uncertainties from the determinations of NRA and NU. In addition, it should be mentioned that the estimated NU (from NRA) from oligotrophic ocean (Sta. 55) may be more or less underestimated if some small phytoplankton, *Prochlorococcus marinus* and *Synechococcus* sp., exist in the subsurface layer (Shimada et al. 1996). The relevant investigations about phytoplankton species are from Shimada et al. (1993; 1996) who indicated that the total fluorescence intensity of the prochlorophytes accounted for 32 to 63% of the sum of the total fluorescence intensity of all fluorescing phytoplankton detected at subsurface chlorophyll maxima in the West Pacific. In other words, the small phytoplankton ( $< 1 \mu\text{m}$ ) consist of 32 to 63 percent of total biomass. According to the reports of Shimada (1993 and 1996), the small phytoplankton in the subsurface are *Prochlorococcus marinus* and *Synechococcus* sp.. The diameter size in *Prochlorococcus marinus* ranges from 0.54 to 0.67  $\mu\text{m}$  and *Synechococcus* sp. ranges from 0.81 to 1.07  $\mu\text{m}$  (Morel et al., 1993). Theoretically, both GF/F and Gelman A/E would undersample *Prochlorococcus marinus* and Gelman A/E would partially undersample *Synechococcus* sp. relative to GF/F. However, Chavez et al. (1995) demonstrated that both glass-fiber GF/F and 0.2  $\mu\text{m}$  membrane filters can retain equivalent amounts of chl *a* in the open ocean waters of the Pacific Ocean. Further,



Venrick et al. (1987) indicated that 1.2  $\mu\text{m}$  GF/C filter passed an average of 4.4 to 8.9 % of the total chlorophyll, compared to 0.45  $\mu\text{m}$  Millipore filters in the Pacific Ocean. Cells smaller than the filter pore sizes can be retained on the filter because particles may clog the filter pores, particularly for large volume filtrations. Furthermore, the pore size of Gelman A/E filter (1.0  $\mu\text{m}$ ) is between GF/F (0.7  $\mu\text{m}$ ) and GF/C (1.2  $\mu\text{m}$ ) filters. Therefore, it is not likely that Gelman A/E would significantly undersample small phytoplankton. Assuming that the maximum missing rate of a Gelman A/E filter is 30 % for small phytoplankton, the missing chlorophyll will be 10 to 19 % (32 to 63 % multiplied by 30 %) of the total biomass obtained by using a Gelman Type A/E filter. In other words, NRA may be underestimated 10 to 19 % using the filter employed in this study.

#### *Comparison of NU estimated from NRA and previous NU data*

In this section, we compare our NU based on NRA estimates with Eppley's data (Table 4-5). Eppley (1989) has compiled the recent estimates from five upwelling areas and reported that the NU is from 1.6 to 8.1  $\text{mg-N m}^{-2} \text{h}^{-1}$  (average  $3.9 \pm 3.1 \text{ mg-N m}^{-2} \text{h}^{-1}$ ). Allen et al. (1996) found NU to be 3.7  $\text{mg-N m}^{-2} \text{h}^{-1}$  in the nutrient-rich water in the center of a cyclonic mesoscale eddy. Our value of 4.0  $\text{mg-N m}^{-2} \text{h}^{-1}$  falls well within this general range of reported values. In coastal regions, Eppley (1989) reported a range of 0.8 to 8  $\text{mg-N m}^{-2} \text{h}^{-1}$ . Our values of 2.3 to 4.1  $\text{mg-N m}^{-2} \text{h}^{-1}$  (average 3.2  $\text{mg-N m}^{-2} \text{h}^{-1}$ ) in the shelf waters outside of the plume of Diluted Changjiang Water also fall quite nicely within these reported values. Eppley (1989) also summarized the NU in oligotrophic oceans and reported that NU values range from 0.13 to 0.73  $\text{mg-N m}^{-2} \text{h}^{-1}$ . With the method of Garside

*Table 4-5. Review of previous comparison of  $^{15}\text{NO}_3^-$  new production<sup>1</sup> vs new production via nitrate reductase activity from different hydrographic realms*

Author ocean	Method	Upwelling	Coastal regions	Oligotrophic
Eppley (1989)	$^{15}\text{NO}_3^-$	1.6 ~ 8.1	0.8 ~ 8.0	0.13 ~ 0.73
Allen et al. (1996)	$^{15}\text{NO}_3^-$ -Chem.	3.7		0.42 ~ 0.63
Eppley and Koeve (1990)	Chem. <sup>2</sup>			0.55 ± 0.50 (day) 0.43 ± 0.28 (night)
This study <sup>3</sup>	$^{15}\text{NO}_3^-$ -NRA	4.0	2.3 ~ 4.1	0.36 and 0.53

1. NP (new production): unit is  $\text{mg-N m}^{-2} \text{h}^{-1}$ .

2. Chem.: Chemiluminescent nitrate analysis.

3. NP (0.36 and 0.53) in this study represent different casts.

(1982) to measure nitrate concentration and avoid the artifact of added  $^{15}\text{NO}_3^-$ , Allen et al. (1996) found that the NU in the oligotrophic North Pacific was  $0.42 \text{ mg-N m}^{-2} \text{ hr}^{-1}$ . In addition, Eppley and Koeve (1990) determined the uptake of nitrate by directly measuring the disappearance of ambient nitrate by using a chemiluminescent nitrate analysis at nM level (Garside, 1982). They reported that the NU values are  $0.55 \pm 0.5 \text{ mg-N m}^{-2} \text{ h}^{-1}$  during the day and  $0.43 \pm 0.28 \text{ mg-N m}^{-2} \text{ h}^{-1}$  at night in the eastern subtropical Atlantic Ocean. Our values of NU estimated from NRA in the oligotrophic Kuroshio ( $0.36$  and  $0.53 \text{ mg-N m}^{-2} \text{ h}^{-1}$ ) are quite comparable to these values. On the other hand, our measured value of NU ( $1.14 \text{ mg-N m}^{-2} \text{ h}^{-1}$ ) is significantly higher than these reported values. Thus, NRA may be a more reliable tool for estimating NP in oligotrophic waters than the traditional procedure of  $^{15}\text{NO}_3^-$  uptake without the simultaneous determination of the ambient concentration of nitrate by using an analytical method with a detection limit in the nanomolar level.

## Conclusions

NRA is almost equivalent to NU under light- and nitrate-replete conditions. Previous field studies failed to find a consistent relationship between NRA and NU probably because earlier NRA assay was inadequate and/or the light, nutrient, and hydrographic effects were not separated suitably. Thus, once the relationship between NRA and NU is established with some determinations of NRA and NU in a study area, the rate of nitrate uptake (NU) can be directly estimated by using NRA data alone. This NRA approach is particularly useful in oligotrophic oceans where the determination of NU by measuring  $^{15}\text{NO}_3^-$  uptake is difficult and suffers a number of limitations.

A positive relationship between NRA and chl *a* was found in this study with the highest ratio of NRA/chl *a* in shelf water and upwelling area while the lowest one was in the oligotrophic ocean. The NRA, NU and NRA/chl *a* in the upwelling water exceeded those in the oligotrophic Kuroshio surface water and in the fresher coastal plume by more than a factor of two. Productivity in the upwelling water was probably supported to a great extent by the utilization of plentiful nitrate. While the coastal plume was also nitrate-replete, the possible presence of other reduced combined nitrogen could have inhibited the uptake of nitrate. In the oligotrophic water, nitrate uptake was limited by the availability of nitrate so that recycled production was made necessary by this nitrate-deficient condition.

## CHAPTER V

THE RELATIONSHIP BETWEEN NRA AND IODINE SPECIATION  
IN THE SOUTHERN EAST CHINA SEA**Introduction**

Dissolved inorganic iodine is a biophilic element which exists in seawater primarily as iodate and iodide (Tsunogai and Henmi, 1971; Trusdale, 1978; Wong, 1991). Iodide is thermodynamically unstable relative to iodate in oxygenated seawater (Sillen, 1961; Wong, 1991). Theoretically, iodide should be undetectable in the oxic environment however, it is frequently found with iodate in the surface oceans (Tsunogai and Henmi, 1971; Tsunogai, 1971; Wong and Brewer, 1974, 1977; Elderfield and Trusdale, 1980; Wong and Zhang, 1992a; Wong, 1995; Campos et al., 1996; Tian et al., 1996). Tsunogai and Sase (1969) first suggested that the formation of iodide in the surface ocean is mediated by the enzyme of bacterial nitrate reductase. Tsunogai and Henmi (1969) suggested that the reduction of iodate may be intertwined with nitrate uptake by phytoplankton. Kuenzler (1969) suggested that zooplankton can excrete iodide under natural conditions. Butler et al. (1981) reported that *Skeletonema costatum* can incorporate iodate during incubation process but other phytoplankton (*D. tertiolecta*, *A. japonica* etc.) do not. Udomkit and Dunstan (1991), Moisan et al. (1994) and Udomkit (1994) found that iodate can be sequestered by marine phytoplankton and that iodide is released in the process simultaneously. Although the presence of iodide in surface waters has long been considered to be biologically mediated, the detailed mechanism is still unknown (Wong, 1991).

Knowledge of the formation of iodide in the surface ocean is still poorly understood, although dissolved iodine in surface oceans does show remarkable evidence of being linked

with biological activity. Wong and Zhang (1992) suggested that the rate of iodide production may be related to nitrate reduction rate since they found that the ratio of iodate to iodide was high ( $<0.5$ ) when the concentration of nitrate plus nitrite was above  $0.5 \mu\text{M}$ , e.g. nitrate reduction was active. Campos et al. (1996) found that iodate is reduced to iodide in surface waters by biological processes and proposed that variations of dissolved iodine in surface waters is associated with primary production. Tian et al. (1996) observed that the monthly variations of dissolved iodine in the Mediterranean Sea and pointed out that iodide concentrations in surface waters increased from  $40 \text{ nM}$  (May) to  $80 \text{ nM}$  (November). In that period of iodide increase, the production in surface waters is mainly supported by recycled nutrients, i.e. regenerated production. Thus, they proposed that the transformation of iodate to iodide in surface waters is associated with the regenerated production.

When considering these different postulations, the nitrate reductase (NR) hypothesis of Tsunogai and Sase (1969) seems to be the most reasonable of those listed since the chemical structures of iodate ( $\text{IO}_3^-$ ) is similar to nitrate ( $\text{NO}_3^-$ ), and since nitrate uptake is a ubiquitous biological activity. In addition, Balch (1985, 1987) and Balch et al. (1987) have successfully used  $^{36}\text{Cl}$ -labelled chlorate to study nitrate transport and the rate of transport of chlorate into the cells has been shown to be linearly related to the rate of nitrate uptake in both laboratory cultures of marine phytoplankton and in field investigations. If this NR hypothesis is proven, iodate reduction may be used as an analogue for studying nitrate uptake and thus new production similar to the approach of using  $^{36}\text{Cl}$ -labelled chlorate (Wong, 1991, Wong and Zhang, 1992). However, there is presently no NR field

data that has been related to the variations of dissolved iodine in the oceans.

This study reports pioneering evidence to support the NR hypothesis that the reduction of iodate to iodide is caused by NR produced by phytoplankton. In addition, the global new production can be estimated by applying a conceptual model of the cycling of dissolved iodine.

### **Materials and methods**

Eight stations were occupied in a transect across the southern East China Sea between May 2 and 15, 1996 aboard the R/V Ocean Research I during Cruise ORI-449 of the Kuroshio Edge Exchange Processes (KEEP) Study. The locations of the station are shown in Fig.5-1. At each station, the measurements of temperature and salinity were the same as the description of Chapter III. Sub-samples were then acquired for the determination of the dissolved iodine species and nitrate reductase activity (NRA).

The sub-samples for the determination of dissolved iodine species were drawn, stored frozen in polyethylene bottles (Wong, 1973), and then returned to the shore-based laboratory for analyses. Both iodate and iodide were determined by using a EG&G-PAR Model 384B-4 polarographic analyzer system with a Model 303A static mercury drop electrode. Iodate was determined directly by differential pulse polarography (DPP) according to the method of Herring and Liss (1974) as modified by Wong and Zhang (1992b). The precision for the determination of iodate was  $\pm 1$  % (RSD) at 100 nM of iodate and the detection limit of iodate was about 20 nM. Iodide was determined directly by cathodic stripping square wave voltammetry by the method of Luther et al. (1988) as

modified by Wong and Zhang (1992b). The precision for the determination of iodide was  $\pm 3\%$  (RSD) at 100 nM of iodide and the detection limit of iodide was approximately 5 nM.

Sub-samples for the determination of NRA and the dissolved iodine species were obtained from the same samples at Stations 49, 50, 51, 52 and 53. At Sta. 55, they were drawn from different casts. NRA was determined on board ship by a slightly modified version of the method of Hochman et al. (1986) and its detailed procedures were described in Chapter III.



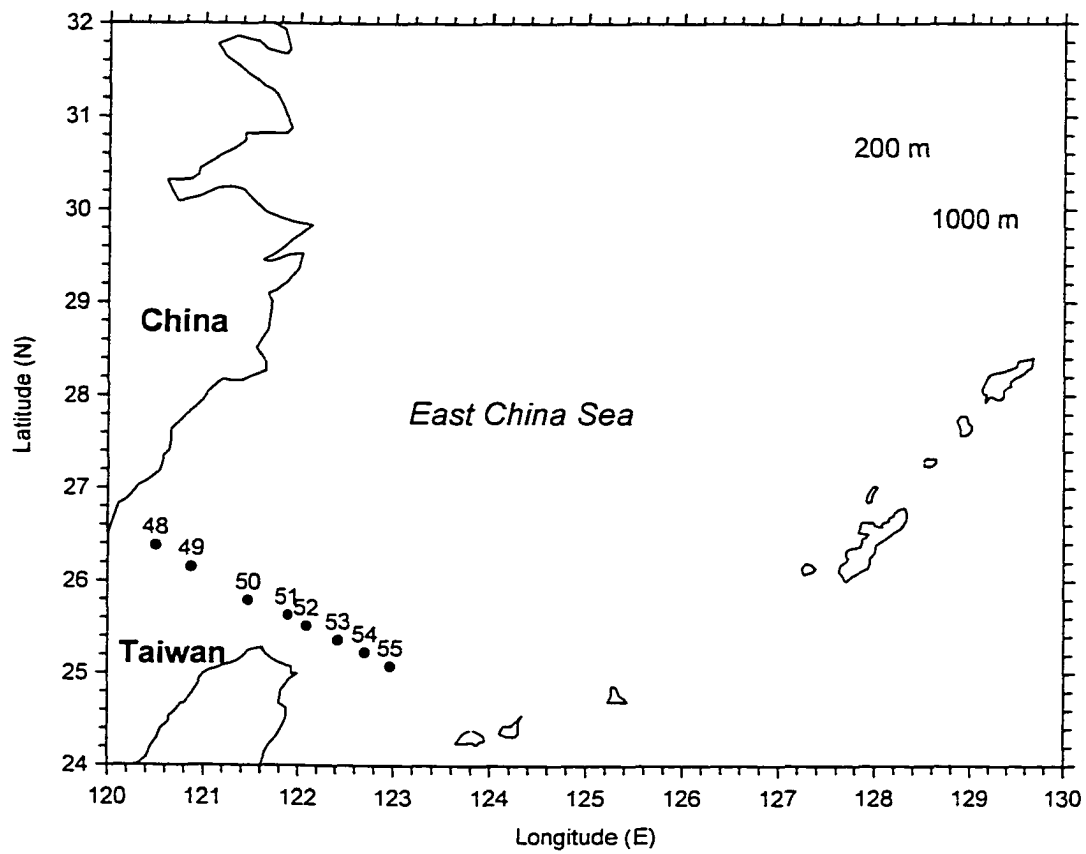


Fig. 5-1. The study area of iodine species in the southern East China Sea.

## **Results and discussions**

### *Hydrography*

The hydrographic characteristics in the southern East China Sea are described in Chapter III and IV. The contours of temperature and salinity in this transect are shown in Figures 5-2 and 5-3, respectively. Briefly, at least four distinct water masses were clearly shown in this transect. The colder and fresher Coastal Water (CW) with low nitrate concentration (see Chapter III) was found at Stations 48 and 49. The warm, intermediate salinity and nitrate-depleted Taiwan Current Warm Water (TCWW) was occasionally found at Sta. 50. The nitrate-rich, more saline, and cold Kuroshio Subsurface Water (KSW) was present at Stations 51, 52 and 53. The center of upwelling seemed to be located at Sta. 52 as indicated by the lowest temperature and highest nitrate concentration observed on the transect. The highest temperature, highest salinity and nitrate impoverished Kuroshio Surface Water was found at Sta. 55. Sta 54 was located at the boundary between Kuroshio Surface Water and Kuroshio Subsurface Water.

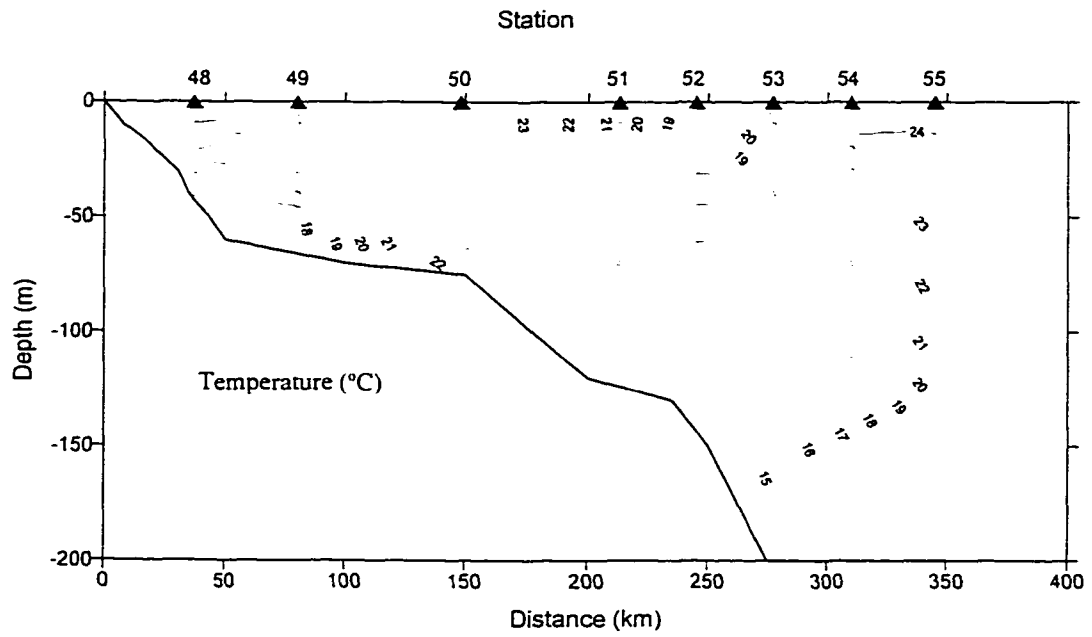


Fig. 5-2. Contours of temperature in the transect along the southern East China Sea.

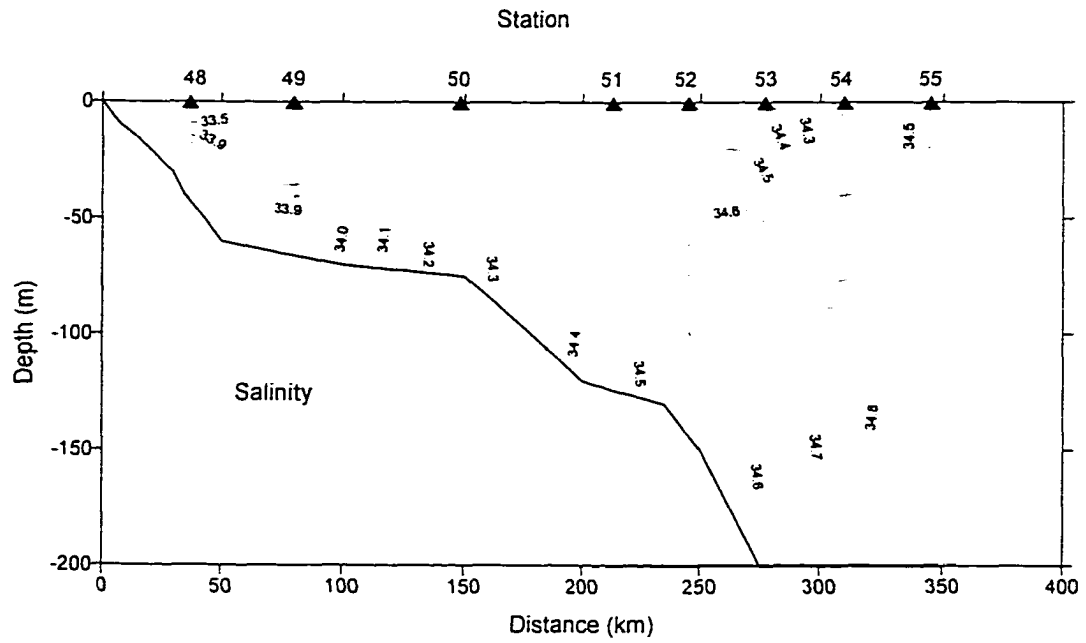


Fig. 5-3. Contours of salinity in the transect along the southern East China Sea.

*Depth profiles of hydrography, NRA, N-IO<sub>3</sub><sup>-</sup>, and N-I<sup>-</sup>*

The vertical distribution of sigma- $\theta$ , nitrate, NRA, N-iodate (N-IO<sub>3</sub><sup>-</sup>) and N-iodide (N-I<sup>-</sup>) at Stations 49, 53 and 55 are shown in Figs 5-4 to 5-6. N-IO<sub>3</sub><sup>-</sup> and N-I<sup>-</sup> represent the concentrations of iodate and iodide which were normalized to a salinity of 35, which corrects any effects of salinity on iodine distribution. The detailed data of NRA, iodine speciation at stations 48, 49, 50, 51, 52, 53, 54 and 55 are shown in appendix E. In the coastal water (Sta. 49), the water column was well mixed (down to ~ 30 m), whereas nitrate was exhausted within the upper 20 m (Fig. 5-4). High NRA was found in the surface layer and values decreased with depth to a low level (20 nM). The concentrations of N-IO<sub>3</sub><sup>-</sup> within the mixed layer in coastal area did not show significant variations and the concentration remained at a low level below 310 nM. Similarly, the distribution of N-I<sup>-</sup> within the mixed layer had the same structure as the N-IO<sub>3</sub><sup>-</sup> distribution. However, slightly higher levels of N-IO<sub>3</sub><sup>-</sup> (< 330 nM) and N-I<sup>-</sup> (140 ~150 nM) were found below the mixed layer at this station. Simultaneously, the gradient of sigma- $\theta$  and nitrate below the mixed layer (20 m) dramatically increased with depth suggesting that another water mass was present in this water column.

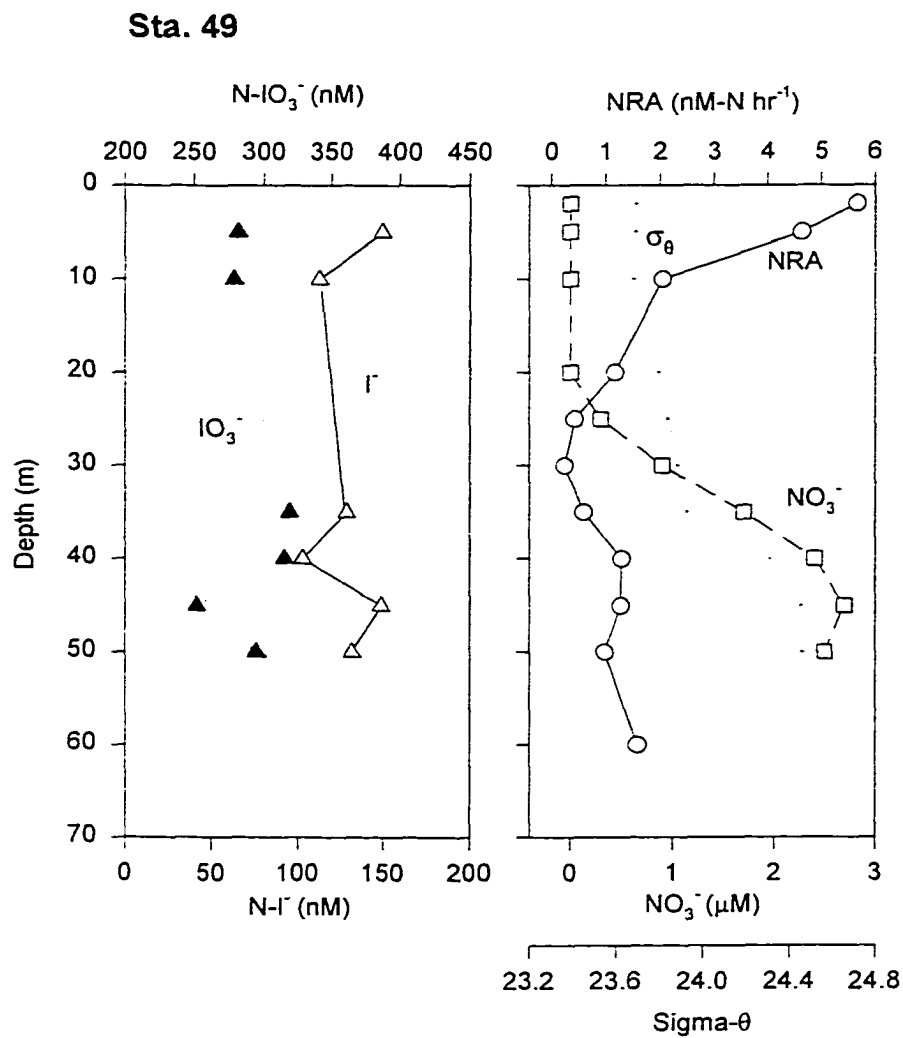


Fig. 5-4. The vertical distribution of  $N-IO_3^-$ ,  $N-I^-$ ,  $NO_3^-$ ,  $\sigma_\theta$ , NRA at Sta. 49.

At Sta. 53, in the upwelling region, cold, nutrient-rich waters were upwelled onto the surface layer and spurred high biological productivity (Fig. 5-5). The highest NRA was found in the surface layer and gradually decreased to below detection levels under the photic zone. Interestingly, the distribution of  $\text{N-I}^-$  above the photic zone closely followed the pattern of NRA. Conversely, the variation of  $\text{N-IO}_3^-$  above the photic zone seemed to show the reverse trend of distribution of NR. High  $\text{N-IO}_3^-$  was found at the base of the photic zone and rapidly decreased towards the surface. Essentially, the depletion of  $\text{N-IO}_3^-$  and increase of  $\text{N-I}^-$  were mutually coupled together and appeared to be mirror-images in the photic zone. Additionally, a tongue of the highest  $\text{N-IO}_3^-$  (390 ~ 420 nM) and lowest  $\text{N-I}^-$  (20- 40 nM) waters were found below the photic zone in the upwelling area where high  $\sigma_{\theta}$  (24.6 - 25.6) and nitrate-rich (8-12  $\mu\text{M}$ ) waters were also present. This suggested that the bottom waters at Stations 51, 52 and 53 are mostly from the Kuroshio Subsurface Water. According to the investigation of Lin (1995), the characteristics of water in the Okinawa Trough were nitrate-rich (11  $\mu\text{M}$ ), high  $\text{N-IO}_3^-$  (450 nM) and low  $\text{N-IO}_3^-$  (8 nM). Thus, the characteristics of dissolved iodine from upwelling origin is iodate-replete and iodide-depleted.

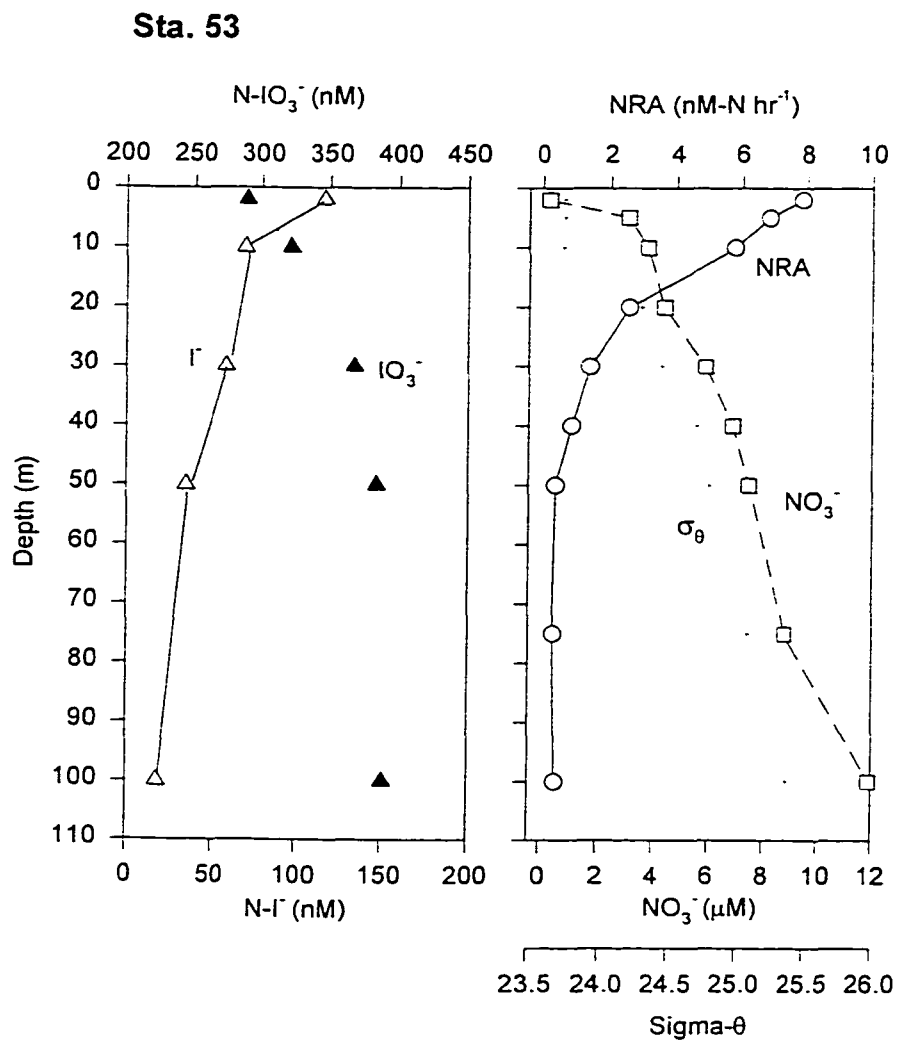


Fig. 5-5. The vertical distribution of N-IO<sub>3</sub><sup>-</sup>; N-I<sup>-</sup>, NO<sub>3</sub><sup>-</sup>; sigma-θ, NRA at Sta. 53.



The surface water in the oligotrophic area (Sta.55) was well mixed (0–40 m) and almost devoid of nitrate above the photic zone (70 to 100 m) (Fig. 5-6). The concentrations of  $\text{N-IO}_3^-$  (245 to 257 nM) and  $\text{N-I}^-$  (154 to 176) within the mixed layer did not vary significantly.  $\text{N-IO}_3^-$  below the mixed layer began to increase from 257 nM to a maximum value (410 nM) at a depth of 200 m, while  $\text{N-I}^-$  began to decrease from 176 nM to a minimum value (11 nM). Overall, the distributions of  $\text{N-IO}_3^-$  and  $\text{N-I}^-$  below the mixed layer at Sta. 55 were similar to those of  $\text{N-IO}_3^-$  and  $\text{N-IO}_3^-$  at upwelling region. They appeared as mirror-images, however, the largely uniform  $\text{N-IO}_3^-$  and  $\text{N-I}^-$  in the surface layer might have resulted from the physical transport of Equatorial Pacific Ocean waters rather than from *in situ* iodate reduction. According to previous investigations, the concentrations of iodide in the surface oceans at the equator of the Pacific Ocean and its adjacent seas ranged from 80 to 220 nM with an average of 150 nM (Cheng et al., 1993; Rue et al., 1997). The Kuroshio originates from the North Equatorial Current and its speed ranges from 1 to 3 knots (equal 44 to 133 km per day) from east of Luzon Island toward Japan along the continental slope of the East China Sea (Nitani, 1972). Assuming that the average speed of Kuroshio is 90 km d<sup>-1</sup> and the distance from the East China Sea to the Equator of Pacific Ocean is 15,000 km so that the turnover time of Kuroshio near the East China Sea is about 170 days. The residence time (10 years) of the surface ocean in the Pacific Ocean is much longer than the residence time of Kuroshio. Thus, the result suggests that the high iodide in the oligotrophic ocean (Sta. 55) may result from the North Equatorial Current.

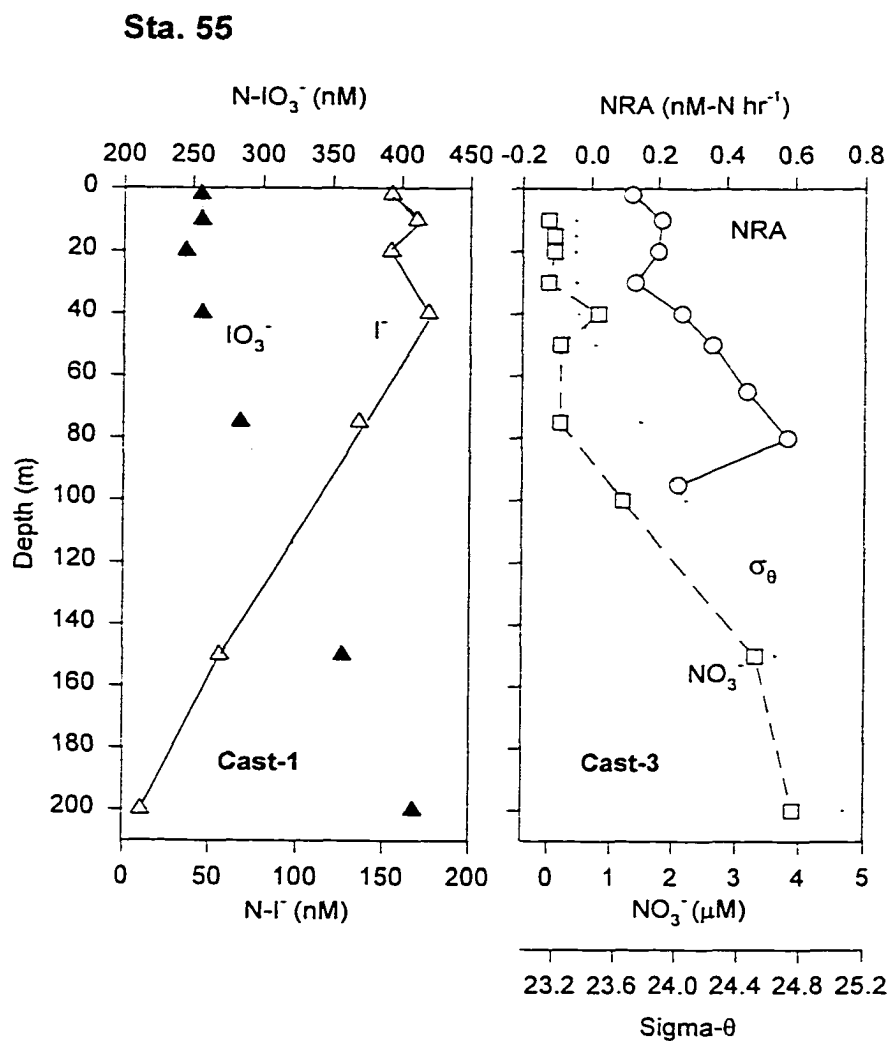


Fig 5-6 The vertical distribution of  $N-IO_3^-$ ,  $N-I^-$ ,  $NO_3^-$ ,  $\sigma_\theta$ , NRA at Sta.55.

### *Reduction of iodate to iodide*

The relationship between  $\text{N-IO}_3^-$  and  $\text{N-I}^-$  in this study transect is shown in Fig. 5-7. For all sampling locations,  $\text{N-IO}_3^-$  and  $\text{N-I}^-$  seemed to follow a negative linear band and the strong relationship between two variables yields a linear correlation:

$$[\text{N-IO}_3^-] = -0.97(\pm 0.05) [\text{N-I}^-] + 416(\pm 6) \quad r^2 = 0.87, n = 54 \quad \text{----- (5-1)}$$

where  $[\text{N-IO}_3^-]$  and  $[\text{N-I}^-]$  are in nM and  $n$  is the number of observations. The slope of the line is about -1 considering statistical uncertainties. Equation 5-1 clearly demonstrates that the production of iodide in surface water seems to be equal to the reduction of iodate. The coupling relationship suggests that the interconversion between iodate and iodide is the main process regulating the speciation of iodine in these waters because the concentrations of total iodine (iodate + iodide) seemed to be constant. In other words, when iodate was taken up or reduced by marine organisms, most of iodate was not accumulated in particulate phase but exuded to the ambient seawater. This situation is sharply contrast with nitrate uptake in which nitrate is incorporated into the particulate phase. Analogous negative relationships between iodate and iodide have been reported by Wong and Zhang (1992a) and Wong (1995) in the South Atlantic Bight. However, Wong and co-worker also found that the relationships between iodate and iodide did not follow the -1:1 linear band when iodate was below 50 nM because some dissolved iodine may be converted to particulate form.

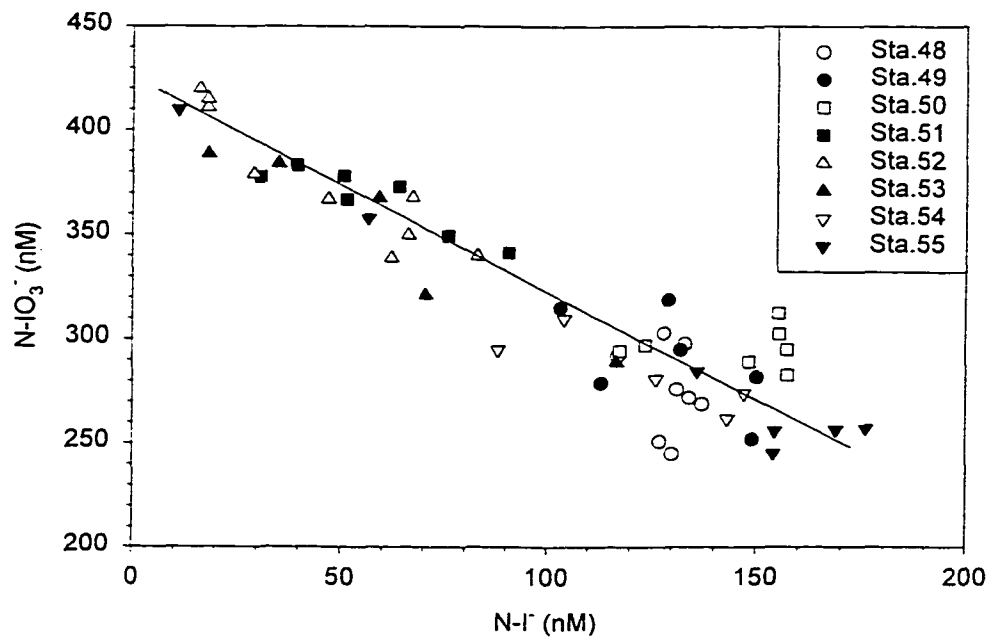


Fig. 5-7. The relationship between  $N-IO_3^-$  and  $N-I^-$  at all stations. Solid line represents the best fit regression line.

*A conceptual model for the cycling of dissolved inorganic iodine*

Undoubtedly, iodate and iodide play reciprocal roles in terms of the strong negative relationship between iodate and iodide in surface oceans. Thus, a conceptual model for the cycling of dissolved inorganic iodine is proposed (Fig. 5-8). (1) The iodate-rich (as well as nitrate-rich) and iodide-free deep water is transported to the surface oceans through upwelling. (2) Nitrate and iodate are simultaneously taken up by phytoplankton in the surface layer. (3) Iodate is quantitatively exuded as iodide rather than retained in the particulate form. Once formed, iodide is not oxidized back to iodate readily because iodide is metastable relative to iodate (Wong, 1980; Luther et al., 1995). Thus, the average concentration of iodate and iodide in surface water may represent the result of iodate reduction over the residence time of oceanic surface waters. If the reduction of iodate is coupled to nitrate uptake (new production), the changes in the speciation of dissolved inorganic iodine in the surface oceans will be an integrator of new production over time. However, the conceptual model is only suitable for upwelling system because the concentration of iodate and iodide in other marine environments may include two components: pre-existing concentration and *in situ* production through either iodate reduction or iodide oxidation.

It should be noted that  $\text{N-I}^-$  and  $\text{N-IO}_3^-$  in the coastal waters ( Stations 48, 49 and 50) did not follow the above linear relationship. Similar uncoupled behaviors of  $\text{N-I}^-$  and  $\text{N-IO}_3^-$  were also reported in the South Atlantic Bight (Wong and Zhang 1992c, Wong, 1995). This may be caused by the transformation of dissolved iodine to particulate organic iodine because iodine is an essential element for marine organisms (Wong, 1991).

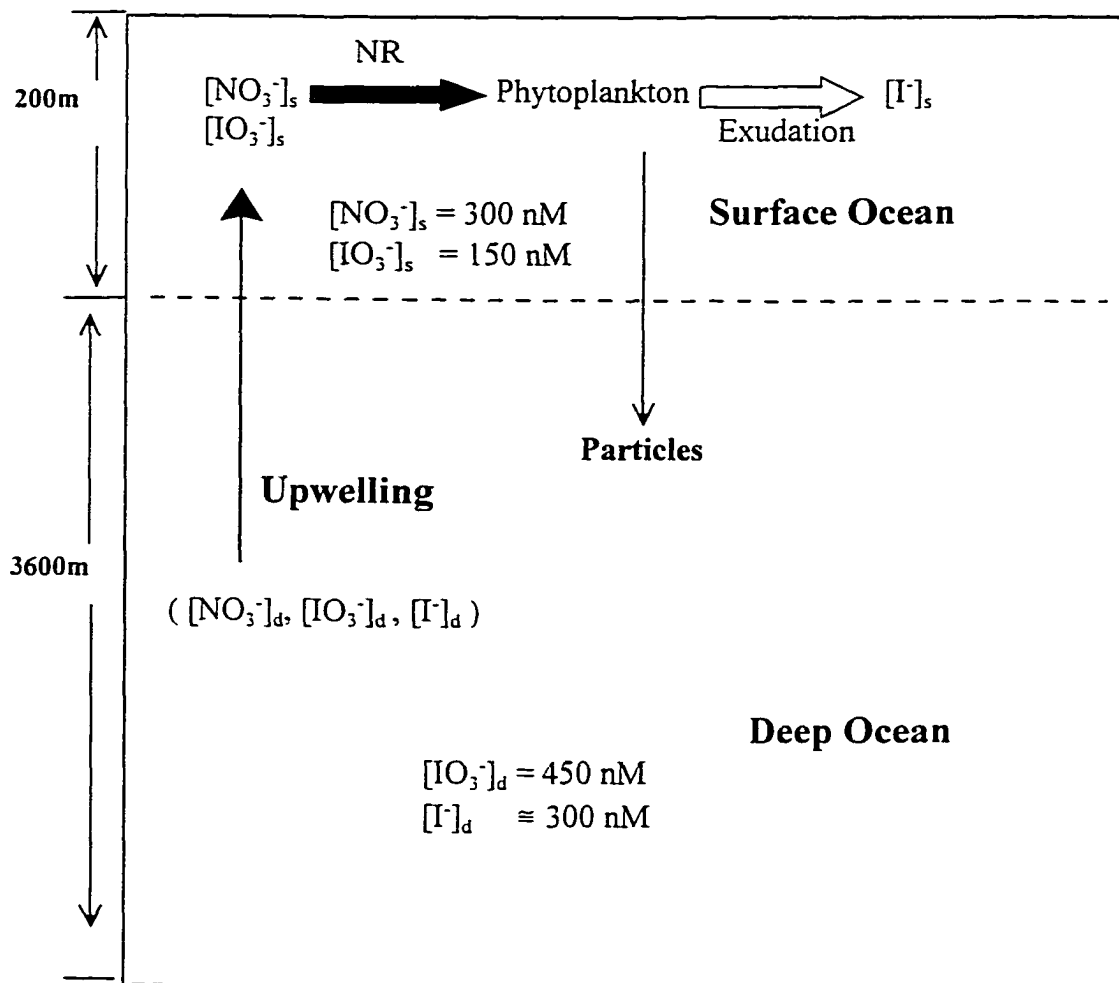


Fig. 5-8. A conceptual model for the cycling of dissolved inorganic iodine species in the surface oceans.

In addition, some iodine may be converted to dissolved organic iodine. Cheng (1998) and Wong and Cheng (1998) have found that a significant quantity of DOI exist in coastal waters.

*The estimation of new production using the production rate of iodate to iodide*

The relationships between  $\text{N-IO}_3^-$  and NRA, and  $\text{N-I}^-$  and NRA in the upwelling water are shown in Fig. 5-9. Both  $[\text{N-IO}_3^-]$  and  $[\text{N-I}^-]$  were strongly correlated to NRA so that

$$[\text{N-I}^-] = 8.0(\pm 1.3) \text{ NRA} + 33(\pm 5) \quad r^2 = 0.71, n = 18 \text{ ----- (5-2)}$$

$$[\text{N-IO}_3^-] = -9.2(\pm 1.1) \text{ NRA} + 389(\pm 4) \quad r^2 = 0.82, n = 18 \text{ ----- (5-3)}$$

where the units of  $[\text{N-IO}_3^-]$  and  $[\text{N-I}^-]$  are nM. NRA unit is in  $\text{nM-N h}^{-1}$  and n is the number of samples. The intercepts in the two equations represent the composition of the source water. The slopes in the two equations have opposite signs but their absolute values were indistinguishable according to statistical uncertainties. The strong correlations among  $\text{N-IO}_3^-$ ,  $\text{N-I}^-$  and NRA provide evidence that the formation of iodide in surface water is mediated by phytoplankton NR. Alternately, the results also clearly illustrate that the reduction of iodate by NR in the upwelling zone is almost identical to the production of iodide.

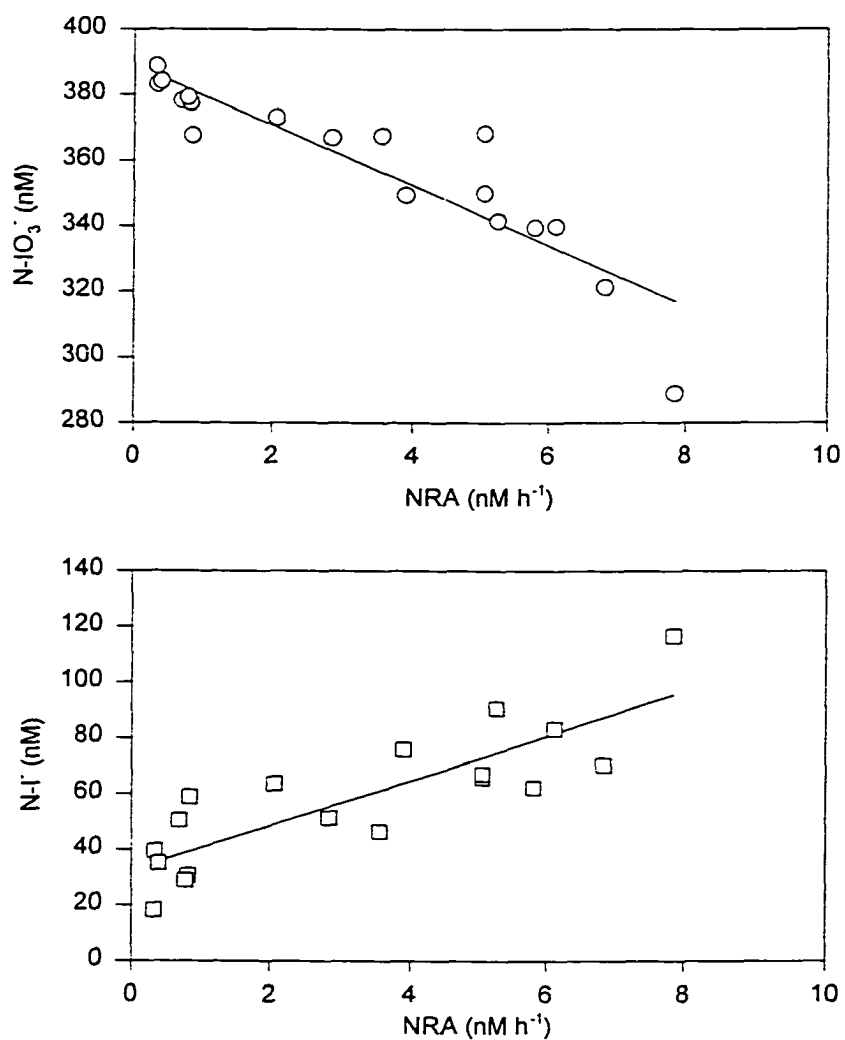


Fig. 5-9. The relationship between NRA and N-IO<sub>3</sub><sup>-</sup> (upper panel), and NRA and N-I<sup>-</sup> (lower panel) in the upwelling areas (Stations 51 to 53).



Furthermore, according to the conceptual model,

$$\delta [N-IO_3^-] = \Delta[N-I^-] = IRA \times \tau \text{ ----- (5-4)}$$

where  $\delta [N-IO_3^-]$  is the deficit in  $[N-IO_3^-]$  and  $\Delta[N-I^-]$  is the enrichment in  $[N-I^-]$  in the upwelling water relative to its source water. IRA is the iodate reduction activity and  $\tau$  is the residence time of the upwelling water which is controlled by the physical dynamics of the upwelling system. If

$$IRA = NRA \times (IRR / NRR) \text{ ----- (5-5)}$$

where IRR is iodate reduction rate and NRR is nitrate reduction rate, therefore, IRR/NRR is the biological discrimination factor of the enzyme nitrate reductase for selecting between  $IO_3^-$  and  $NO_3^-$ . Then, equations (5-4) and (5-5) can be combined and rewritten as follows.

$$(\delta [N-IO_3^-] / NRA) = (IRR / NRR) \times \tau \text{ ----- (5-6)}$$

Where  $\delta [N-IO_3^-]/NRA$  is the slope of the relationship between  $\delta [N-IO_3^-]$  and NRA or  $9.2(\pm 1.0) \text{ nM-IO}_3^- \text{ nM}^{-1}\text{-NO}_3^- \text{ h}^{-1}$  in this case. The value of (IRR/NRR) is still unknown to date. Moisan et al., 1994 reported that iodate uptake rates ranged between 0.003 and 0.24  $\text{n mol-IO}_3^- \mu\text{g chl } a \text{ h}^{-1}$  in laboratory cultures, and 0.08 and 0.26  $\text{n mol-IO}_3^- \mu\text{g chl } a \text{ h}^{-1}$  in two field experiments. Assuming that the average IRR is about 0.10 ( $\pm 0.01$ )  $\text{n mol-IO}_3^- \mu\text{g-chl } a \text{ h}^{-1}$ . The NRA was determined twice at Sta. 52 by measuring  $^{15}\text{N}$ -labelled nitrate uptake and the average value was 8  $\text{nmol NO}_3^- \mu\text{g chl } a \text{ h}^{-1}$  (Chapter IV). If the average values of the reported iodate uptake rates ( $0.10 \pm 0.01$ ) and nitrate uptake rates (8) at Sta. 52 are used, then (IRR/NRR) can be estimated to be about 0.0125 (1/80) and  $\tau$  may be estimated to be  $31 \pm 3$  days. Thus, the residence time in this upwelling system was about one month. By using the nitrate uptake approach (Chapter IV), the residence time of

upwelling water in the southern East China Sea is 30 days. The new production in the upwelling zone (Sta. 51, 52 and 53) can be estimated as following equation.

$$NP = \Delta[N-I^-] / \tau \times (NRR / IRR) \text{ ----- (5-7)}$$

Where NP represents the new production in the upwelling zone and  $\Delta[N-I^-]$  represents the enrichment in  $[N-I^-]$  the photic zone.  $\tau$  and NRR/IRR are assumed to be 30 days and 80. The background of  $N-I^-$  in the upwelling water is 16 nM (from the deepest sample). The enrichments of iodide at Stations 51, 52 and 53 are 1166, 1860, and 1787  $\mu\text{mol m}^{-2}$ , respectively. The production rates of iodide at these three stations are 39, 62, 60  $\mu\text{mol m}^{-2} \text{d}^{-1}$ . Thus, the nitrate uptake or NP will be 1.8, 2.9, and 2.8  $\text{mg-N m}^{-2} \text{h}^{-1}$  at Sta. 51, 52 and 53, and the average NP is 2.5  $\text{mg-N m}^{-2} \text{h}^{-1}$ . Comparison of the NP obtained from iodine approach with other two approaches (NRA and  $^{15}\text{NO}_3^-$  uptake incubation), suggests that the NP values from iodine approach agree well with these two distinct methods (Table 5-1).

By using the nitrate uptake approach (NRA and  $^{15}\text{NO}_3^-$  uptake), the residence time of upwelling water in the southern East China Sea is 30 days. By using the mass balance of oxygen, the upwelled rate of subsurface water in East China Sea was estimated to be 5  $\text{m d}^{-1}$  (Liu et al. 1992b). Since the water depth at the shelf edge in the upwelling zone is about 100~130 m, the residence time of the upwelling water will be 20 to 26 d. Comparison of the data obtained from the iodine approach with two different means, suggests that the iodine approach seems to be reasonable.

The relationships between  $N-\text{IO}_3^-$  and NRA, and  $N-I^-$  and NRA outside of the upwelling zone at Sta. 49, 50, 55 (the data at Sta. 55 from different casts) are shown in Fig. 5-10. These data points of  $N-\text{IO}_3^-$  and  $N-I^-$  are far from the linear regression line in the

upwelling area and the sources of  $\text{N-IO}_3^-$  and  $\text{N-I}^-$  not only came from pre-existing concentrations but also contained *in situ* input or output of dissolved iodine. Thus, the conceptual model of dissolved iodine can not be used in the marine environment with high pre-existing dissolved iodine speciation.

*Table 5-1. NU and turnover time of upwelled water in the southern East China Sea*

Station	Iodine system NU	<sup>15</sup> NO <sub>3</sub> <sup>-</sup> incubation NU	NRA & NU	Oxygen system
51	1.8	nd	1.7	nd
52	2.9	3.9	2.9	nd
53	2.8	nd	1.9	nd
turnover time (τ, day)	30	27	35	20-26

The unit of NP is mg-N m<sup>-2</sup> h<sup>-1</sup> and nd is no data.

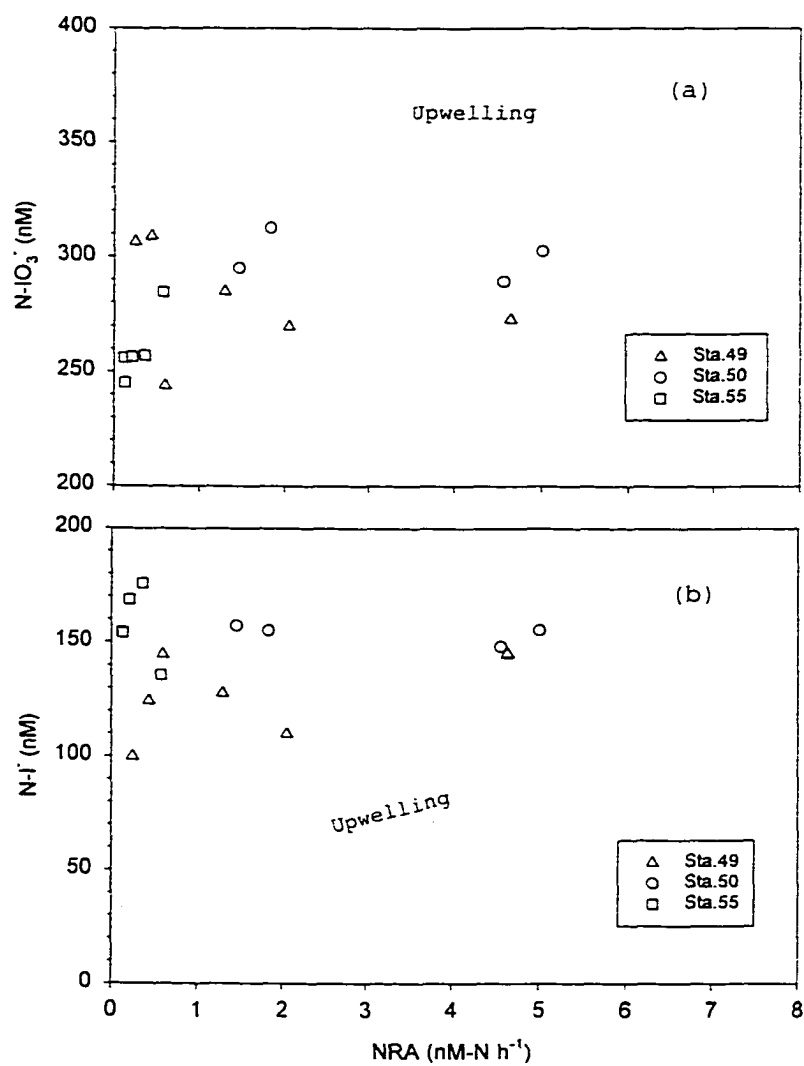


Fig. 5-10. The relationship between NRA and  $\text{N-IO}_3^-$  (upper panel), and NRA and  $\text{N-I}^-$  (lower panel) at Stations 49, 50 and 55. Dotted line is the relationship in the upwelling areas.

*Estimating global new production from global iodate depletion in the surface oceans*

Because the  $\text{NO}_3^-$  uptake rate and NRA were strongly correlated to each other under illuminated and nitrate-rich environments, with an average ratio of 1 (Chapter III), the NRA may represent the rate of  $\text{NO}_3^-$  uptake or new production in this environment. If the conceptual model of dissolved iodine is expanded to a global scale, the deficit of iodate or the production of iodide in surface oceans relative to the deep oceans may be equal to the accumulation of global new production over the residence time of surface oceans. The global new production can be estimated by the following equation.

$$\text{NP} = \delta [\text{N-IO}_3^-] / \tau \times (\text{NRR} / \text{IRR}) \text{ ----- (5-8)}$$

Where NP represents the global new production.  $\delta [\text{N-IO}_3^-] / \tau$  represents the deficient rate of iodate per year in the surface ocean and NRR/IRR is assumed to be 80. The average deficit of iodate in the surface oceans relative to the deep oceans is about  $0.15 \mu\text{M}$  (Wong, 1991, 1995). The average thickness of the surface mixed layer is 200 m. Then, the iodate deficit in the mixed layer is  $3 \times 10^4 \mu\text{mol m}^{-2}$ . Assuming the residence time of the surface waters in the oceans is about  $30 \pm 10$  years, the deficient rate of iodate by its reduction to iodide in the surface ocean is  $1000 \pm 300 \mu\text{mol m}^{-2} \text{y}^{-1}$ . Thus, the nitrate uptake or NP will be  $8 \pm 3 \times 10^4 \mu\text{mol-N m}^{-2} \text{y}^{-1}$  or  $6.4 \pm 2.4 \text{ g-C m}^{-2} \text{y}^{-1}$ . The global primary production is estimated to be from 44 to 50  $\text{Gt-C y}^{-1}$  (average  $47 \text{ Gt-C y}^{-1}$ ,  $1 \text{ Gt} = 10^{15} \text{ g}$ ) using different productivity algorithms (Antoine et al., 1996; Longhurst et al., 1995; Behrenfeld and Falkowski, 1997). The global oceanic primary production can be expressed as 122 to 139  $\text{g-C m}^{-2} \text{y}^{-1}$  with an average value  $130 \text{ g-C m}^{-2} \text{y}^{-1}$  (the area of the ocean is about  $3.6 \times 10^{14} \text{ m}^2$ ). Then, the *f* ratio will be about 0.03 to 0.07. The global new production has been

estimated to be 3.4 to 22 Gt C y<sup>-1</sup> with an average 9 Gt C y<sup>-1</sup> in previous literature (Chapter I) and  $f$  ratio should be estimated to be 0.07 to 0.47 (the global primary production is assumed 47 Gt-C y<sup>-1</sup>). The agreement between the values estimated from the dissolved iodine species and the reported values is actually rather remarkable in view of the preliminary nature in the approach taken here. For example, the value of (IRR/NRR) is poorly known. Furthermore, if there is any oxidation of iodate to iodide during the residence time of the surface oceans, then the reduction of iodate, the global new production, and the  $f$  ratio, will be underestimated.

## **Conclusions**

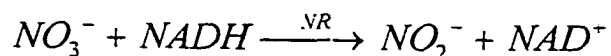
The results from this study provide field evidence that supports the idea that the depletion of iodate in the surface oceans is caused by a biological mediated reduction of iodate to iodide through the activity of the enzyme nitrate reductase. In the process, the iodate reappears in the dissolved phase as iodide almost quantitatively so that little of the iodate processed by the organisms is sequestered in the particulate phase. Thus, the depletion of iodate and the enrichment of iodide relative to the composition of the source water of a surface water mass represent an integration of NRA through the life time of the water mass. Global new production may be estimated from the global depletion of iodate or enrichment of iodide in the surface oceans.



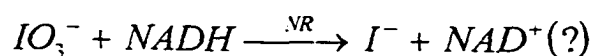
## CHAPTER VI

THE REDUCTION OF IODATE TO IODIDE BY NITRATE  
REDUCTASE IN MARINE PHYTOPLANKTON**Introduction**

Earlier investigations on the reduction of  $\text{IO}_3^-$  to  $\text{I}^-$  by phytoplankton yielded inconsistent results. Butler et al. (1981) indicated that *Skeletonema costatum* can incorporate iodate but other phytoplankton (*D. tertiolecta*, *A. japonica* etc.) do not. In recent studies, when the experimental conditions were stringently controlled, consistent results were observed. Moisan et al. (1994) demonstrated that several species of phytoplankton (*Thalassiosira oceanica* Hasle, *Skeletonema costatum*, *Emiliana huxleyi*, and *Dunaliella tertiolecta*) and natural marine phytoplankton can assimilate iodate. Udomkit (1994) reported that the uptake of iodate and the production of iodide were observed in certain phytoplankton cultures simultaneously. Tsunogai and Sase (1969) suggested that the reduction of iodate to iodide in the surface ocean may be mediated by the enzyme nitrate reductase. These results support the hypothesis that iodide formation in the surface ocean may be caused by the biologically mediated reduction of iodate through the activity of the enzyme nitrate reductase (NR). It is well documented that nitrate reductase involves nitrate reduction so that the reduction of nitrate to nitrite can be expressed as below.



Although the NR hypothesis has long been suspected, the direct evidence that NR catalyzes the reduction of iodate to iodide (as below) has seldom been reported.



Furthermore, direct measurement of iodate to iodide catalyzed by NR is very difficult. The objectives of this study were to develop a method for measuring iodate reduction by NR, to demonstrate that NR also reduces iodate to iodide, and to relate the rate of nitrate reduction to the rate of iodate reduction. In this research, a method based on the  $^{125}IO_3^-$  technique of Woittiez et al. (1991) was used for estimating the reduction of iodate to iodide in both phytoplankton cultures and in field collected marine phytoplankton.

## Materials and methods

### *Reagents*

All chemicals used were ACS reagent-grade.

Iodate ( $^{125}IO_3^-$ ) radiotracer preparation:  $^{125}IO_3^-$  solution was prepared by the method of Wong and coworkers (Takayanagi and Wong, 1986; Wong and Zhang, 1992). In this method,  $^{125}I^-$  stock (from New England Nuclear) was oxidized to  $^{125}IO_3^-$  with sodium hypochlorite under slightly basic conditions. The excess oxidizing agent was then destroyed with sodium sulfite. The high activity of  $^{125}I^-$  (1 mCi) was diluted to 1  $\mu$ Ci/ml with a 0.1 M  $Na_2CO_3$  solution containing ~ 1 mM KBr. Five ml of 1  $\mu$ Ci/ml  $^{125}I^-$  was pipetted into a 100 ml polyethylene bottle containing 10 ml of 0.5 M NaCl, 0.1 ml of 0.25 M KBr, and 0.1 ml of 50  $\mu$ M iodide ( $I^-$ ). Then, 0.2 ml of 0.2% of NaOCl was added to the solution. The solution was left standing for 1 hr before the addition of 0.1 ml of 0.4 M  $Na_2SO_3$  solution. The resulting  $^{125}IO_3^-$  solution was loaded into an AG1x8 column (i.d. 1 cm, length 14-15 cm,

nitrate form, flow rate about 2 ml/min)(Wong and Brewer, 1974). The first 5 ml of eluate was discarded. The rest of the  $^{125}\text{IO}_3^-$  eluate was collected in a 100 ml polypropylene bottle. The final solution was  $0.22 \mu\text{Ci/ml}$  in  $^{125}\text{IO}_3^-$  and  $0.22 \mu\text{M}$  in  $\text{IO}_3^-$ . At the beginning of the experiment, the concentration of  $\text{IO}_3^-$  and the activity of  $^{125}\text{IO}_3^-$  were adjusted to  $5.1 \mu\text{M}$  and  $0.18 \mu\text{Ci/ml}$  by using a working standard of iodate ( $20 \mu\text{M}$ ).

Iodate standard solution ( $20 \mu\text{M}$ ): Dry potassium iodate at  $80^\circ\text{C}$  for over night. Cool it in a desiccator. Add a 2.14 g of potassium iodate to a 1000-ml volumetric flask. Dissolve to the mark and its concentration of iodate is 10 mM. Store in a refrigerator. This solution is stable at least for 12 months. Pipet 1 ml of 10 mM of primary standard to a 50-ml flask and dilute to mark to make the secondary standard ( $200 \mu\text{M}$ ). Pipet 10 ml of  $200 \mu\text{M}$  of secondary standard to a 100-ml flask and dilute to mark and its concentration is  $20 \mu\text{M}$ .

Phosphate buffer solution ( $150 \text{ mM}$ , pH 7.8): Dissolve 39.19 g of  $\text{K}_2\text{HPO}_4$  in a small volume of distilled deionized water (DDW) in a 1000-ml of volumetric flask. Dilute the solution to volume and adjust its pH to 7.8 with phosphoric acid and NaOH.

NADH solution ( $6.5 \text{ mM}$ ): Dissolve 0.215 g Nicotinamide Adenine Dincieotide (NADH, reduced form, Sigma Co., N-6005) in a small volume of DDW in a 50-ml of flask and dilute the solution to volume. Store this solution in refrigeration ( $4^\circ\text{C}$ ) and keep it fresh.

Nitrate reductase (NR): Nitrate reductase ( $7.1 \text{ units/ml}$ , Sigma Co.) is stored at  $-70^\circ\text{C}$

without further purification.

Toluene: A.C.S. grade toluene (MCB) is used without further purification.

Solution of Pd<sup>-2</sup> (from PdCl<sub>2</sub>): Dissolved 0.1 g of PdCl<sub>2</sub> in a small volume of DDW (with little 1 M HCl) and dilute the solution to 100 ml. The concentration of Pd<sup>-2</sup> is 1000 μg/ml solution. Then dilute the stock solution (1000 μg/ml) to 500 μM Pd<sup>-2</sup>. The pH of both solutions is adjusted to 1.0 before experiment with HCl and NaOH.

Solution of Hydrazin: Dissolve 20 g of hydrazin in a small volume of DDW in a 100-ml of flask and dilute the solution to volume.

Charcoal: A.C. S. charcoal (DARCO, activated carbon) is used without further purification.

Artificial Seawater: Make a 5 liters of artificial seawater according to the method of Strickland and Parsons (1972).

### Apparatus

A Bicon, EG & G / Ortec, Model M127 / N gamma counting system was used. The counting system includes a high voltage power supply (0 ~ 3 KV), a 7.6 cm x 7.6 cm well-type NaI-Tl crystal detector, and a signal processor. When a sample is detected in the detector, the signal is first pre-amplified and then processed in a single channel analyzer with another amplifier (Ortec 490B). Finally, the signal of radiation is counted by a counter (Ortec 772) connected to a timer (Ortec 719). The precision of this counting system was about 1 % for 1 μCi/ml of <sup>125</sup>I.

### Phytoplankton cultures

*Skeletonema costatum* cultures (Greville) Cleve (SKEL) were obtained from the Provasoli-Guillard Center for The Culture of Marine Phytoplankton. *S. costatum* were

cultured in 1000-ml borosilicate Erlenmeyer flasks of  $f/2$  culture medium (Guillard and Ryther, 1962). Cultures grew in log phase at  $21 \pm 1$  °C on a 13:11 h light-dark cycle at an irradiance of  $65 \mu\text{mol photons m}^{-2}\text{s}^{-1}$  prior to the experiments on iodide production rate and the reduction of iodate to iodide with NR.

A volume of 30 ml of *S. costatum* culture was filtered for determining the rate of iodide production by NR. The analytical procedures for iodate reduction were the same as described in determination of iodate reduction by NR. NRA and chl *a* were measured with the same methods employed in the field investigation.

#### Natural phytoplankton assemblages

Water samples were collected at a depth of 0.3 m at Ocean View Beach in Norfolk, VA ( $36^{\circ}58'$  N,  $76^{\circ}16'$  W) on 10 and 14 July 1998 (at high tide 10:00 and 13:30), respectively. Other samples were collected at Lynnhaven Inlet in Virginia Beach, VA ( $36^{\circ}55'$  N,  $76^{\circ}06'$  W) on 16 July 1998, at low (10:10) and high tide (15:50). They were transported back to the laboratory, and then processed within 1 hr of sample collection.

Other sub-samples were obtained for the determination of chlorophyll *a* and nitrate reductase activity. Chl *a* was determined by the method of Strickland and Parsons (1972) and NRA was determined by a modified version of Hochman et al. (1986) method (see Chapter II).

#### *Procedures*

##### Determination of iodate reduction by NR

The analytical scheme for measuring iodate reduction by NR is shown in Fig. 6-1. One liter of seawater or 30 ml of the phytoplankton culture was filtered through a 47 mm

GF/C glass fiber filter. After filtration, the filtrate was discarded and the filter was transferred to a 50 ml pyrex beaker containing 1 ml of phosphate buffer, 50  $\mu$ l of toluene, 0.2 ml of NADH, and 0.1 ml solution of  $^{125}\text{IO}_3^-$  (0.18  $\mu\text{Ci/ml}$ ) and  $\text{IO}_3^-$  (5.1  $\mu\text{M}$ ). The beaker was agitated for 10 minutes at room temperature to turn the mixtures into a slurry. A 0.5 ml aliquot of the slurry was transferred with an Eppendorff pipette to a beaker containing 50 mg of charcoal, 0.5 ml of 500  $\mu\text{M}$  of  $\text{Pd}^{+2}$  solution and 10 ml of artificial seawater. The mixture was then stirred for 10 minutes on a stirrer and then filtered through a 25 mm GF/C glass fiber filter. The filter was placed in a 5 ml polyethylene vial and the activity of iodine on the filter was determined by a gamma counter. This fraction was called charcoal-adsorbable-palladium iodide ( $\text{PdCl}_2$ ). It contains primarily iodide while iodate was excluded. Another 0.5 ml aliquot of the slurry was transferred to a 50 ml beaker containing 20 mg of hydrazin, 100  $\mu\text{g}$   $\text{Pd}^{+2}$ , 50 mg charcoal and 10 ml of artificial seawater. The solution was stirred for 10 minutes and filtered through a 25 mm GF/C glass fiber filter. After filtration, the filtrate was discarded and the filter was again placed in a 5 ml polyethylene vial and the activity on the filter was determined by a gamma counter. This fraction was called charcoal-adsorbable total iodine including both iodate and iodide. In a control experiment, the same experiment was run without the enzyme extract.

#### Data processing

It is assumed that the ratio between radioactive  $^{125}\text{IO}_3^-$  and non-radioactive  $\text{IO}_3^-$  is constant throughout the iodate reduction and the radioactive  $^{125}\text{IO}_3^-$  is reduced to  $^{125}\text{I}^-$  at an analogous rate as the non-radioactive  $\text{IO}_3^-$  reduced to  $\text{I}^-$ . The iodate reduction rate can be calculated as following equation:

$$\text{Assuming } [A-\text{IO}_3^-]_0 = [A-\text{IO}_3^-]_t + [A-\text{I}^-]_t$$

$$[A-\text{IO}_3^-]_t = [A-\text{IO}_3^-]_0 - [A-\text{I}^-]_t$$

$$\frac{[A-\text{IO}_3^-]_t}{[\text{IO}_3^-]_t} = \frac{[A-\text{IO}_3^-]_0}{[\text{IO}_3^-]_0}$$

where  $[A-\text{IO}_3^-]_0$  represents the initial radioactivity of iodate.  $[A-\text{IO}_3^-]_t$  and  $[A-\text{I}^-]_t$  represent the radioactivity of iodate and iodide at a given time, respectively.  $[\text{IO}_3^-]_0$  represents the initial concentration of non-radioactivity iodate, and  $[\text{IO}_3^-]_t$  is the non-radioactivity iodate concentration at a given time. These three values of  $[A-\text{IO}_3^-]_0$ ,  $[\text{IO}_3^-]_0$ , and  $[\text{IO}_3^-]_t$  are known, thus

$$\text{the iodate reduction rate (IRR)} = [\text{IO}_3^-]_t / t = \left( \frac{[A-\text{IO}_3^-]_0}{[\text{IO}_3^-]_0} \times [\text{IO}_3^-]_t \right) / t$$

$$\text{the iodide production rate (IPR)} = [\text{I}^-]_t / t = ([\text{IO}_3^-]_0 - [\text{IO}_3^-]_t) / t$$

$t$  is the reaction time which is equal to 10 minutes in this experiment.

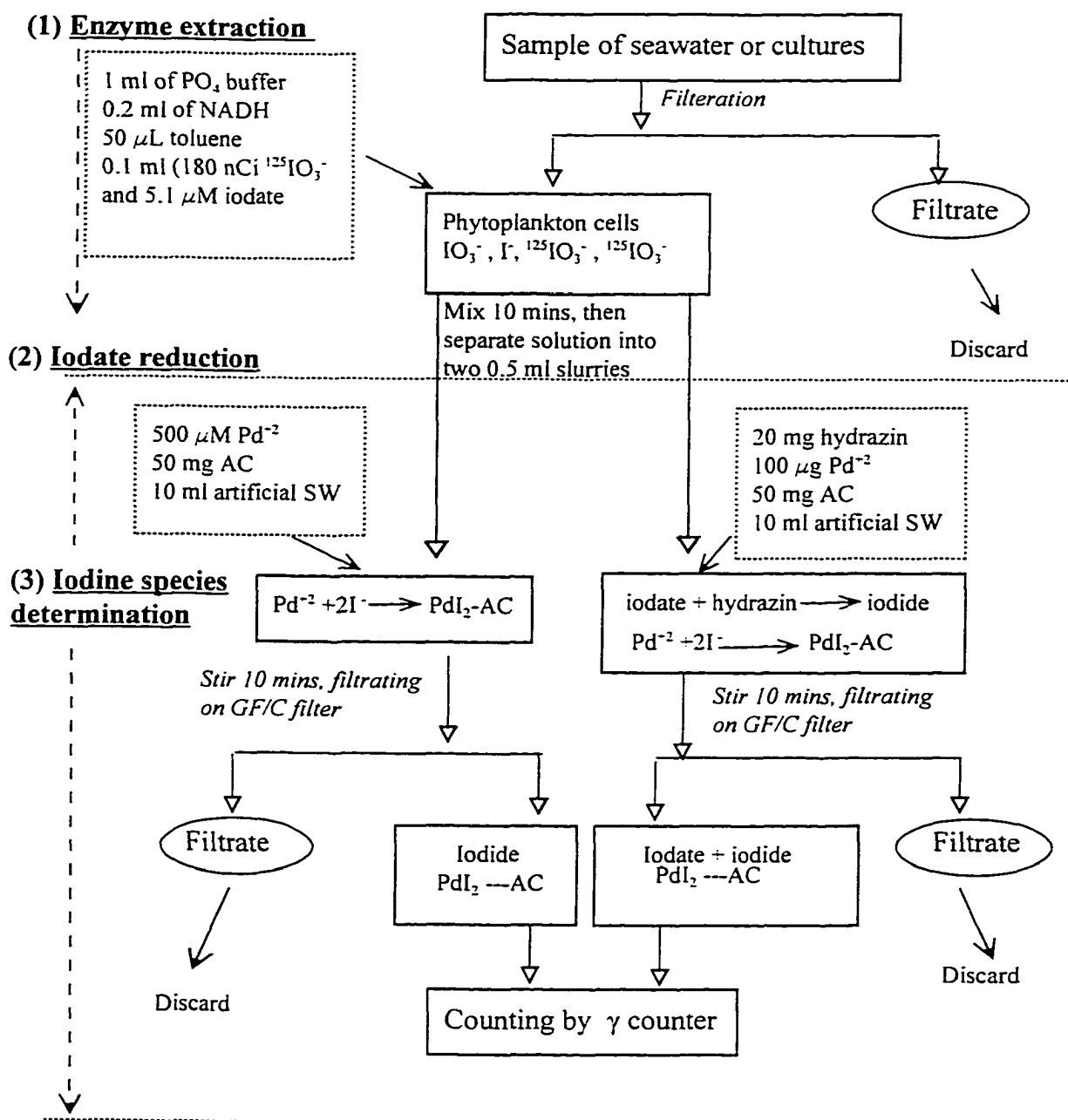


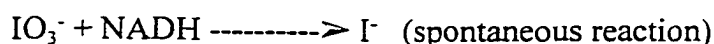
Fig. 6-1. The analytical scheme of reduction of iodate to iodide mediated by nitrate reductases. AC: activated charcoal.



## Results and discussions

### *Experimental blank*

Because iodide absorption by activated charcoal is variable, an iodide blank correction is necessary for calculating the rate of iodate reduction by NR. Thus, iodide blank experiments were conducted. The results are shown in Fig. 6-2. Treatment A contains reagents, but no NADH and NRA. Treatment B contains reagents and NADH, but no NRA. Treatment C contains reagents, and both NADH and NRA (NRA = 42,000 nM h<sup>-1</sup>, from Sigma Co.). In Fig. 6-2, the fractions of iodide gradually increased from treatment A (8%) to treatment B (19%), and to treatment C (25%). Simultaneously, the fractions of iodate gently decreased from treatment A (92%) to treatment B (81%) to treatment C (75%). In treatment A, this result demonstrates that iodide is indeed absorbed by activated charcoal even though there was no any iodate reduction. In treatment B, this result indicates that some of iodate was reduced to iodide even without the catalyzer, nitrate reductase. In other words,



the reaction of the reduction of iodate to iodide reacting with NADH may be spontaneous. This result supports the idea that the redox couple of NADPH/NADP<sup>+</sup> (reduced nicotinamide-adenine-dinucleotide phosphate) is a dominate route for electron transfer in biochemical processes (Morel, 1983; Weast et al., 1988; Wong, 1991; Tian et al., 1996). Thus, the combination of Type B (containing reagents and NADH but without NRA) is chosen as the controlling experiment. The reduction of iodate to iodide mediated by NR was found in treatment C while its rate of iodate reduction, 1 nM h<sup>-1</sup>, was very low relative

to the activity of NR (42,000 nM h<sup>-1</sup>).

#### *Comparison of commercial NR and marine NR*

It has been reported that iodate can be taken up effectively by cultures of *S. costatum* (Butler et al., 1981; Moisan et al. 1994). Therefore, NR extracted by *S. costatum* was used to determine the rate of iodate reduction. The result is shown in Fig. 6-3 where the fraction of iodide gradually increased from treatment A (8%) to treatment B (10%) and dramatically increased to treatment C (73%). Concomitantly, the fractions of iodate gently decreased from treatment A (92%) to treatment B (90%) and dramatically dropped to treatment C (27%). The variations of iodide fractions for treatments A and B were similar to the previous results while there was a big difference for treatment C. In other words, about 73% of iodate was reduced to iodide mediated by NR extracted from *S. costatum*.

The rate of iodate reduction by marine NR (73 % or 33 nM h<sup>-1</sup>) was much higher than that from Sigma NR (25% or 1 nM h<sup>-1</sup>). The total iodate concentration in the initial stage was different, but it indicated that marine NR was more effectively catalyzed by the iodate reduction than terrestrial NR. Furthermore, the activity in Sigma NR (42,000 nM h<sup>-1</sup>) was two orders of magnitude higher than marine NR extracted from *S. costatum* (400 nM h<sup>-1</sup>), while the rate of iodate reduction in the former was much lower than in the latter. Thus, *S. costatum* NR was used to replace the NR (from Sigma Co.) in this study.

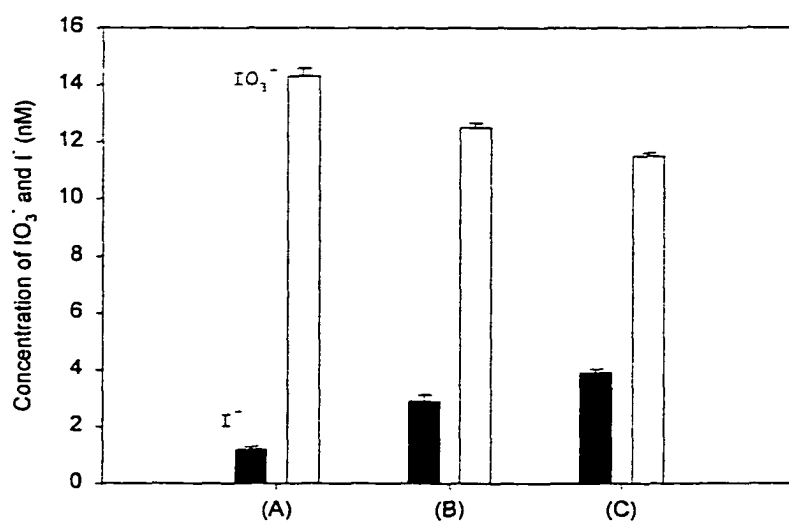


Fig. 6-2. The concentration of iodide and iodate in iodate reduction experiment (NR from Sigma Co.).  
(A): reagent only  
(B): reagent + NADH  
(C): reagent + NADH + NR

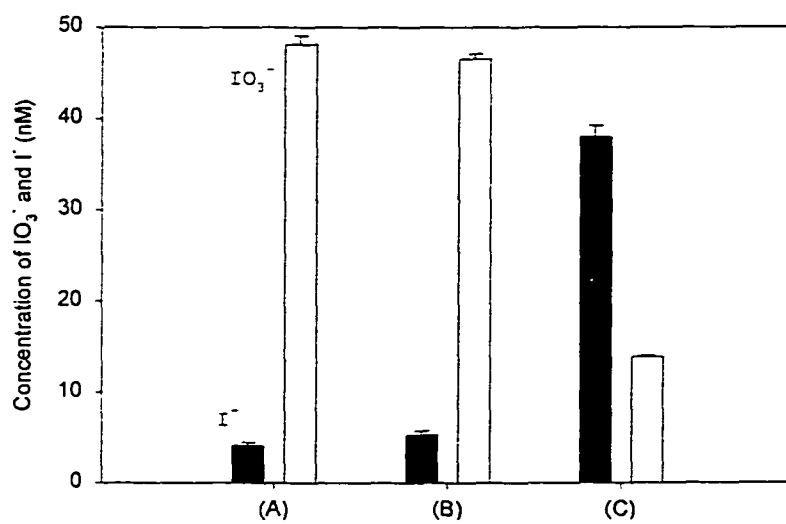


Fig. 6-3. The concentration of iodide and iodate in iodate reduction experiment (NR from *S. costatum*).  
(A): reagent only  
(B): reagent + NADH  
(C): reagent + NADH + NR

### *Effect of reaction time*

In order to gain the optimum reaction time of iodate reduction by NR, reaction time was varied while the other parameters such as pH, NADH, iodate concentration and phosphate buffer were fixed. The relationship between concentrations of dissolved inorganic iodine and reaction time are presented in Fig. 6-4. The concentration of iodide increased rapidly and almost linearly with time up to about 10 minutes of reaction time. At longer reaction times, no further increase in the concentration of iodide was found. Concomitantly, the concentration of iodate decreased rapidly and approximately linearly decreased up to a stable level about 10 minutes of reaction time. At longer reaction times, no further decrease in the concentration of iodate was found. Thus, a reaction time of 10 minutes was chosen in the analytical scheme.

The change in the concentration of iodide and iodate with reaction time suggests that the reduction of iodate to iodide was controlled by the enzyme activity in the first 10 minutes of reaction. At longer reaction times, there was no further reduction. This may suggest a result of the exhaustion of NADH through its reaction with iodate, and auto-degradation of NADH and/or the auto-degradation of NR. The exhaustion of iodate was unlikely since > 80% of the added iodate by the reaction was still present when its reduction ceased. Eppley (1978) reported that the incubation time for NR was 30 minutes, but the current incubation time is getting shorter and become 20 minutes (Hochman et al., 1986) and 10 minutes (Berges and Harrison, 1995). These results support that the activity of NR may be degraded quickly when NR was extracted from phytoplankton cells without appropriate storage.

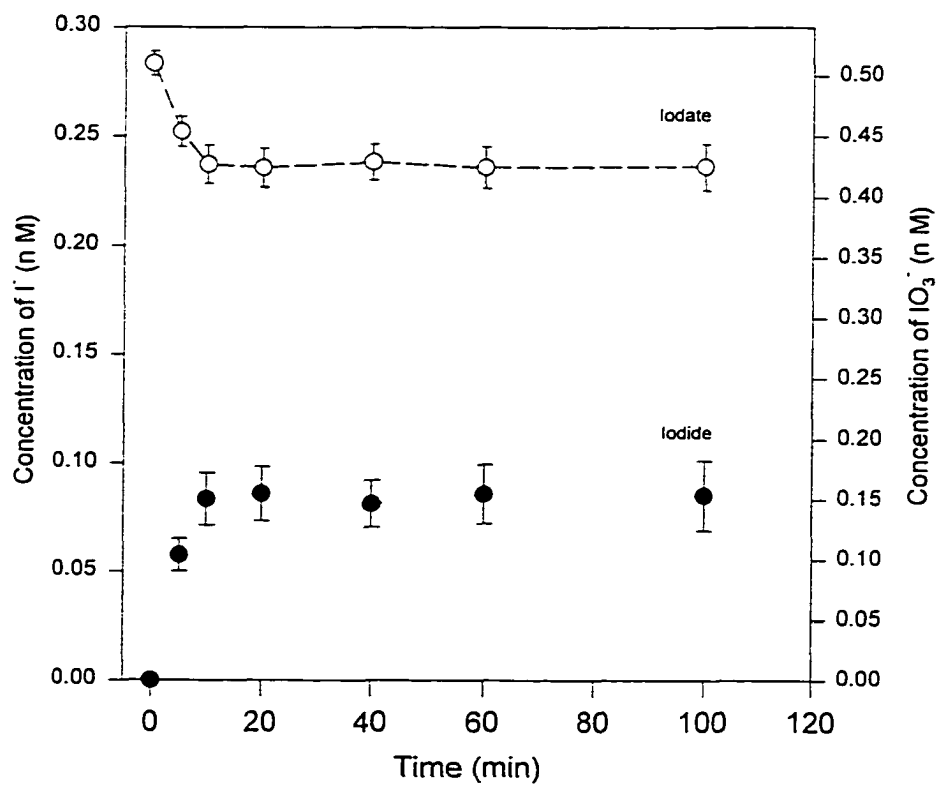


Fig. 6-4. The reduction of iodate to iodide by *S. costatum* NR at different reaction times.

*Effect of the concentration of  $IO_3^-$* 

The optimum iodate concentration for iodate reduction by NR was determined by using a culture of *S. costatum*. The concentration of added iodate was between 0.02 and 0.43  $\mu\text{M}$  (final concentration) while the other parameters were held constant. The rates of production of iodide at the different iodate concentrations are shown in Fig.6-5. The rate increased linearly with the concentration of added iodate from 0.02 to 0.17  $\mu\text{M}$  (the slope between the rate of production of iodide and ambient iodate concentration =  $22.4(\pm 2.6)$  ( $\text{nM h}^{-1}/\mu\text{M}$ ),  $r^2=0.97$ ). The maximum rate of about 7  $\text{nM h}^{-1}$  ( $V_{\text{max}}$ ) was reached at a concentrations of added iodate of about 0.32  $\mu\text{M}$ . Above 0.32  $\mu\text{M}$  of added iodate, there was no detectable change in the rate of iodide production with further increase in the concentration of added iodate. Thus, the reaction rate was limited only at the concentration of added iodate below 0.32  $\mu\text{M}$ . The  $K_m$  (Michaelis constant) can be calculated from both slope and  $V_{\text{max}}$  and its value is about 0.16 ( $= 7/22.4$ )  $\mu\text{M}$ . In order to assure that iodate is present in excess in the reaction scheme, a concentration of added 0.4  $\mu\text{M}$  iodate was used. The shape of the curve relating the rate of the production of iodide to the concentration of iodate was consistent with that of a reaction controlled by enzyme activities (Voet and Voet, 1995). However, the data set was too limited to be treated rigorously by using the Michaelies-Menten equation.

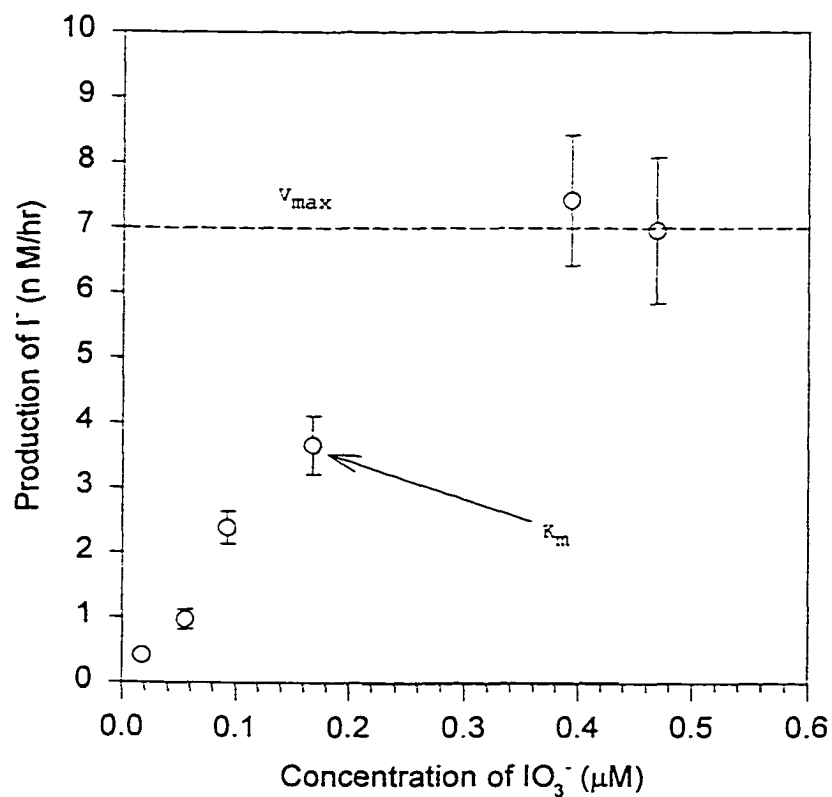


Fig. 6-5. The production of iodate and iodide catalyzed by NR at different iodate concentrations.

(Error bars represent 1 standard deviation, dotted line is the best fit line.)



*Iodate reduction by NR extracted from euxenic cultures of S. costatum and from natural phytoplankton assemblages*

The reduction of iodate to iodide was observed in the NR extracted from an euxenic culture of *S. costatum* and from four natural phytoplankton assemblages (Table 6-1). The iodate reduction activity (IRA) in this investigation ranged from 0.008 to 0.064  $\text{nmol-I}^- \mu\text{g chl } \alpha^{-1} \text{ h}^{-1}$ . Higher IRA (0.064  $\text{nmol-I}^- \mu\text{g chl } \alpha^{-1} \text{ h}^{-1}$ ) was found in an euxenic culture of *S. costatum*. For four natural phytoplankton assemblages IRA ranged from 0.008 to 0.019 and averaged 0.014  $\text{nmol-I}^- \mu\text{g chl } \alpha^{-1} \text{ h}^{-1}$ . NR extracted from *S. costatum* seems to have higher ability to catalyze the reduction of iodate to iodide than natural marine phytoplankton. Moisan et al., (1994) indicated that the uptake rate of iodate by euxenic culture of *Thalassiosira oceanica*, *S. costatum*, *Emiliania huxleyi* and *Dunaliella* ranged from 0.003 to 0.24  $\text{nmol-I}^- \mu\text{g chl } \alpha^{-1} \text{ h}^{-1}$  and field phytoplankton assemblages ranged from 0.08 to 0.26  $\text{nmol-I}^- \mu\text{g chl } \alpha^{-1} \text{ h}^{-1}$ . Udomkit (1994) reported that the removal rate by *S. costatum* ranged from 0.004 to 0.023  $\text{nmol-IO}_3^- \mu\text{g chl } \alpha^{-1} \text{ h}^{-1}$  and the rate of iodide production in this species ranged from 0.0004 to 0.003  $\text{nmol-I}^- \mu\text{g chl } \alpha^{-1} \text{ h}^{-1}$ . Assuming uptake of iodate and production of iodide represent reduction of iodate to iodide, the values in this study are similar to these reports.

Table 6-1. The reduction rate of iodate to iodide by nitrate reductase from natural phytoplankton that were collected in Chesapeake Bay, VA and from one phytoplankton culture (*S. costatum*)

Taxa	Chl- <i>a</i> ( $\mu\text{g/L}$ )	IRA ( $\text{nM h}^{-1}$ )	SIRA ( $\text{nmol } \mu\text{g-chl-}a^{-1} \text{ h}^{-1}$ )	NRA ( $\text{nM h}^{-1}$ )	SNRA ( $\text{nmol } \mu\text{g-chl-}a^{-1} \text{ h}^{-1}$ )	NRA/IRA
<i>S. costatum</i>	176 $\pm$ 2	11.2 $\pm$ 0.3	0.064 $\pm$ 0.002	494 $\pm$ 25	2.81 $\pm$ 0.14	44 $\pm$ 3
Natural phytoplankton assemblages						
Lynnhaven (July 10)	8.6 $\pm$ 0.3	0.12 $\pm$ 0.05	0.0143 $\pm$ 0.005	4.8 $\pm$ 0.2	0.56 $\pm$ 0.03	39 $\pm$ 15
Lynnhaven (July 14)	7.2 $\pm$ 0.2	0.058 $\pm$ 0.038	0.008 $\pm$ 0.005	4.8 $\pm$ 0.2	0.67 $\pm$ 0.04	83 $\pm$ 55
Ocean View (low tide, July 16)	9.6 $\pm$ 0.3	0.181 $\pm$ 0.054	0.019 $\pm$ 0.006	17.9 $\pm$ 0.9	1.86 $\pm$ 0.11	99 $\pm$ 30
Ocean View (high tide, July 16)	6.0 $\pm$ 0.2	0.093 $\pm$ 0.042	0.015 $\pm$ 0.007	8.0 $\pm$ 0.4	1.33 $\pm$ 0.08	86 $\pm$ 39
Average NRA/IRA in natural phytoplankton assemblages						77 $\pm$ 19
IRA: iodate reduction rate SIRA: chlorophyll <i>a</i> specific iodate reduction rate (IRA/chl <i>a</i> ) NRA: nitrate reductase activity SNRA: chlorophyll <i>a</i> specific nitrate reductase activity (NRA/chl <i>a</i> )						

*The relationship between IRA and NRA*

The rate of reduction of iodate in the four field samples was linearly related with NRA (Fig. 6-6) such that

$$\text{NRA} = 101 (\pm 45) \text{IRA} + 3 (\pm 6), \quad r^2 = 0.71$$

The strong correlation between iodate reduction and NRA is consistent with a coupling between iodate reduction and nitrate reduction as suggested by Tsunogai and Sase (1969). The ratio of NRA/IRA in the four field samples is about 100 which is agreement well with the previous estimation (NRA/IRA = 80, Chapter V). If new production can be represented by NRA, then, it can also be estimated by the depletion of iodate in the residence time of the surface ocean and the ratio of NRA/IRA (Chapter V). While the former is known moderately well, the latter was still somewhat uncertain. In this study, the value varies near 50 %. It is likely to vary with species composition and with geographical location. Thus, further work is needed to obtain a more reliable global average NRA/IRA.

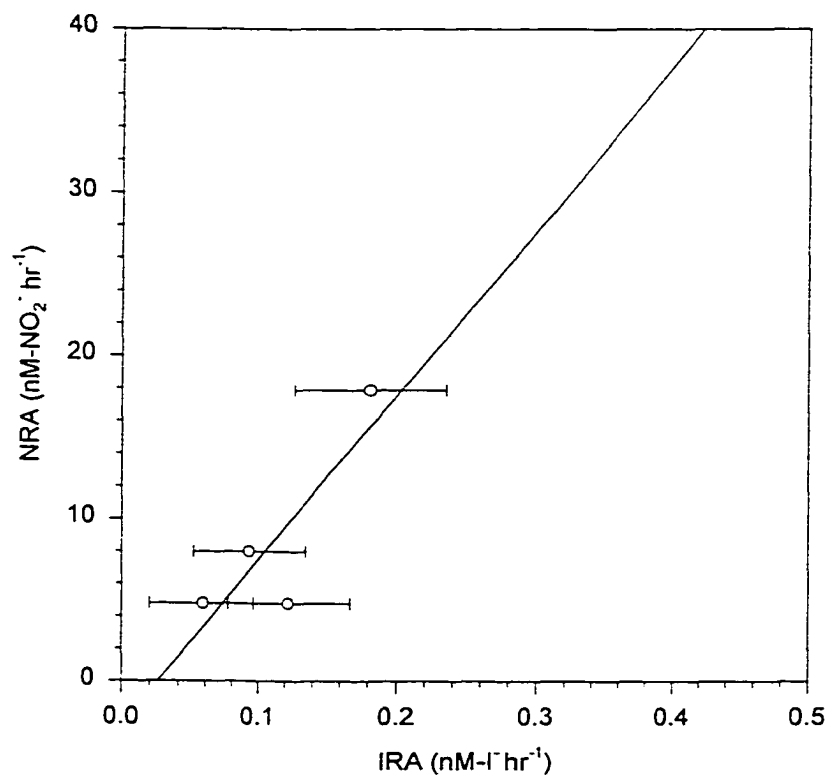


Fig. 6-6. The relationship between iodide production activity (IRA) and nitrate reductase activity (NRA) in four field samples.

## Conclusions

A method for estimating the reduction of iodate to iodide by nitrate reductase extracted from an euxenic culture of *S. costatum* by using  $^{125}\text{IO}_3^-$  was established. The reduction of  $\text{IO}_3^-$  to  $\text{I}^-$  catalyzed by NR was observed in an euxenic culture of *S. costatum* and four natural phytoplankton assemblages. The rates were  $0.064 \text{ n mol I}^- \mu\text{g chl a}^{-1} \text{ h}^{-1}$  in the former and  $0.008$  to  $0.019 \text{ n mol I}^- \mu\text{g chl a}^{-1} \text{ h}^{-1}$  in the latter. These results strongly support that the reduction of iodate to iodide is catalyzed by nitrate reductase. Iodate reduction rate was linearly related to nitrate reductase activity. The slope (ratio) between NRA and IRA was 100, which agreed well with the previous estimation (NRA/IRA = 80).

In addition, the result also indicates that iodate reduction may be coupled to nitrate reduction.

## CHAPTER VII

### SUMMARY AND DIRECTIONS FOR FUTURE RESEARCH

#### Summary

An improved NRA assay was established for measuring nitrate reductase activity demonstrating that the sensitivity of this method is about five times higher than that used in previous studies. While the measurements of NRA and  $^{15}\text{NO}_3^-$  uptake (NU) in a field sampling program may be affected differently under different light- and nitrate-conditions, NRA and NU are strongly, quantitatively and linearly related to each other under light- and nitrate-replete conditions. Previous field studies suffered because they had little success in finding a consistent relationship between NRA and NU. This was probably due to the fact that these environmental effects were overlooked, and the method used for the determination of NRA was inadequate. The relationship between NRA and NU may be established with a relatively small number of simultaneous determinations of NRA and NU. Once the relationship is found for a study area, it may be used for estimating NP from the determination of NRA alone. Since NRA may be determined readily on board ship with relative simplicity, it is a powerful, time-saving and economical supplementary tool for expanding the present data base on NU in the marine environment. This experimental approach is especially helpful in estimating NU in the oligotrophic oceans where the determination of NU by measuring  $^{15}\text{NO}_3^-$  uptake is difficult to be performed.

For the reduction of iodate to iodide catalyzed by NR from phytoplankton, both laboratory experiments and field investigations strongly support the idea that NR significantly involves the reduction of iodate to iodide. Additionally, the preliminary result

suggests that iodate reduction is coupled to nitrate reduction so that the rate of iodate reduction can be used to estimate the rate of nitrate uptake, new production.

### **Directions for future research**

If most NU ( $^{15}\text{NO}_3^-$  incubation technique) estimates are misleading due to stimulation by the addition of excess substrates, is the estimate of NU and  $f$  ratio in the oligotrophic ocean still reliable? Preliminary NRA data demonstrated that NRA may be a suitable candidate to estimate new production, but some important questions regarding the relationship between NRA and NU have not been answered. For example, although a good correlation between NRA and NU was found in the East China Sea, further work is needed to test whether this correlation may be applied to the marine environment in general. In addition, the ratio of the rate of iodate reduction to the rate of nitrate uptake is still somewhat uncertain. Therefore, I propose to do the following studies for the future research:

1. Test whether the ratio of nitrate reductase activity (NRA) to  $^{15}\text{NO}_3^-$  uptake (NU) can be applied to the marine environment.
2. Study the relationship between NRA and NU in oligotrophic waters by using a sensitive chemiluminescence technique to determine low nitrate concentration.
3. Study the ratio of the rate of iodate reduction to NRA in different marine environments.
4. Re-evaluate the oceanic global new production with the new ratio of the rate of iodate reduction to NRA.

Future research will provide a further understanding of the nitrate uptake processes,

an accurate estimation of new production in the oligotrophic oceans, and the relationship between iodate reduction and nitrate reduction in different marine environments.



## REFERENCES

- Allen, C. B., J. Kanda, and E. A. Laws (1996) New production and photosynthetic rates within and outside a cyclonic mesoscale eddy in the North Pacific subtropical gyre. *Deep-Sea Research*, **43**, 917-936.
- Antoine, D., J.-M. Andre, and A. Morel (1996) Oceanic primary production 2. Estimation at global scale from satellite (coastal zone color scanner) chlorophyll. *Global Biogeochemical Cycles*, **10**, 57-69.
- Apaicio, P. J. and J. M. Maldonado (1978) Regulation of nitrate assimilation in photosynthetic organisms. In: Nitrogen Assimilation of Plants. E. J. Hewitt and c. V. cutting, editors, Academic Press, New York, pp. 207-215.
- Balch, W. M. (1985) Differences between dinoflagellates and diatoms in the uptake of  $^{36}\text{Cl-ClO}_3$ , an analogue of  $\text{NO}_3$ . In: Toxic Dinoflagellates, D. Anderson, A. White and D. Baden, editors. Elsevier, New York. pp. 121-123.
- Balch, W. M. (1987) Studies of nitrate transport by marine phytoplankton using  $^{36}\text{Cl-ClO}_3$ , as a transport analogue - I. Physiological findings. *Journal of Phycology*, **23**, 107-118.
- Balch, W. M., C. Garside, and E. H. Renger (1987) Studies of nitrate transport by marine phytoplankton using  $^{36}\text{Cl-ClO}_3$ , as a transport analogue - II. Field observations. *Deep-Sea Research*, **34**, 221-236.
- Beardsley, R. C., R. Limeburner, H. Yu, and G. A. Cannon (1985) Discharge of the Changjiang (Yangtze River) into the East China Sea. *Continental Shelf Research*, **4**, 57-76.
- Beevers, L. and R. H. Hageman (1980) Nitrate and nitrite reduction. In: The biochemistry of Plants. B. J. Mifflin, editor, Academic Press, New York, 5, pp. 115-168.
- Behrenfeld, M.J. and P.G. Falkowski (1997) Photosynthetic rates derived from satellite-based chlorophyll concentration. *Limnology and Oceanography*, **42**, 1-20.
- Berger, W. H. (1989) Global maps of ocean productivity. In: Productivity of the ocean: present and past. W. H. Berger, V. S. Smetacek and G. Wefer, editors, Wiley & Sons, New York, pp. 429-455.
- Berges, J. A. and P. J. Harrison (1993) Relationship between nucleoside diphosphate kinase activity and light-limited growth rate in marine diatom *Thalassiosira pseudonana* (Bacillariophyceae). *Journal of Phycology*, **29**, 45-53.

- Berges, J. A. and P. J. Harrison (1995a) Nitrate reductase activity quantitatively predicts the rate of nitrate incorporation under steady state light limitation: A revised assay and characterization of the enzyme in three species of marine phytoplankton. *Limnology and Oceanography*, **40**, 82-93.
- Berges, J. A. and P. J. Harrison (1995b) Relationships between nitrate reductase activity and rates of growth and nitrate incorporation under steady-state light or nitrate limitation in the marine diatom *Thalassiosira pseudonana* (Bacillariophyceae). *Journal of Phycology*, **31**, 85-95.
- Berges, J. A., W. P. Cochlan, and P. J. Harrison (1995) Laboratory and field responses of algal nitrate reductase to diel periodicity in irradiance, nitrate exhaustion, and the presence of ammonia. *Marine Ecology Progressive Series*, **124**, 259-269.
- Berges, J. A. (1997) Algal nitrate reductase. *European Journal of Phycology*, **32**, 3-8.
- Bienfang, P. K. and D. A. Ziemann (1992) The role of coastal high latitude ecosystems in global export production. In: Primary productivity and biogeochemical cycles in the sea. P.G. Falkowski and A. D. Woodhead, editors, Plenum, New York, pp. 285-297.
- Blasco, D. and H. L. Conway (1982) Effect of ammonium on the regulation of nitrate assimilation in natural phytoplankton populations. *Journal of Experimental Marine Biology and Ecology*, **61**, 157-168.
- Blasco, D., J. J. MacIssac, T. T. Packard, and R. C. Dugdale (1984) Relationship between nitrate reductase and nitrate uptake in phytoplankton in the Peru upwelling region. *Limnology and Oceanography*, **29**, 275-286.
- Blasco, D. and T. T. Packard (1974) Nitrate reductase measurements in upwelling regions. 1. Significance of the distribution off Baja California and northwest Africa. *Tethys*, **6**, 239-246.
- Brandão, A. C. M., A. de L. R. Wagener, and K. Wagener (1994) Model experiments on the diurnal cycling of iodine in seawater. *Marine Chemistry*, **46**, 25-31.
- Bronk, D. A., P. M. Glibert, and B. B. Ward (1994) Nitrogen uptake, dissolved organic nitrogen release, and new production. *Science*, **265**, 1843-1846.
- Bruland, K. (1983) Trace elements in sea-water. In: Chemical Oceanography. J. P. Riley and R. Chester, editors, Academic Press, Orlando, FL., **8**, p. 157.
- Butler, E. C. V., J. D. Smith, and N. S. Fischer (1981) Influence of phytoplankton on iodine speciation in seawater. *Limnology and Oceanography*, **26**, 382-386.

- Campos, M. L. A. M., A. M. Farrenkopf, T. D. Jickells, and G. W. Luther, III (1996) A comparison of dissolved iodine cycling at the Bermuda Atlantic Time-series Station and Hawaii Ocean Time-series Station. *Deep-Sea Research*, **43**, 455-466.
- Carpenter, E. J. (1983) Nitrogen fixation by marine *oscillatoria* (*Trichodesmium*) in the world's oceans. In: Nitrogen in the marine environment. E. J. Carpenter and D. G. Capone, editors, Academic Press, INC., New York.
- Chavez, F. P. (1989) Size distribution of phytoplankton in the central and eastern tropical Pacific. *Global Biogeochemical Cycles*, **3**, 27-35.
- Chavez, F. P., K. R. Buck, R. R. Bidigare, D. M. Karl, D. Hebel, M. Latasa, and L. Campbell (1995) On the chlorophyll *a* retention properties of glass-fiber GF/F filters. *Limnology and Oceanography*, **40**, 428-433.
- Chavez, F. P. and R. T. Barber (1987) An estimate of new production in the equatorial Pacific. *Deep-Sea Research*, **34**, 1229-1243.
- Chavez, F. P. and J. R. Toggweiler (1995) Physical estimates of global new production: the upwelling contribution. In: Upwelling in the ocean, modern processes and ancient records. S. P. Summerhayes, K.-C. Emeis, M. V. Angel, R. L. Smith, and B. Zeitzschel, editors, John Wiley & Sons Ltd, West Sussex, England, pp. 313-320.
- Chen, C. T. A. (1996) The Kuroshio intermediate water is the major source of nutrients on the East China Sea continental shelf. *Oceanography Acta*, **19**, 523-527.
- Chen, C. T. A., R. Ruo, S. -C. Pai, C. -T. Liu, and G. T. F. Wong (1995) Exchange of water masses between the East China Sea and the Kuroshio off northeastern Taiwan. *Continental Shelf Research*, **15**, 19-39.
- Chen, S.-T. (1997) Biogeochemical behavior of nutrients and their fluxes in the Minjiang river estuary. *Chinese Journal of Oceanology and Limnology*, **15**, 150-155.
- Chen, Y.-L. L. (1995) Phytoplankton composition and productivity in response to the upwelling off northeastern Taiwan. *Process National Sciences Council, ROC Part B: Life Sciences*, **19**, 66-72.
- Chen, Y. -L. L., H. -B. Lu, F. -K. Shiah, G. -C. Gong, K. -K. Liu, and J. Kanda (1999) New production and *f*-ratio on the continental shelf of the East China Sea: Comparisons between nitrate inputs from the subsurface Kuroshio Current and the Changjiang river. *Estuarine Coastal and Shelf Science*, **48**, 59-76.
- Cheng, X. (1998) Non-volatile dissolved organic iodine in marine water. Ph. D. Dissertation, Old Dominion University, Norfolk, VA.

- Cheng, X., G. Guohui, and P. Zhang (1993) Zonal discrepancy of iodine in the West Pacific Ocean and its adjacent seas. *Acta Oceanologica Sinica*, **12**, 405-415.
- Chern, C. -S. and J. Wang (1990) On the mixing of waters at a northern offshore area of Taiwan. *Terrestrial, Atmospheric and Oceanic Sciences*, **1**, 297-306.
- Chern, C. -S., J. Wang, and D. -P. Wang (1990) The exchange of Kuroshio and East China Sea Shelf water. *Journal of Geophysical Research*, **95**, 16017-16023.
- Chuang, W. -S. and W. -D. Liang (1994) Seasonal variability of the Kuroshio water across the continental shelf northeast of Taiwan. *Journal of Oceanography*, **50**, 531-542.
- Codispoti, L. (1983) Nitrogen in upwelling systems. In: Nitrogen in the marine environment. E. J. Carpenter and D. G. Capone, editors, Academic Press.
- Collos, Y (1982) Transient situations in nitrate assimilation by marine diatoms. 3. Short-term uncoupling of nitrate uptake and reduction. *Journal of Experimental Marine Biology and Ecology*, **62**, 285-295.
- Collos, Y and G. Slawyck (1977) Nitrate reductase activity as a function of *in situ* nitrate uptake and environmental factors of euphotic zone profiles. *Journal of Experimental Marine Biology and Ecology*, **29**, 119-130.
- Delwiche, C. C. (1981) The nitrogen cycle and nitrous oxide. In: Denitrification, Nitrification and Atmospheric Nitrous Oxide. C. C. Delwiche, editor, Wiley, New York. pp. 1-15.
- Dickson, M. -L. and P. A. Wheeler (1995) Nitrate uptake rates in a coastal upwelling regime: A comparison of PN-specific, absolute, and Chl *a*-specific rates. *Limnology and Oceanography*, **40**, 533-543.
- Ditullio, G. R. and E. A. Laws (1983) Estimates of phytoplankton N uptake based on <sup>14</sup>CO<sub>2</sub> incorporation into protein. *Limnology and Oceanography*, **28**, 177-185.
- Dortch, O., S. I. Ahmed and T. T. Packard (1979) Nitrate reductase and glutamate dehydrogenase activities in *Skeletonema costatum* as measures of nitrogen assimilation rates. *Journal of Plankton Research*, **1**, 169-185.
- Dugdale, R. C. and J. J. Goering (1967) Uptake of new and regenerated forms of nitrogen in marine production. *Limnology and Oceanography*, **12**, 196-206.
- Dugdale, R. C. and F. P. Wilkerson (1986) The use of <sup>15</sup>N to measure nitrogen uptake in eutrophic oceans; experimental considerations. *Limnology and Oceanography*, **31**, 673-689.

- Dugdale, R. C. and F. P. Wilkerson (1989) New production in the upwelling center at Point Conception, California: temporal and spatial patterns. *Deep-Sea Research*, **36**, 985-1007.
- Dugdale, R. C., F. P. Wilkerson, and M. J. Minas (1995) The role of a silicate pump in driving new production. *Deep-Sea Research*, **42**, 697-719.
- Dugdale, R. C., F. P. Wilkerson and A. Morel (1990) Realization of new production in coastal upwelling areas: A means to compare relative performance. *Limnology and Oceanography*, **35**, 822-829.
- Edmond, J. M., A. Spivack, B. C. Grant, M. H. Hu, Z. Chen, S. Chen, and X. Zeng (1985) Chemical dynamics of the Changjiang estuary. *Continental Shelf Research*, **4**, 17-36.
- Elderfield, H. and V. W. Truesdale (1980) On the biophilic nature of iodine in seawater. *Earth and Planetary Science Letter*, **50**, 105-114.
- Eppley, R. W. (1978) Nitrate reductase in marine phytoplankton, p. 217-233. In: Handbook of hydrological methods. J. A. Hellebust and J. S. Craigie, editors, Cambridge.
- Eppley, R. W. (1989) New production: History, methods, problems. In: Productivity of the Ocean: Present and Past, W. H. Berger, V. S. Smetacek and G. Wefer, editors, Wiley, New York. pp. 85-97.
- Eppley, R. W. and W. Koeve (1990) Nitrate use by plankton in the eastern subtropical North Atlantic, March-April 1989. *Limnology and Oceanography*, **35**, 1781-1788.
- Eppley, R. W. and B. J. Peterson (1979) Particulate organic matter flux and planktonic new production in the deep ocean. *Nature*, **282**, 677-680.
- Eppley, R. W. and J. L. Coatsworth (1968) Nitrate and nitrite uptake by *Ditylum brightwellii*. Kinetics and mechanisms. *Journal of Phycology*, **4**, 151-156.
- Eppley, R. W., J. L. Coatsworth, and L. Solórzano (1969) Studies of nitrate reductase in marine phytoplankton. *Limnology and Oceanography*, **14**, 194-205.
- Eppley, R. W., T. T. Packard, and J. J. MacIsaac (1970) Nitrate reductase in Peru current phytoplankton. *Marine Biology*, **6**, 195-199.
- Eppley, R. W., J. H. Sharp, E. H. Renger, M. J. Perry, and W. G. Harrison (1977) Nitrogen assimilation by phytoplankton and other microorganisms in the surface waters of the central north Pacific Ocean. *Marine Biology*, **39**, 111-120.

- Fitzwater, S. E., G. A. Knauer, and J. H. Martin (1982) Metal contamination and its effect on primary production measurements. *Limnology and Oceanography*, **27**, 544-551.
- Gao, Y., G. J. Smith, and R. S. Alberte (1992) Light regulation of nitrate reductase in *Ulva fenestrata* (Chlorophyceae). *Marine Biology*, **112**, 691-696.
- Gardner, W. S., D. Wynne, and W. M. Dunstan (1976) Simplified procedure for the manual analysis of nitrate in seawater. *Marine Chemistry*, **4**, 393-396.
- Garside, C. (1982) A chemiluminescent technique for the determination of nanomolar concentrations of nitrate, nitrate and nitrite, or nitrite alone in seawater. *Marine Chemistry*, **11**, 159-167.
- Garside, C. (1991) Shift-up and the nitrate kinetics of phytoplankton in upwelling systems. *Limnology and Oceanography*, **36**, 1239-1243.
- Garside, C., T. C. Malone, O. A. Roels, and B. A. Sharfstein (1976) An evaluation of sewage derived nutrients and their influence on the Hudson Estuary and New York Bight. *Estuarine Coastal Marine Science*, **4**, 281-289.
- Giri, L. and C. S. Ramadoss (1979) Physical studies on assimilatory nitrate reductase from *Chlorella vulgaris*. *Journal of Biological Chemistry*, **254**, 11703-11712.
- Glibert, P. M., F. Lipschultz, J. J. Mccarthy, and M. A. Altabet (1982) Isotope dilution models of uptake and remineralization of ammonium by marine plankton. *Limnology and Oceanography*, **27**, 639-650.
- Glibert, P. M. and J. C. Goldman (1981) Rapid ammonium uptake by marine phytoplankton. *Marine Biology Letters*, **2**, 25-31.
- Goldman, J. C., C. D. Taylor, and P. M. Glibert (1981) Nonlinear time-course uptake of carbon and ammonium by marine phytoplankton. *Marine Ecology Progress Series*, **6**, 137-148.
- Gong, G. -C. (1992) Chemical hydrography of the Kuroshio front in the sea northeast of Taiwan. Ph.D. Dissertation, Institute of oceanography, National Taiwan University, 204 pp.
- Gong, G. -C. and K. -K. Liu (1995) Summertime hydrography and control of nutrient distribution in the East China Sea. In: Global fluxes of carbon and its related substances in the coastal Sea-Ocean-Atmosphere System. S. Tsunogai, K. Iseki, I. Koike and T. Oba, editors, M & J. International, Yokohama, Yokohama, Japan. 188. pp. 46-52.

- Gong, G. -C., K. -K. Liu, and S. -C. Pai (1995) Prediction of nitrate concentration from two end member mixing in the southern East China Sea. *Continental Shelf Research*, **15**, 827-842.
- Gong, G. -C., W. -R. Yang, and Y. -H. Wen (1993) Correlation of chlorophyll-*a* concentration and sea tech fluorometer fluorescence in seawater. *Acta Oceanographica Taiwanica*, **31**, 117-126.
- Gong, G. -C., J. Chang, and Y. -H. Wen (1999) Estimation of annual primary production in the Kuroshio waters northeast of Taiwan using a photosynthesis-irradiance model. *Deep-Sea Research*, **46**, 93-108.
- Guillard, R. R. L. and J. H. Ryther (1962) Studies on marine planktonic diatoms. I. *Cyclotella nana* Hustedt and *Detonula confervaacea* (cleve) Gran. *Canadian Journal of Microbiology*, **8**, 229-39.
- Gruber, N. and J. L. Sarmiento (1997) Global patterns of marine nitrogen fixation and denitrification. *Global Biogeochemical Cycles*, **11**, 235-266.
- Harrison, W. G. (1973) Nitrate reductase during a dinoflagellate bloom. *Limnology and Oceanography*, **18**, 457-465.
- Harrison, W. G. (1983) The time-course of uptake of inorganic and organic nitrogen compounds by phytoplankton from the Eastern Canadian Arctic: A comparison with temperature and tropical populations. *Limnology and Oceanography*, **28**, 1231-1237.
- Harrison, W. G., T. Platt, and M. R. Lewis (1985) The utility of light-saturation model for estimating marine primary productivity in the field: a comparison with conventional "simulated" *in situ* methods. *Canadian Journal of Fisheries and Aquatic Science*, **42**, 864-872.
- Harrison, W. G., T. Platt, and M. R. Lewis (1987) *f*-Ratio and its relationship to ambient nitrate concentration in coastal waters. *Journal of Plankton Research*, **9**, 235-248.
- Herring, J. J. and P. S. Liss (1974) A new method for the determination of iodine species in seawater. *Deep-Sea Research*, **21**, 777-783.
- Hochman, A., A. Nissany, D. Wynne, B. Kaplan, and T. Berman (1986) Nitrate reductase: an improved assay method for phytoplankton. *Journal of Plankton Research*, **8**, 385-392.
- Hsueh, Y., J. Wang, and C. S. Chern (1992) The intrusion of the Kuroshio across the continental shelf northeast of Taiwan. *Journal of Geophysical Research*, **97**, 14323-

14330.

- Jickell, T. D., S. S. Boyd, and A. H. Knapp (1988) Iodine cycling in the Sargasso Sea and the Bermuda inshore waters. *Marine Chemistry*, **24**, 61-82.
- Karl, D. M. (1992) The oceanic carbon cycle: Primary production and carbon flux on the oligotrophic North Pacific Ocean. *Processes of International symposium on global Change (IGBP)*. Tokorozawa, Japan.
- Kokkinakes, S. A. and P. A. Wheeler (1987) Nitrogen uptake and phytoplankton growth in coastal upwelling regions. *Limnology and Oceanography*, **32**, 1112-1123.
- Kuenzler, E. J. (1969) Elimination of iodine, cobalt, iron and zinc by marine zooplankton. In: symposium on Radioecology Process 2<sup>nd</sup> National Symposium on Radioecology. D. T. Nelson and E. C. Evans, editors, Washington, D.C., USAEC, pp. 462-473.
- Lalli, C. M. and T. R. Parsons (1994) Biological Oceanography: An introduction. Pergamon, Oxford, UK.
- Laws, E. A. (1984) Isotope dilution models and the mystery of the vanishing <sup>15</sup>N. *Limnology and Oceanography*, **29**, 379-386.
- Laws, E. A., W. G. Harrison and G. R. Ditullio (1985) A comparison of nitrogen assimilation rates based on <sup>15</sup>N uptake and autotrophic protein synthesis. *Deep-Sea Research*, **32**, 85-95.
- Li, Y. H. (1995) Material exchange between the East China Sea and the Kuroshio Current. *Terrestrial, Atmospheric and Oceanic Sciences*, **5**, 625-631.
- Lin, C. -Y., C. -Z. Shyu, and W. -H. Shih (1992) The Kuroshio fronts and cold eddies off northeastern Taiwan observed by NOAA-AVHRR imageries. *Terrestrial, Atmospheric and Oceanic Sciences*, **3**, 225-242.
- Lin, J. -R. (1995) Dissolved iodine in the southern East China Sea. M.S. Thesis. National Taiwan University, Taipei, Taiwan.
- Liu, K.-K. (1979) Geochemistry of inorganic nitrogen compounds in two marine environments: The Santa Barbara Basin and the ocean off Peru. Ph.D. Dissertation, University of California, Los Angeles.
- Liu, K. -K., G. -C. Gong, S. Lin, C. -Z. Zhyu, S. -C. Pai, C. -L. Wei, and S. -Y. Chao (1992a) Response of Kuroshio upwelling to the onset of northeast monsoon in the sea north of Taiwan: observations and a numerical simulation. *Journal of Geophysical Research*, **97**, 12511-12526.



- Liu, K. -K., G. -C. Gong, S. Lin, C. -Z. Zhyu, C. -Y. Yang, C. -L. Wei, S. -C. Pai and C. -K. Wu (1992b) The year-round upwelling at the shelf break near the northern tip of Taiwan as evidenced by chemical hydrography. *Terrestrial, Atmospheric and Oceanic Sciences*, **3**, 234-276.
- Longhurst, A., S. Sathyendranath, T. Platt, and C. Caverhill (1995) An estimate of global primary production in the ocean from satellite radiometer data. *Journal of Plankton Research*, **17**, 1245-1271.
- Luther, G. W. III and H. Cole (1988) Iodine speciation in Chesapeake Bay waters. *Marine Chemistry*, **24**, 315-325.
- Luther, G. W. III, C. B. Swartz and W. J. Ullman (1988) Direct determination of iodide in seawater by cathodic stripping square wave voltammetry. *Analytical Chemistry*, **60**, 1721-1724.
- Luther, G. W. III, J. Wu and J. B. Cullen (1995) Redox chemistry of iodine in seawater revisited: frontier molecular orbital theory considerations. *American Chemical Society Symposium Series*, **24**, 133-155.
- MacIsaac, J. J., R. C. Dugdale, R. T. Barber, D. Blasco, and T. T. Packard (1985) Primary production cycle in an upwelling center. *Deep-Sea Research*, **32**, 503-529.
- Martin, J. H. (1990) Glacial-interglacial CO<sub>2</sub> change: The iron hypothesis. *Paleoceanography*, **5**, 1-13.
- Martin, J. H., G. A. Knauer, D. M. Karl, and W. W. Broenkow (1987) Carbon cycling in the northeast Pacific. *Deep-Sea Research*, **34**, 267-285.
- McCarthy, J. J. and R. W. Eppley (1972) A comparison of chemical, isotopic, and enzymatic methods for measuring nitrogen assimilation of marine phytoplankton. *Limnology and Oceanography*, **17**, 371-382.
- McCarthy, J. J., C. Garside, and J. L. Nevins (1992) Nitrate supply and phytoplankton uptake kinetics in the euphotic layer of a Gulf Stream warm-core ring. *Deep-Sea Research*, **39**: S393-S403.
- McCarthy, J. J., C. Garside, J. L. Nevins, and R. T. Barber (1996) New production along 140°W in the equatorial Pacific during and following the 1992 El Niño event. *Deep-Sea Research*, **43**, 1065-1093.
- Milliman, J. D. and Q. Jin (1985) Introduction. *Continental Shelf Research*, **4**, 1-4.
- Moisan, T. A., W. M. Dunstan, A. Udomkit, and G. T. F. Wong (1994) The uptake of

- iodate by phytoplankton. *Journal of Phycology*, **30**, 580-587.
- Morel A, Y.-H. Ahn, F. Partensky, D. Vaultot, and H. Claustre (1993) *Prochlorococcus* and *Synechococcus*: a comparative study of their optical properties in relation to their size and pigmentation. *Journal of Marine Research*, **51**, 617-649.
- Morris, A. W. and J. P. Riley (1963) The determination of nitrate in sea-water. *Analytica Chimica Acta*, **29**, 272-279.
- Najjar, R. G., J. L. Sarmiento, and J. R. Toggweiler (1992) Downward transport and fate of organic matter in the oceans: Simulations with a general circulation mode. *Global Biogeochemical Cycles*, **6**, 45-76.
- Nitani, H. (1972) Beginning of the Kuroshio. In: Kuroshio. H. Stommel and K. Yoshida, editors, University of Washington Press, Seattle, Washington, pp. 129-163.
- Packard, T. T. and D. Blasco (1974) Nitrate reductase activity in upwelling regions. 2. Ammonia and light dependence. *Tethys*, **6**, 269-280.
- Packard, T. T., D. Blasco, J. J. MacIsaac, and R. C. Dugdale (1971) Variations of nitrate reductase activity in marine phytoplankton. *Investigation Pesquera*, **35**, 209-219.
- Packard, T. T., M. Denis, and P. Garfield (1988) Deep-ocean metabolic CO<sub>2</sub> production: Calculation from ETS activity. *Deep-Sea Research*, **35**, 371-392.
- Packard, T. T., R. C. Dugdale, J. J. Goering, and R. T. Barber (1978) Nitrate reductase activity in the subsurface waters of the Peru current. *Journal of Marine Research*, **36**, 59-76.
- Pai, S. -C., C. -C. Yang, and J. P. Riley (1990) Formation kinetics of the pink azo dye in the determination of nitrite in natural waters. *Analytica Chimica Acta*, **232**, 345-349.
- Parsons, T. R. and M. Takahashi (1977) *Biological Oceanographic Processes*. 2nd ed. Pergamon, Oxford. pp.332.
- Parsons, T. R., Y. Maita, and C. M. Lalli (1984) *A Manual of Chemical and Biological Methods for Seawater Analysis*. Pergamon Press. Oxford. pp.173.
- Platt, T., C. L. Gallegos, and W. G. Harrison (1980) Photoinhibition of photosynthesis in natural assemblages of marine phytoplankton. *Journal of Marine Research*, **38**, 687-701.
- Platt, T., P. Jauhari, and S. Sathyendranath (1992) The importance and measurement of

- new production. In: Primary productivity and biogeochemical cycles. P. G. Falkowski and A. D. Woodhead, editors, Plenum, New York, pp. 273-284.
- Platt, T., S. Sathyendranath, C. M. Caverhill, and M. R. Lewis (1988) Ocean primary production and available light: Further algorithms for remote sensing. *Deep-Sea Research*, **33**, 149-163.
- Platt, T., S. Sathyendranath, O. Ulloa, W. G. Harrison, N. Hoepffner, and J. Goes (1992) Nutrient control of phytoplankton photosynthesis in the Western North Atlantic. *Nature*, **356**, 229-231.
- Post, W. M., F. P. Chavez, P. J. Mulholland, J. Pastor, T. -H. Peng, K. Prentice, and T. Webb III (1992) Climatic feedbacks in the global carbon cycle. In: The Science of Global Change: The Impact of Human Activities on the Environment. D. Dunnette and R. O'Brien, editors, Washington, D. C., American Chemical Society, pp. 392-412.
- Rebello, A. D., F. W. Herms, and K. Wagener (1990) The cycling of iodine as iodate and iodide in a tropical estuarine system. *Marine Chemistry*, **29**, 77-93.
- Rhee, G. Y. (1979) Continuous culture in phytoplankton ecology. In Droop, M. R. & Jannasch, H. W. [Eds.] *Advances in Aquatic Microbiology*. Academic Press, London, pp. 150-207.
- Rue, E. L., G. J. Smith, G. A. Cutter, and K. W. Bruland (1997) The response of trace element redox couples to suboxic conditions in the water column. *Deep-Sea Research*, **44**, 113-134.
- Sarmiento, J. L. and C. Le Quere (1996) Oceanic carbon dioxide uptake in a model of century-scale global warming. *Science*, **274**, 1346-1350.
- Sarmiento, J. L., R. D. Slater, M. J. R. Fasham, H. W. Ducklow, J. R. Toggweiler, and G. T. Evans (1993) A seasonal three-dimensional ecosystem model of nitrogen cycling in the North Atlantic euphotic zone. *Global Biogeochemical Cycles*, **7**, 417-450.
- Sathyendranath, S., A. Longhurst, C. M. Caverhill, and T. Platt (1995) Regionally and seasonally differentiated primary production in the North Atlantic. *Deep-Sea Research*, **42**, 1773-1802.
- Sathyendranath, S., T. Platt, E. P. W. Horne, W. G. Harrison, O. Ulloa, R. Outerbridge, and N. Hoepffner (1991) Estimation of new production on the ocean by compound remote sensing. *Nature*, **353**, 129-133.

- Shaffer, G. (1996) Biogeochemical cycling in the global ocean. 2. New production, Redfield ratios, and remineralization in the organic pump. *Journal of Geophysical Research*, **111**, 3723-3745.
- Shiah, F. K., G. C. Gong, and K. K. Liu (1995) A preliminary survey on primary productivity measured by the  $^{14}\text{C}$  assimilation method in the KEEP area. *Acta Oceanographica Taiwanica*, **34**, 1-15.
- Shimada, A., T. Maruyama and S. Miyachi (1996) Vertical distributions and photosynthetic action spectra of two oceanic picophytoplankters, *Prochlorococcus marinus* and *Synechococcus sp.* *Marine Biology*, **127**, 15-23.
- Simada, A., T. Hasegawa, I. Umeda, N. Kadoya, and T. Maruyama (1993) Spatial mesoscale patterns of West Pacific picophytoplankton and analyzed by flow cytometry: their contribution to subsurface chlorophyll maxima. *Marine Biology*, **115**, 209-215.
- Siegenthaler, U. and J. L. Sarmiento (1993) Atmospheric carbon dioxide and the ocean. *Nature*, **365**, 119-125.
- Sillen, L. G. (1961) The physical chemistry of seawater. In: Oceanography. Mary Sears, editor, AAAS Publ. No. 67, Washington, pp. 549-581.
- Slawyk, G. and Y. Collos (1976) An automated assay for the determination of nitrate reductase in marine phytoplankton. *Marine Biology*, **34**, 23-26.
- Slawyk, G., B. Coste, Y. Collos, and M. Rodier (1997) Isotopic and enzymatic analyses of planktonic nitrogen utilisation in the vicinity of Cape Sines (Portugal) during weak upwelling activity. *Deep-Sea Research*, **44**, 1-25.
- Smith, G. J., R. C. Zimmerman, and R. S. Alberte (1992) Molecular and physiological responses of diatoms to variable levels of irradiance and nitrogen availability: Growth of *Skeletonema costatum* in simulated upwelling conditions. *Limnology and Oceanography*, **37**, 989-1007.
- Solomonson, L. P., G. H. Toumer, R. L. Hall, R. Borchers, and J. L. Bailey (1975) Reduced nicotinamide adenine dinucleotide-nitrate reductase of *Chlorella vulgaris*. *Journal of Biological Chemistry*, **250**, 4120-4127.
- Solomonson, L. P. and M. J. Barber (1990) Assimilatory nitrate reductase: functional properties and regulation. *Annual Review of Plant Physiology and Plant Molecular Biology*, **41**, 225-253.
- Spokes, L. J. and P. S. Liss (1996) Photochemically induced redox reactions in seawater,

II. Nitrogen and iodine. *Marine Chemistry*, **54**, 1-10.

- Strickland, J. D. H. and T. R. Parsons (1972) A practical handbook of seawater analysis. *Fisheries Research Board of Canada. Bulletin*, 167, 2nd edition, pp.310.
- Su, J. L., B. X. Guan, and J. Z. Jiang (1990) The Kuroshio. Part I. Physical features. *Ocean. Marine Biology Annual Review*, **28**, 11-71.
- Sun, X. (1987) Analysis of the surface path of the Kuroshio in the East China Sea (in Chinese with English abstract). Essays on the investigation of Kuroshio. X. Sun, editor, Ocean Press, Beijing, pp. 1-14.
- Takayanagi, K. and G. T. F. Wong (1986) the oxidation of iodide to iodate for the polarographic determination of total iodine in natural waters. *Talanta*, **33**, 451-454.
- Tang, T. Y. and Y. J. Yang (1993) Low frequency current variability on the shelf break northeast of Taiwan. *Journal of Oceanography*, **49**, 193-210.
- Tian, R. C., J. C. Marty, E. Nicolas, J. Chiavérini, D. Ruiz-Pino and M. D. Pizay (1996) Iodine speciation: a potential indicator to evaluate new production versus regenerated production. *Deep-Sea Research*, **43**, 723-738.
- Timmermans, K. R., W. Stolte and H. J. W. de Baar (1994) Iron-mediated effects on nitrate reductase in marine phytoplankton. *Marine Biology*, **121**, 389-396.
- Truesdale, V. W. (1978) Iodine in inshore and off-shore marine waters. *Marine Chemistry*, **6**, 1-12.
- Truesdale, V. W. (1994) A re-assessment of Redfield correlations between dissolved iodine and nutrients in oceanic waters and a strategy for further investigations of iodine. *Marine Chemistry*, **48**, 43-56.
- Tsunogai, S. (1971) Iodine in deep water of the ocean. *Deep-Sea Research*, **18**, 913-919.
- Tsunogai, S. and T. Henmi (1971) Iodine in the surface water of the ocean. *Journal of Oceanographic Society of Japan*, **27**, 67-72.
- Tsunogai, S. and T. Sase (1969) Formation of iodide-iodine in the ocean. *Deep-Sea Research*, **16**, 489-496.
- Udomkit, A. (1994) Iodate transformation by marine phytoplankton, Ph.D. Dissertation, Oceanography Department, Old Dominion University, Norfolk, VA.
- Udomkit, A. and W. M. Dunstan (1991) Preliminary study on the influence of

phytoplankton on iodine speciation. *Journal of Phycology*, **27**, 73.

- Venrick, E. L., S. L. Cummings, and C. A. Kemper (1987) Picoplankton and the resulting bias in chlorophyll retained by traditional glass-fiber filters. *Deep-Sea Research*, **34**, 1951-1956.
- Voet, D. and J. Voet (1995) *Biochemistry*. John Wiley & Sons, 2nd edition, pp. 1361.
- Wada, E. and A. Hattori (1991) Nitrogen in the Sea: Forms, Abundances, and Rate Processes. CRC Press, Boca Raton, 208 pp.
- Walsh, J. J. (1976) Herbivory as a factor in patterns of nutrient utilization in the sea. *Limnology and Oceanography*, **21**, 1-13.
- Ward, B. B., K. A. Kilpatrick, E. H. Renger, and R. W. Eppley (1989) Biological nitrogen cycling in the nitracline. *Limnology and Oceanography*, **34**, 493-513.
- Wheeler, P. A. (1983) Phytoplankton nitrogen metabolism. In "Carpenter, E. J., Capone, D. G. Nitrogen in the marine environment. Academic Press, New York, pp. 309-346.
- Wilkerson, F. P. and R. C. Dugdale (1987) The use of large shipboard barrels and drifters to study the effects of coastal upwelling on phytoplankton dynamics. *Limnology and Oceanography*, **32**, 368-382.
- Woittiez, J. R. W., Van der Sloot, G. D. Wals, B. J. T. Nieuwendijk, and J. Zonderhuis (1991) The determination of iodide, iodate, total inorganic iodine and charcoal-adsorbable iodine in sea water. *Marine Chemistry*, **34**, 247-259.
- Wong, G. T. F. (1973) The marine chemistry of iodate. M. S. Thesis, Massachusetts Institute of Technology.
- Wong, G. T. F. (1980) The stability of dissolved inorganic species of iodine in seawater. *Marine Chemistry*, **9**, 45-73.
- Wong, G. T. F. (1991) The marine geochemistry of iodine. *Reviews in Aquatic Sciences*, **4**, 45-73.
- Wong, G. T. F. (1995) Dissolved iodine across the Gulf stream Front and in the south Atlantic Bight. *Deep-Sea Research*, **42**, 2005-2023.
- Wong, G. T. F. and P. G. Brewer (1974) The determination and distribution of iodate in South Atlantic waters. *Journal of Marine Research*, **32**, 25-36.

- Wong, G. T. F. and P. G. Brewer (1977) The marine chemistry of iodine in anoxic basins. *Geochimica et Cosmochimica Acta*, **41**, 151-159.
- Wong, G. T. F. and X. Cheng (1998) Dissolved organic iodine in marine waters: Determination, occurrence and analytical implications. *Marine Chemistry*, **59**, 271-281.
- Wong, G. T. F., G. -C. Gong, K. -K. Liu, and S. -C. Pai (1998) 'Excess nitrate' in the East China Sea. *Estuarine, Coastal and Shelf Science*, **46**, 411-418.
- Wong, G. T. F., S. -C. Pai, K. -K. Liu, C. -T. Liu, and C. T. A. Chen (1991) Variability of the chemical hydrography at the frontal region between the East China Sea and the Kuroshio northeast of Taiwan. *Estuarine, Coastal and Shelf Science*, **33**, 105-120.
- Wong, G. T. F. and L. Zhang (1992a) Changes in iodine-speciation across coastal hydrographic fronts in southeastern United States continental shelf waters. *Continental Shelf Research*, **12**, 717-733.
- Wong, G. T. F. and L. Zhang (1992b) Chemical removal of oxygen with sulfite for the polarographic or voltammetric determination of iodate and iodide in seawater. *Marine Chemistry*, **38**, 109-116.
- Wong, G. T. F. and L. Zhang (1992c) The determination of total inorganic iodine in seawater by cathodic stripping square wave voltammetry. *Talanta*, **39**, 355-360.
- Zhang, J (1996) Nutrient elements in large Chinese estuaries. *Continental Shelf Research*, **16**, 1023-1045.
- Zhang, J. -Z. and M. Whitfield (1986) Kinetics of inorganic redox reactions in seawater. I. The reduction of iodate by bisulfide. *Marine Chemistry*, **19**, 121-137.
- Zimmerman, R. C. J. N. Kremer, and R. C. Dugdale (1987) Acceleration of nutrient uptake by phytoplankton in a coastal upwelling ecosystem: a modelling analysis. *Limnology and Oceanography*, **32**, 359-367.

## APPENDICES

## APPENDIX A

## RECIPE OF f/2 SOLUTION

The recipe of culture medium is prepared as follows: the seawater was enriched with nutrients based on the medium "f" devised by Guillard and Ryther (1962) but the concentrations of nutrients were diluted to half the strength of the original recipe, f/2.

The fundamental compounds for 1 liter of f/2 are:

**Major nutrients:**

NaNO <sub>3</sub>	883	μM
NaH <sub>2</sub> PO <sub>4</sub> · H <sub>2</sub> O	36.3	μM
Na <sub>2</sub> SiO <sub>3</sub> · 9H <sub>2</sub> O	54	μM

**Trace metals:**

Na <sub>2</sub> · EDTA <sup>-</sup>	11.7	μM
FeCl <sub>3</sub> · 6H <sub>2</sub> O <sup>+</sup>	11.7	μM
CuSO <sub>4</sub> · 5H <sub>2</sub> O	0.04	μM
ZnSO <sub>4</sub> · 7H <sub>2</sub> O	0.08	μM
CoCl <sub>2</sub> · 6H <sub>2</sub> O	0.05	μM
MnCl <sub>2</sub> · 4H <sub>2</sub> O	0.9	μM
Na <sub>2</sub> MoO <sub>4</sub> · 2H <sub>2</sub> O	0.03	μM

**Vitamins:**

Thiamin· HCl	0.1	mg
Biotin	0.5	μg
B <sub>12</sub>	0.5	μg



## APPENDIX B

### CALCULATION OF NRA

The activity of nitrate reductase is calculated as below:

$$\text{NRA (nM-NO}_2^- \text{ h}^{-1}\text{)} = \frac{(A_{\text{sample}} - A_{\text{blank}})}{S_{\text{standard}} \times T} \times \frac{V_{\text{standard}} \times V_{\text{mixture}}}{V_{\text{nitrite}} \times V_{\text{sample}}}$$

$A_{\text{sample}}$  and  $A_{\text{blank}}$  represent the absorbance of the sample and the blank.

$S_{\text{standard}}$  is the slope of the calibration curve for nitrite standard.

$V_{\text{standard}}$  is the final volume of nitrite standard in nitrite absorbance measurement.

T is the incubation time.

$V_{\text{mixture}}$  represents the total volume in the solution of nitrate reductase.

$V_{\text{nitrite}}$  is the volume of the nitrite determination.

$V_{\text{sample}}$  is the filtration volume of seawater or phytoplankton culture.

For example, the filtration volume ( $V_{\text{sample}}$ ) of seawater is 4 liters.  $A_{\text{sample}}$  and  $A_{\text{blank}}$  are equal

to 0.050 and 0.010. The  $V_{\text{standard}}$ ,  $V_{\text{mixture}}$ , and  $V_{\text{nitrite}}$  are 2.2 ml, 1.7 ml and 1 ml. T is 5 minutes and  $S_{\text{standard}}$  is 0.096 Abs./ $\mu\text{M}$ . NRA is calculated as follows.

$$\text{NRA (nM-NO}_2^- \text{ h}^{-1}\text{)} = \frac{(0.050 - 0.010)}{(0.096 \times 5 \text{ min})} \times \frac{(2.2 \times 1.7)}{(1 \times 4)} = 4.68$$

## APPENDIX C

## NRA, HYDROGRAPHY AND RELEVANT DATA IN THE EAST CHINA SEA

NRA, hydrography and relevant data in the East China Sea.

Sta.	Depth (m)	T (°C)	S	NO <sub>3</sub> <sup>-</sup> (μM)	PAR %	Chl a (mg m <sup>-3</sup> )	NRA (nM h <sup>-1</sup> )	Spe. NRA (nM h <sup>-1</sup> mg <sup>-1</sup> m <sup>3</sup> )
11	2	16.34	33.434	0.3	100.0	0.856	10.58	12.36
	5	16.32	33.436	0.3	36.1	0.849	11.50	13.55
	10	16.31	33.453	0.5	15.1	0.769	9.60	12.48
	15	16.01	33.645	1.8	7.4	0.758	9.33	12.31
	20	15.13	33.833	3.5	3.5	0.399	8.71	21.83
	30	14.61	33.788	4.1	0.1	0.211	3.47	16.45
	35	14.53	33.791	4.4	0.0	0.173	2.66	15.38
	40	14.50	33.770	4.5	0.0	0.206	2.28	11.07
	50	14.45	33.769	5.5	0.0	0.199	2.00	10.05
	55	14.45	33.773	5.4	0.0	0.273	1.82	6.67
15	2	17.54	34.485	2.1	nd	0.496	4.46	11.18
	5	17.54	34.595	1.4	100.0	0.572	4.19	7.33
	10	17.55	34.485	1.6	65.0	0.432	4.83	11.18
	20	17.55	34.482	2.1	25.6	0.392	5.38	13.72
	30	17.54	34.525	1.8	13.3	0.386	3.75	9.72
	40	17.54	34.474	1.7	5.3	0.437	2.12	4.85
	50	17.54	34.484	1.9	1.7	0.357	1.12	3.14
	60	17.14	34.412	2.1	0.0	0.403	0.85	2.11
	70	16.79	34.423	4.3	0.0	0.306	0.49	1.60
	80	16.41	34.347	4.6	0.0	0.197	0.46	2.34
90	15.43	34.227	5.2	0.0	0.341	0.41	1.20	
26	2	17.70	34.181	0.1	100.0	2.438	15.35	6.30
	5	17.65	34.235	0.1	45.5	1.951	15.20	7.79
	10	17.40	34.171	0.1	14.3	1.951	15.05	7.71
	15	17.28	34.203	0.5	4.4	1.744	15.40	8.83
	20	17.27	34.182	0.4	0.6	1.201	16.59	13.81
	25	17.25	34.189	1.5	0.0	0.891	16.75	18.80
	30	17.23	34.202	nd	0.0	0.825	13.47	16.33
	50	16.91	34.234	nd	0.0	0.244	1.84	7.54
	60	16.74	34.269	5.5	0.0	0.248	1.83	7.38
	75	14.75	34.223	5.4	0.0	0.211	1.78	8.44

nd: no data

## APPENDIX C (Continued)

NRA, hydrography and relevant data in the East China Sea.

Sta.	Depth (m)	T (°C)	S	NO <sub>3</sub> <sup>-</sup> (μM)	PAR %	Chl a (mg m <sup>-3</sup> )	NRA (nM h <sup>-1</sup> )	Spe. NRA (nM h <sup>-1</sup> mg <sup>-1</sup> m <sup>3</sup> )
30	2	15.44	30.124	5.9	100.0	0.851	4.55	5.35
	5	15.44	30.442	6.0	70.6	0.890	4.16	4.67
	10	15.28	30.313	6.0	50.3	1.139	5.34	4.69
	15	13.62	32.544	7.2	22.6	1.197	5.35	4.47
	20	15.52	33.663	6.1	9.9	nd	1.53	nd
	25	15.73	33.672	5.4	4.0	0.357	1.27	3.56
	30	15.80	33.795	6.4	0.9	0.250	1.23	4.92
	35	15.87	33.795	nd	0.0	0.246	1.24	5.04
	40	16.30	nd	nd	0.0	nd	1.80	nd
45	16.94	nd	nd	0.0	nd	1.80	nd	
45	2	21.59	34.273	0.1	100.0	0.971	6.43	6.62
	5	21.59	34.324	0.1	71.6	0.962	4.93	5.16
	10	21.58	34.266	0.1	40.8	0.822	4.63	5.63
	15	21.54	34.268	0.1	22.7	0.818	3.43	4.16
	20	21.49	34.252	0.2	12.6	0.862	2.63	3.05
	25	21.39	34.238	0.0	7.1	0.603	nd	nd
	30	21.17	34.236	0.2	4.1	0.319	0.93	2.92
	40	21.22	34.277	0.5	1.1	0.173	0.73	4.22
	50	21.24	34.313	0.6	0.0	0.120	0.63	5.25
	60	21.22	34.345	1.0	0.0	0.095	nd	nd
	75	19.70	34.439	6.3	0.0	0.124	nd	nd
	90	16.92	34.447	7.3	0.0	0.191	nd	nd
49	2	nd	nd	0.0	100.0	0.700	5.67	8.10
	5	20.95	33.867	0.0	48.6	0.694	4.64	6.68
	10	20.95	33.908	0.0	41.4	0.649	2.05	3.16
	20	21.00	33.902	0.0	17.3	0.700	1.17	1.68
	25	20.44	33.954	0.3	11.0	0.694	0.44	0.63
	30	20.32	33.897	0.9	7.0	0.649	0.25	0.38
	35	19.97	33.918	1.7	4.4	0.140	0.60	4.29
	40	19.88	34.098	2.4	2.9	0.117	1.30	11.11
	45	18.93	33.885	2.7	1.2	0.124	1.28	10.32
50	17.84	33.847	2.5	0.1	0.120	0.99	8.25	
60	17.73	33.960	nd	0.0	nd	1.59	nd	

nd: no data

## APPENDIX C (Continued)

NRA, hydrography and relevant data in the East China Sea.

Sta.	Depth (m)	T (°C)	S	NO <sub>3</sub> <sup>-</sup> (μM)	PAR %	Chl a (mg m <sup>-3</sup> )	NRA (nM h <sup>-1</sup> )	Spe. NRA (nM h <sup>-1</sup> mg <sup>-1</sup> m <sup>3</sup> )
50	2	nd	34.238	0.0	nd	0.543	4.56	8.40
	5	23.78	34.240	0.0	nd	0.572	nd	nd
	10	23.77	34.240	0.0	nd	0.545	5.00	9.17
	15	23.78	34.241	0.0	nd	0.523	nd	nd
	20	23.79	34.242	0.0	nd	0.554	3.93	7.09
	25	23.79	34.238	0.2	nd	0.556	nd	nd
	30	23.78	34.240	0.0	nd	0.512	nd	nd
	35	23.72	34.266	0.1	nd	0.410	nd	nd
	40	23.56	34.257	0.3	nd	0.434	1.83	4.22
	45	23.49	34.268	0.4	nd	0.299	nd	nd
	50	23.46	34.269	1.3	nd	0.279	nd	nd
	60	23.44	34.269	0.7	nd	0.293	1.46	4.98
51	2	20.58	34.435	1.6	nd	0.809	5.25	6.49
	5	20.56	34.455	2.0	nd	0.813	3.90	4.80
	10	20.59	34.434	1.5	nd	0.707	2.06	2.91
	20	20.61	34.427	1.7	nd	0.751	2.85	3.80
	30	20.39	34.439	3.4	nd	0.720	3.07	4.26
	40	20.38	34.429	3.7	nd	0.528	0.70	1.33
	50	19.55	34.437	4.3	nd	0.550	0.34	0.62
	60	19.32	34.571	6.3	nd	0.412	0.83	2.02
	70	18.99	34.455	7.2	nd	0.290	nd	nd
	80	18.49	34.484	10.4	nd	0.129	nd	nd
90	17.53	34.538	12.0	nd	0.106	nd	nd	
52-1	2	18.46	34.449	4.2	100.0	0.887	6.11	6.89
	5	18.45	34.449	5.1	61.7	0.769	5.80	7.54
	10	18.45	34.458	5.1	35.5	0.652	5.04	7.73
	15	18.43	34.484	5.7	13.4	0.710	4.14	5.82
	20	18.27	34.470	6.0	5.5	0.612	5.04	8.20
	30	18.05	34.502	7.1	2.1	0.583	3.56	5.28
	40	17.51	34.584	9.4	0.7	0.691	0.79	4.14
	50	16.33	34.605	11.1	0.0	0.091	0.78	7.88
	60	16.00	34.613	12.5	0.0	0.099	0.75	7.58
	75	15.27	34.610	11.7	0.0	0.056	0.55	9.82
100	15.23	34.605	11.1	0.0	0.098	0.45	4.59	

nd: no data

## APPENDIX C (Continued)

NRA, hydrography and relevant data in the East China Sea.

Sta.	Depth (m)	T (°C)	S	NO <sub>3</sub> <sup>-</sup> (μM)	PAR %	Chl a (mg m <sup>-3</sup> )	NRA (nM h <sup>-1</sup> )	Spe. NRA (nM h <sup>-1</sup> mg <sup>-1</sup> m <sup>3</sup> )
52-3	2	18.95	34.632	3.8	100.0	0.949	10.36	10.92
	10	18.93	34.477	4.7	37.0	0.867	9.61	11.08
	15	18.74	34.476	4.4	nd	0.882	nd	nd
	20	18.31	34.486	5.0	13.8	0.747	6.91	9.25
	25	18.11	nd	4.8	nd	0.829	nd	nd
	30	17.68	34.504	5.4	6.1	0.700	2.07	2.96
	40	16.59	34.582	8.2	2.9	0.335	1.02	3.04
	50	15.83	34.627	9.4	1.6	0.180	nd	nd
	60	15.68	34.628	11.1	0.7	0.062	nd	nd
	75	15.59	34.626	11.6	0.2	0.055	nd	nd
100	15.32	34.620	11.8	0.0	0.039	nd	nd	
53	2	22.11	34.111	0.1	100.0	2.438	7.85	9.20
	5	22.10	34.148	0.1	45.5	1.951	6.83	6.67
	10	22.13	34.155	0.1	14.3	1.951	5.78	5.34
	20	20.25	34.152	0.5	4.4	1.744	2.56	4.55
	30	19.71	34.152	0.4	0.6	1.201	1.39	5.70
	40	18.87	34.154	1.5	0.0	0.891	0.85	5.25
	50	18.66	34.151	nd	0.0	0.825	0.40	4.00
	75	17.72	34.232	nd	0.0	0.244	0.33	5.00
	100	16.47	34.205	5.5	0.0	0.248	0.40	10.89
	150	nd	34.204	5.4	0.0	0.211	nd	nd
55-3	2	23.93	34.624	0.2	100.0	0.065	0.12	1.85
	5	23.94	nd	0.2	nd	nd	nd	nd
	10	23.94	34.617	0.0	40.4	0.067	0.21	3.13
	20	23.94	34.622	0.0	25.5	0.071	0.20	2.82
	30	23.94	34.642	0.0	16.3	0.074	0.13	1.76
	40	23.83	34.824	0.8	10.4	0.082	0.27	3.29
	50	23.63	34.778	0.0	6.4	0.087	0.36	4.14
	65	23.22	34.803	0.0	2.5	0.223	0.46	2.06
	80	22.78	34.830	0.5	0.4	0.202	0.58	2.87
	95	22.42	34.853	0.7	0.0	0.142	0.26	1.83
111	22.03	nd	0.9	0.0	0.033	nd	nd	

nd: no data

## APPENDIX C (Continued)

NRA, hydrography and relevant data in the East China Sea.

Sta.	Depth (m)	T (°C)	S	NO <sub>3</sub> <sup>-</sup> (μM)	PAR %	Chl a (mg m <sup>-3</sup> )	NRA (nM h <sup>-1</sup> )	Spe. NRA (nM h <sup>-1</sup> mg <sup>-1</sup> m <sup>3</sup> )
55-5	2	24.06	34.618	0.1	100.0	0.055	0.11	2.00
	10	24.04	34.618	0.1	nd	nd	nd	nd
	15	23.99	34.615	0.0	nd	nd	nd	nd
	20	23.97	34.614	0.0	nd	nd	nd	nd
	30	23.94	34.615	0.0	33.7	0.055	0.14	2.55
	40	23.91	34.689	0.0	22.6	0.055	0.29	5.27
	50	23.41	34.771	2.4	14.2	0.058	0.39	6.72
	75	22.52	34.850	2.6	5.4	0.229	0.65	2.84
	100	21.73	34.888	3.7	1.4	0.095	0.38	4.00
	151	19.13	34.905	4.7	nd	nd	nd	nd
	203	18.38	34.862	3.3	nd	nd	nd	nd

nd: no data

## APPENDIX D

## NRA, NU AND HYDROGRAPHIC DATA IN THE EAST CHINA SEA

NRA, NU and hydrographic data in the East China Sea.

Sta.	Depth (m)	T (°C)	S	NO <sub>3</sub> <sup>-</sup> (μM)	PAR %	Chl a (mg m <sup>-3</sup> )	NRA (nM h <sup>-1</sup> )	NU (nM h <sup>-1</sup> )	NU/NRA
11	2	16.34	33.434	0.3	100.0	0.856	10.58	11.03	1.04
	5	16.32	33.436	0.3	36.1	0.849	11.50	11.58	1.01
	10	16.31	33.453	0.5	15.1	0.769	9.60	12.70	1.32
	15	16.01	33.645	1.8	7.4	0.758	9.33	6.36	0.68
	20	15.13	33.833	3.5	3.5	0.399	8.71	0.61	0.07
	30	14.61	33.788	4.1	0.1	0.211	3.47	0.35	0.10
	35	14.53	33.791	4.4	0.0	0.173	2.66	0.33	0.12
	40	14.50	33.770	4.5	0.0	0.206	2.28	0.44	0.19
	50	14.45	33.769	5.5	0.0	0.199	2.00	0.28	0.14
55	14.45	33.773	5.4	0.0	0.273	1.82	0.38	0.21	
15	2	17.54	34.485	2.1	nd	0.496	4.46	5.03	1.28
	5	17.54	34.595	1.4	100.0	0.572	4.19	4.57	1.09
	10	17.55	34.485	1.6	65.0	0.432	4.83	6.03	1.25
	20	17.55	34.482	2.1	25.6	0.392	5.38	5.27	0.98
	30	17.54	34.525	1.8	13.3	0.386	3.75	3.19	0.85
	40	17.54	34.474	1.7	5.3	0.437	2.12	1.00	0.47
	50	17.54	34.484	1.9	1.7	0.357	1.12	0.21	0.19
	60	17.14	34.412	2.1	0.0	0.403	0.85	nd	nd
	70	16.79	34.423	4.3	0.0	0.306	0.49	nd	nd
	80	16.41	34.347	4.6	0.0	0.197	0.46	nd	nd
90	15.43	34.227	5.2	0.0	0.341	0.41	0.45	1.10	
26	2	17.70	34.181	0.1	100.0	2.438	15.35	36.52	2.38
	5	17.65	34.235	0.1	45.5	1.951	15.20	24.36	1.60
	10	17.40	34.171	0.1	14.3	1.951	15.05	8.70	0.58
	15	17.28	34.203	0.5	4.4	1.744	15.40	3.70	0.24
	20	17.27	34.182	0.4	0.6	1.201	16.59	1.72	0.10
	25	17.25	34.189	1.5	0.0	0.891	16.75	1.13	0.07
	30	17.23	34.202	nd	0.0	0.825	13.47	0.62	0.05
	50	16.91	34.234	nd	0.0	0.244	1.84	0.42	0.23
	60	16.74	34.269	5.5	0.0	0.248	1.83	1.47	0.80
75	14.75	34.223	5.4	0.0	0.211	1.78	0.82	0.46	

nd: no data

## APPENDIX D (Continued)

NRA, NU and hydrographic data in the East China Sea.

Sta.	Depth (m)	T (°C)	S	NO <sub>3</sub> <sup>-</sup> (μM)	PAR %	Chl a (mg m <sup>-3</sup> )	NRA (nM h <sup>-1</sup> )	NU (nM h <sup>-1</sup> )	NU/NRA
30	2	15.44	30.124	5.9	100.0	0.851	4.55	1.34	0.30
	5	15.44	30.442	6.0	70.6	0.890	4.16	3.26	0.78
	10	15.28	30.313	6.0	50.3	1.139	5.34	5.38	1.01
	15	13.62	32.544	7.2	22.6	1.197	5.35	5.37	1.00
	20	15.52	33.663	6.1	9.9	nd	1.53	1.44	0.94
	25	15.73	33.672	5.4	4.0	0.357	1.27	0.77	0.61
	30	15.80	33.795	6.4	0.9	0.250	1.23	0.75	0.61
	35	15.87	33.795	nd	0.0	0.246	1.24	0.61	0.49
	40	16.30	nd	nd	0.0	nd	1.80	1.45	0.81
	45	16.94	nd	nd	0.0	nd	1.80	1.06	0.59
52-1	2	18.46	34.449	4.2	100.0	0.887	6.11	nd	nd
	5	18.45	34.449	5.1	61.7	0.769	5.80	nd	nd
	10	18.45	34.458	5.1	35.5	0.652	5.04	nd	nd
	15	18.43	34.484	5.7	13.4	0.710	4.14	nd	nd
	20	18.27	34.470	6.0	5.5	0.612	5.04	nd	nd
	30	18.05	34.502	7.1	2.1	0.583	3.56	nd	nd
	40	17.51	34.584	9.4	0.7	0.691	0.79	nd	nd
	50	16.33	34.605	11.1	0.0	0.091	0.78	nd	nd
	60	16.00	34.613	12.5	0.0	0.099	0.75	nd	nd
	75	15.27	34.610	11.7	0.0	0.056	0.55	nd	nd
	100	15.23	34.605	11.1	0.0	0.098	0.45	nd	nd
52-3	2	18.95	34.632	3.8	100.0	0.949	10.36	13.50	1.30
	10	18.93	34.477	4.7	37.0	0.867	9.61	nd	nd
	15	18.74	34.476	4.4	nd	0.882	nd	nd	nd
	20	18.31	34.486	5.0	13.8	0.747	6.91	6.51	0.94
	25	18.11	nd	4.8	nd	0.829	nd	nd	nd
	30	17.68	34.504	5.4	6.1	0.700	2.07	4.51	2.18
	40	16.59	34.582	8.2	2.9	0.335	1.02	0.42	0.41
	50	15.83	34.627	9.4	1.6	0.180	nd	nd	nd
	60	15.68	34.628	11.1	0.7	0.062	nd	nd	nd
	75	15.59	34.626	11.6	0.2	0.055	nd	nd	nd
	100	15.32	34.620	11.8	0.0	0.039	nd	nd	nd

nd: no data



## APPENDIX D (Continued)

NRA, NU and hydrographic data in the East China Sea.

Sta.	Depth (m)	T (°C)	S	NO <sub>3</sub> <sup>-</sup> (μM)	PAR %	Chl a (mg m <sup>-3</sup> )	NRA (nM h <sup>-1</sup> )	NU (nM h <sup>-1</sup> )	NU/NRA
55-3	2	23.93	34.624	0.2	100.0	0.065	0.12	1.88	15.67
	5	23.94	nd	0.2	nd	nd	nd	nd	nd
	10	23.94	34.617	0.0	40.4	0.067	0.21	nd	nd
	20	23.94	34.622	0.0	25.5	0.071	0.20	1.40	7.00
	30	23.94	34.642	0.0	16.3	0.074	0.13	1.00	7.69
	40	23.83	34.824	0.8	10.4	0.082	0.27	1.15	4.26
	50	23.63	34.778	0.0	6.4	0.087	0.36	0.56	1.56
	65	23.22	34.803	0.0	2.5	0.223	0.46	nd	nd
	80	22.78	34.830	0.5	0.4	0.202	0.58	nd	nd
	95	22.42	34.853	0.7	0.0	0.142	0.26	0.84	3.23
	111	22.03	nd	0.9	0.0	0.033	nd	nd	nd
55-5	2	24.06	34.618	0.1	100.0	0.055	0.11	nd	nd
	10	24.04	34.618	0.1	nd	nd	nd	nd	nd
	15	23.99	34.615	0.0	nd	nd	nd	nd	nd
	20	23.97	34.614	0.0	nd	nd	nd	nd	nd
	30	23.94	34.615	0.0	33.7	0.055	0.14	nd	nd
	40	23.91	34.689	0.0	22.6	0.055	0.29	nd	nd
	50	23.41	34.771	2.4	14.2	0.058	0.39	nd	nd
	75	22.52	34.850	2.6	5.4	0.229	0.65	nd	nd
	100	21.73	34.888	3.7	1.4	0.095	0.38	nd	nd
	151	19.13	34.905	4.7	nd	nd	nd	nd	nd
203	18.38	34.862	3.3	nd	nd	nd	nd	nd	

nd: no data

## APPENDIX E

IODATE, IODIDE, AND RELEVANT DATA IN THE SOUTHERN  
EAST CHINA SEA

Iodate, iodide, and relevant data in the southern East China Sea.

Sta.	Depth (m)	T (°C)	S	NO <sub>3</sub> <sup>-</sup> (μM)	Chl a (mg m <sup>-3</sup> )	NRA (nM h <sup>-1</sup> )	N-IO <sub>3</sub> <sup>-</sup> (nM)	N-I <sup>-</sup> (nM)
48	2	19.08	32.496	0.0	0.623	nd	nd	nd
	5	19.31	32.815	0.0	0.858	nd	303	128
	10	20.13	33.562	0.6	0.465	nd	269	137
	15	20.92	34.183	0.5	0.743	nd	292	117
	20	20.31	34.191	0.9	0.335	nd	298	133
	25	19.27	34.128	0.8	0.346	nd	272	134
	30	18.13	33.960	1.0	0.213	nd	276	131
	35	17.31	33.920	1.6	0.140	nd	nd	nd
	40	16.77	33.847	1.2	0.099	nd	nd	nd
49	2	nd	nd	0.0	0.700	5.67	nd	nd
	5	20.95	33.867	0.0	0.694	4.64	282	150
	10	20.95	33.908	0.0	0.649	2.05	279	113
	20	21.00	33.902	0.0	0.700	1.17	nd	nd
	25	20.44	33.954	0.3	0.694	0.44	nd	nd
	30	20.32	33.897	0.9	0.649	0.25	nd	nd
	35	19.97	33.918	1.7	0.140	0.60	319	129
	40	19.88	34.098	2.4	0.117	1.30	315	103
	45	18.93	33.885	2.7	0.124	1.28	252	149
	50	17.84	33.847	2.5	0.120	0.99	295	132
50	2	nd	34.238	0.0	0.543	4.56	289	148
	5	23.78	34.240	0.0	0.572	nd	nd	nd
	10	23.77	34.240	0.0	0.545	5.00	302	155
	15	23.78	34.241	0.0	0.523	nd	294	119
	20	23.79	34.242	0.0	0.554	3.93	nd	nd
	25	23.79	34.238	0.2	0.556	nd	nd	nd
	30	23.78	34.240	0.0	0.512	nd	nd	nd
	35	23.72	34.266	0.1	0.410	nd	283	157
	40	23.56	34.257	0.3	0.434	1.83	313	155
	45	23.49	34.268	0.4	0.299	nd	nd	nd
	50	23.46	34.269	1.3	0.279	nd	297	124
	60	23.44	34.269	0.7	0.293	1.46	295	157

## APPENDIX E (Continued)

Iodate, iodide, and relevant data in the southern East China Sea.

Sta.	Depth (m)	T (°C)	S	NO <sub>3</sub> <sup>-</sup> (μM)	Chl a (mg m <sup>-3</sup> )	NRA (nM h <sup>-1</sup> )	N-IO <sub>3</sub> <sup>-</sup> (nM)	N-I <sup>-</sup> (nM)
51	2	20.58	34.435	1.6	0.809	5.25	342	91
	5	20.56	34.455	2.0	0.813	3.90	349	76
	10	20.59	34.434	1.5	0.707	2.06	373	64
	20	20.61	34.427	1.7	0.751	2.85	nd	nd
	30	20.39	34.439	3.4	0.720	3.07	367	51
	40	20.38	34.429	3.7	0.528	0.70	378	50
	50	19.55	34.437	4.3	0.550	0.34	383	39
	60	19.32	34.571	6.3	0.412	0.83	378	30
	70	18.99	34.455	7.2	0.290	nd	nd	nd
	80	18.49	34.484	10.4	0.129	nd	nd	nd
	90	17.53	34.538	12.0	0.106	nd	nd	nd
52-1	2	18.46	34.449	4.2	0.887	6.11	340	83
	5	18.45	34.449	5.1	0.769	5.80	339	62
	10	18.45	34.458	5.1	0.652	5.04	350	66
	15	18.43	34.484	5.7	0.710	4.14	nd	nd
	20	18.27	34.470	6.0	0.612	5.04	368	67
	30	18.05	34.502	7.1	0.583	3.56	367	47
	40	17.51	34.584	9.4	0.691	0.79	nd	nd
	50	16.33	34.605	11.1	0.091	0.78	379	29
	60	16.00	34.613	12.5	0.099	0.75	411	18
	75	15.27	34.610	11.7	0.056	0.55	415	18
	100	15.23	34.605	11.1	0.098	0.45	420	10
53	2	22.11	34.111	0.1	2.438	7.85	289	117
	5	22.10	34.148	0.1	1.951	6.83	nd	nd
	10	22.13	34.155	0.1	1.951	5.78	321	70
	20	20.25	34.152	0.5	1.744	2.56	367	59
	30	19.71	34.152	0.4	1.201	1.39	384	35
	40	18.87	34.154	1.5	0.891	0.85	nd	nd
	50	18.66	34.151	nd	0.825	0.40	388	18
	75	17.72	34.232	nd	0.244	0.33	nd	nd
	100	16.47	34.205	5.5	0.248	0.40	nd	nd
	150	nd	34.204	5.4	0.211	nd	nd	nd

## APPENDIX E (Continued)

Iodate, iodide, and relevant data in the southern East China Sea.

Sta.	Depth	T	S	NO <sub>3</sub> <sup>-</sup>	Chl a	NRA	N-IO <sub>3</sub> <sup>-</sup>	N-I <sup>-</sup>	Depth
	(m)	(°C)		(μM)	(mg m <sup>-3</sup> )	(nM h <sup>-1</sup> )	(nM)	(nM)	(m)
54	2	24.45	nd	nd	nd	nd	nd	nd	
	10	24.45	nd	nd	nd	nd	281	126	
	20	23.90	nd	nd	nd	nd	274	147	
	30	21.87	nd	nd	nd	nd	262	143	
	50	21.16	nd	nd	nd	nd	295	88	
	70	19.89	nd	nd	nd	nd	310	104	
55-3	2	23.93	34.624	0.2	0.065	0.12	256	154	2*
	5	23.94	nd	0.2	nd	nd			
	10	23.94	34.617	0.0	0.067	0.21	257	169	10*
	20	23.94	34.622	0.0	0.071	0.20			
	30	23.94	34.642	0.0	0.074	0.13	245	154	20*
	40	23.83	34.824	0.8	0.082	0.27			
	50	23.63	34.778	0.0	0.087	0.36	257	176	40*
	65	23.22	34.803	0.0	0.223	0.46			
	80	22.78	34.830	0.5	0.202	0.58	285	136	75*
	95	22.42	34.853	0.7	0.142	0.26			
111	22.03	nd	0.9	0.033	nd	358	56		
						150*	410	11	
200*									

nd: no data; \* denotes the depth of iodate and iodide at Sta.55.

## VITA

Name: Chin-Chang Hung  
 Date of Birth: July 17, 1966  
 Place of Birth: Taiwan, Republic of China  
 Telephone: 757-683-5978  
 Fax: 757-683-5303  
 E-mail: [chung@odu.edu](mailto:chung@odu.edu)  
 Address: 4600 Elkhorn Ave.  
 Department of Ocean, Earth & Atmospheric Sciences  
 Old Dominion University, Norfolk, VA 23529

Education: 1999 Doctor of Philosophy in Chemical Oceanography  
 Department of Ocean, Earth & Atmospheric Sciences  
 Old Dominion University, Norfolk, VA, 23529  
 1993 M.S., Chemical Oceanography, National Taiwan  
 University, Taipei, Taiwan  
 1988 B.A., Oceanography, National Taiwan Ocean University,  
 Keelung, Taiwan

## Selected Publication:

- Hung, C.-C. and Wei, C.-L. (1992) Th-234 scavenging in the water column off southwestern Taiwan. *Terrestrial, Atmospheric and Oceanic Sciences*, **3**, 183-197.
- Wei, C.-L. and C.-C. Hung (1993) The effect of isotopic equilibration time on the determination of  $^{234}\text{Th}$  in seawater. *Journal Radioanalytical and Nuclear Chemistry Letters*, **175**, 155-159.
- Hung, C.-C., Wei, C.-L. and Chen, M.-P. (1994) Scavenging phenomenon in the surface water of Kuroshio Exchange Edge Processes (KEEP) area elucidated by  $^{234}\text{Th}/^{238}\text{U}$  disequilibria. *Acta Oceanography Taiwanica*, **33**, 81-96.
- Wei, C.-L. and C.-C. Hung (1998) Particle scavenging in the upper water column off Mindoro Island, Philippine:  $^{234}\text{Th}/^{238}\text{U}$  disequilibria. *Estuarine, Coastal and Shelf Sciences*, **46**, 351-358.
- Hung, C.-C., G. T. F. Wong, K.-K. Liu, F.-K. Shiah, and G.-C. Gong (1998) The effects of environmental conditions on the relationship between nitrate reductase activity and  $^{15}\text{NO}_3^-$  uptake: field observations in the East China Sea. *Limnology and Oceanography*, (currently in revision).
- Wong, G. T. F. and C. -C. Hung (1998) Speciation of dissolved iodine: an integrator of new production in the oceans. *Continental Shelf Research*, submitted.